ISSN 2217-379X

University of Novi Sad,
Faculty of Technical Sciences,
DEPARTMENT OF GRAPHIC
ENGINEERING AND DESIGN

Volume **17**
Issue **3**
September **2026**

JGED

JOURNAL OF GRAPHIC ENGINEERING AND DESIGN

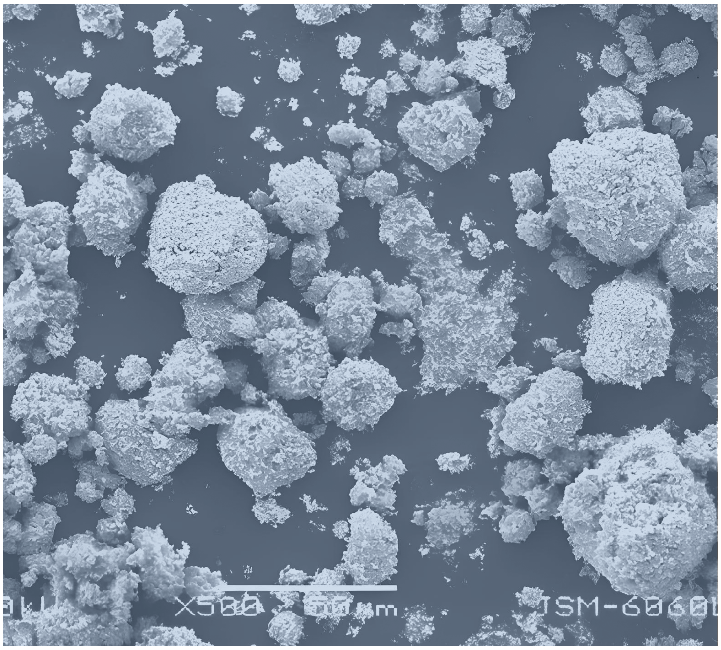

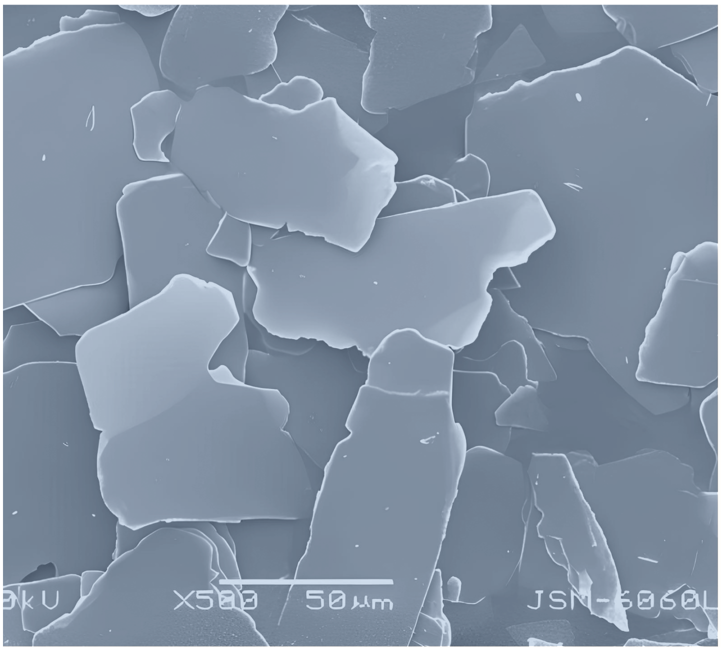

JGED

JOURNAL OF GRAPHIC ENGINEERING AND DESIGN

3/2026

Volume 17, Number 3, September 2026.

Published by

UNIVERSITY OF NOVI SAD, SERBIA
Faculty of Technical Sciences
Department of Graphic Engineering and Design

PUBLISHED BY

University of Novi Sad
Faculty of Technical Sciences
DEPARTMENT OF GRAPHIC ENGINEERING AND DESIGN

Address:
Faculty of Technical Sciences,
Department of Graphic
Engineering and Design,

Trg Dositeja Obradovića 6
21000 Novi Sad, Serbia

Telephone numbers:
+381 21 485 26 20
+381 21 485 26 26
+381 21 485 26 21

Fax number:
+381 21 485 25 45

Email:
jged@uns.ac.rs

Web address:
www.grid.uns.ac.rs/jged

Frequency: 4 issues per year
Printing: Faculty of Technical Sciences,
Department of Graphic Engineering and Design

Circulation: 200

Electronic version of journal available on
www.grid.uns.ac.rs/jged

E-ISSN 2217-9860

The journal is abstracted/indexed
in the Scopus and Directory of Open Access Journals

CIP - Katalogizacija u publikaciji
Biblioteka Matice srpske, Novi Sad
655
JGED : Journal of Graphic Engineering and Design /
editor Dragoljub Novaković. - Vol. 1, No. 1 (nov. 2010) -
Sciences, Department of Graphic Engineering and
Design,
2010-. 30 cm
Četiri puta godišnje
ISSN 2217-379X
COBISS.SR-ID 257662727

JOURNAL OF GRAPHIC
ENGINEERING AND DESIGN

Volume 17, Number 3, September 2026.

Contents

Original scientific paper
http://doi.org/10.24867/JGED-2026-3-005

A study of optical properties of coatings based on functional pigments and cellulose nanocrystals across the solar spectrum

ABSTRACT

This study investigates the optical properties of coatings based on functional pigments and cellulose nanocrystal (CNC) across the solar spectrum (UV-VIS-NIR: 200-2500 nm). The coatings were formulated using CNC aqueous suspension as a sustainable, bio-based binder. Four different pigment types (one IR-absorbing and three pearlescent) were incorporated into the CNC matrix and coated onto the translucent paper substrate. Spectrophotometric measurements revealed significant differences in optical properties among coatings. The coating based on IR-absorbing pigment exhibited the highest overall absorbance, especially in the NIR region, the lowest reflectance across the entire solar spectrum, but the highest transmittance in the NIR (≈85-90% between ≈900-1800 nm). Coatings based on the pearlescent pigments showed lower overall absorbance but higher UV reflectance. The results highlight the potential of using CNCs as a binder with functional pigments to create sustainable functional coatings on transparent substrates where more light, less heat, and higher UV absorption are needed.

KEY WORDS
functional pigments, optical properties, coatings, solar spectrum, cellulose nanocrystals

Mirica Karlovits
Blaž Likozar
Uroš Novak

National Institute of Chemistry, Ljubljana, Slovenia

Corresponding author:
Mirica Karlovits
e-mail:
mirica.karlovits@ki.si

First received: 11.12.2025.
Revised: 6.2.2026.
Accepted: 6.4.2026.

Introduction

The design of coatings that control solar radiation in a spectrally selective way is increasingly important in energy, transportation, packaging, and advanced functional surfaces. The coating and pigment industries have developed a broad range of functional pigments designed to interact selectively with solar radiation. Solar energy can be transferred, reflected, or absorbed by surfaces that are exposed to sunlight. Solar spectrum consists of 52% NIR radiation (700-2500 nm), 43% visible (VIS) light (400-700 nm), and 5% ultraviolet (UV) radiation (280-400 nm). Near infrared light plays an important role in heat generation (La Notte at al., 2020; Mara et al., 2023).

Pigments are important materials in industrial coatings that not only provide colour but also impart special properties such as thermal control.

The classification of pigments can be approached from several perspectives, such as their chemical composition, source (origin), color, crystallographic structure, their interaction with light, and, most importantly, their functional properties. Pearlescent pigments belong to the group of special effect pigments and are composed of plate-shaped crystals unlike conventional pigments. The transmission through a coating containing pearlescent pigments is influence by two effect the absorption of the pigment and interference effects. Silica or mica are almost transparent materials for light. However, metal oxides like titania or iron oxide absorbs UV-light and can for this decrease the transmission in the spectral area of UV-light (Ahn et al., 2022; Greiler & Mahltig, 2021). NIR pigments are mainly classified into two groups: inorganic compounds and organic compounds. A preference for organic pigments is reported due to their non-toxicity, biocompatibility, and their cost-effectiveness.

In addition, organic reflective materials are soluble in standard solvents, thereby increasing compatibility with polymers. The addition of NIR pigments to coatings offers a wide range of benefits. One of the standout advantages is the enhanced durability of the coatings, the reduced thermal degradation (Mansour & Farha, 2025; Rossi, Russo & Bouchakour Rahmani, 2020).

The choice of binder plays an equally important role in determining the optical properties of the coating. Cellulose nanocrystals (CNCs) also known as cellulose nanowhiskers or nanocrystalline cellulose, derived from renewable biomass, offer a sustainable alternative to conventional polymer binders. CNCs are typically produced from lignocellulosic biomass (i.e., plants), due to the natural abundance and commercial availability of these sources. There is also growing interest in valorizing other lignocellulose biomass to produce CNCs, including nonwoody plants (e.g., bamboo, sugar cane and maize), as well as bast fibers from plants such as ramie, hemp, and jute (Frka-Petesic et al., 2023).

CNCs exhibit high mechanical strength, rigidity, and optical transparency, making them ideal for applications in nanocomposites, coatings, and drug delivery. CNCs typically exhibit rod-like shapes with widths ranging from 3 to 20 nm (Tofanica et al., 2025). Their nanoscale dimensions minimize light scattering, enabling the formation of clear films even at relatively high solid content. Furthermore, CNC-based matrices provide environmental benefits by reducing reliance on petroleum-derived polymers and support circular economy principles (Droguet et al., 2022; Jeon, Oh & Kim, 2025; Ruberto et al., 2024).

Recent studies have demonstrated the feasibility of CNC-based coatings for optical and barrier applications, including photonic films and effect pigments, highlighting their potential for sustainable functional coatings (Chen, Zhang & Wu, 2023; Xu et al., 2018). Sirviö et al. showed that CNCs exhibited very high UV-absorption properties, especially in UVA and UVB regions and high transparency in the visible light region (around 90% with 0.1% of CNCs). The fabricated CNCs functioned as lightweight-reinforcing fillers with high UV-absorption capability when incorporated into a poly(vinyl alcohol) (PVA) matrix (Sirviö et al., 2016).

Yang et al. (2024) investigate VO_2 nano-rod coated mica composites pearlesecnt pigment for temperature control packaging. Furthermore, in the study conducted by Toy, E. et al., the effect of particle size on color and NIR reflectivity of $(Fe,Cr)_2O_3$ black pigment was investigated (Toy et al., 2025).

In this context, the present work focuses on coatings formulated with various types of pigments and CNC as a binder. The primary objective was to evaluate the spectral absorbance, reflectance, and transmittance of these coatings across the UV-VIS-NIR range. By combining functional pigments with a bio-based binder, this work aims to advance solutions for thermal control without deterioration of the optical properties of coatings.

Materials and methods

The CNC aqueous suspension (2-5 wt.% solids) used in this study as a binder was provided by the manufacturer *Nanocrystacell*, Slovenia (Table 1). Four different types of coatings were formulated using various pigment types (Table 2), which were incorporated into the CNC suspension (20 wt% pigment concentration). A translucent paper substrate (G = 100 g/m²) was used, which was coated using a K Control Coater/meter bar (wire diameter: 0.05 mm, wet film deposit: 4 µm). The paper was conditioned to a standard atmosphere of (23 ± 1)°C and (50 ± 2)% relative humidity for 24 hours before coating.

A Scanning Electron Microscope- SEM (JSM-5610JOEL) was used to evaluate the pigment morphology and pigment size distribution. The absorption (A), transmission (T), reflectance (R) spectra of coatings were obtained with Lambda 950 UV-VIS-NIR spectrometer (PerkinElmer, USA). Spectral data were collected over a broad wavelength range from 200 nm to 2500 nm, covering the ultraviolet, visible, and near-infrared regions of the electromagnetic spectrum. A step size of 10 nm was selected to ensure high-resolution spectral profiles. This approach enabled a comprehensive analysis of how each pigment influences light-matter interactions within the coating.

Table 1
Properties of cellulose nanocrystals (CNCs)

Parameter	Specification
Chemical name	$C_6O_5H_{10}$
Color	White-translucent
Form	Aqueous suspension, 2-5wt.% solids
Surface	Hydrophilic
Average size (Scherrer method, SEM)	10-15 nm wide,150-300 nm length
Crystallinity (XRD: Segal method)	90.3%
Initial decomposition temperature	285°C
Density	Aqueous gel: 1.04 g/cm^3
Lihnin content	Negligible

Table 2

Properties of pigments

Label	Trade name	Form	Pigment type	Chemical composition	Particle size
HRP	Iriotec® 9230	Powder	IR-absorbing pigment	Tin antimony grey cassiterite	90% < 10 µm
EP1	Miraval® 5424	Powder	Pearlescent pigment	Synthetic calcium aluminum borosilicate (59-77%) coated with titanium dioxide (22-32%), silicone dioxide (1-8%) and stannic oxide (0-1%)	20-200 µm
EP2	Symic E001	Powder	Pearlescent pigment	Mixture of synthetic flurophlogopite (79-90%), titanium dioxide (10-20%) and tin oxide (< 1%)	20-150 µm
EP3	Colorstream® T10-03	Powder	Multi-color effect pigment	Silicon dioxide (51-64%) coated with rutile titanium dioxide (35-45%) and tin oxide (1-4%)	5-50 µm

Results and discussion

Scanning electron image analysis

A 500x magnification scanning electron microscope (SEM) image of each of the four pigments utilised in this study is displayed in Figure 1.

Figure 1/a shows clusters of pigment particles with predominantly rounded or polyhedral shapes, while Figure 1/b-c shows a »corn flake« morphology, in which the particles appear as thin, irregular flakes with sharp edges and comparatively smooth surfaces.

Pigment labelled IRP (Iriotec® 9230) is a mica-based layer pigment with 90% of particles smaller than 10 µm. Infrared-absorbing pigments are functional materials designed to absorb light in the near-infrared (NIR) region of the electromagnetic spectrum (typically 700-2500 nm) while often remaining transparent or only slightly colored in the visible range.

Pigment labelled EP1 (Miraval® 5424) is based on borosilicate glass and are therefore exceptionally transparent with a high sparkle and low color influence on colored formulations with a particle size of 20-200 µm.

Pigment labelled EP2 (Symic E001) is an interference silver pigment based on synthetic mica. It is a mixture of synthetic fluorphlogopite, titanium dioxide and tin oxide. It is a pearlescent pigment based on artificial mica.

Pigment labelled EP3 (Colorstream® T10-03 Tropic Sunrise) is a multicolor effect industrial pigment. It exhibits iridescent color gradients and limitless styling possibilities with ever-changing highlights.

It offers interference, improved chroma and pearlescent effects. It is based on synthetically manufactured silicon dioxide platelets coated with titanium dioxide (Specialchem, 2026).

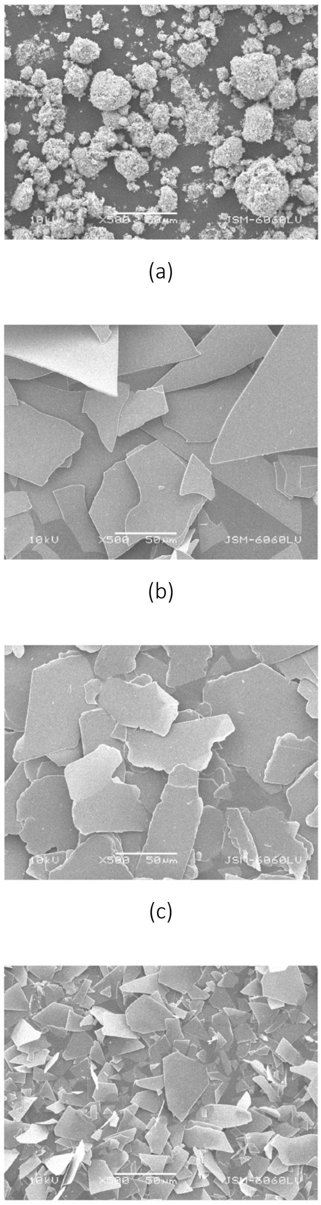

(a) (b) (c) (d)

» **Figure 1:** *SEM images of pigments: a) IRP, b): EP1, c) EP2 and d) EP3 at 500x magnification*

Optical properties of coatings

Figure 2 presents the absorbance (A, %) of four coatings based on different pigments measured across the solar spectrum from 200 to 2500 nm, covering the UV, visible (VIS), and near-infrared (NIR) regions.

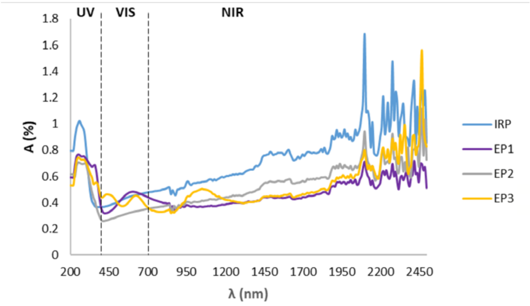

» **Figure 2:** *Absorbance spectra of various coatings in the UV-VIS-NIR regions*

Coating based on infrared absorbing pigment (labelled IRP) has the highest overall absorbance, especially in the NIR region (700-2450 nm), where it rises steadily, with the highest peak at 2100 nm, reaching A = 1.7%.

In the UV region coating based on IRP starts high (~0.8-1%) but dips near 450 nm before gradually increasing again. In the visible region (400-700 nm) absorbance decreased considerably for all coatings. The IR-absorbing pigment is specifically tuned to absorb near-infrared (NIR) radiation. It functions by capturing the energy of IR photons and converting them into thermal energy before they can pass through a substrate (like a window or plastic sheet).

Pigment IRP, however, is a light-colored pigment that absorbs heat and light just like black pigment. In light-colored coatings, it contributes to shorter drying times and higher production capaticies at lower energy cost (Susonity, 2025). On the other side, coatings based on pigments EP1-EP3 have much lower absorbance and remain relatively flat across the spectrum, with slight increases in the NIR region.

The difference in NIR absorbance between coatings based on IRP and EP pigments becomes substantial above 1200 nm, and especially beyond 2000 nm, where IRP's performance is significantly higher.

Compared with pigments of other colors, black pigments like carbon black absorb visible light (400-700 nm), as well as near-infrared (NIR) light (700-2500 nm), which accounts for approximately 50% of solar radiation to store heat (Mansour & Farha, 2025).

Figure 3 presents the reflectance (R, %) of different coatings across the entire solar spectrum.

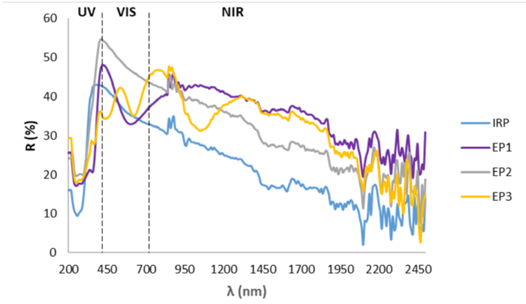

» **Figure 3:** *Reflectance spectra of various coatings in the UV-VIS-NIR regions*

As noted in Figure 3, all coatings show moderate reflectance in the UV region (200-400 nm). Coatings based on EP pigments (EP1-EP3) exhibit higher UV reflectance, especially EP2, which peaks above 54% at 420 nm. Coating based on IRP shows the lowest reflectance in the entire solar spectrum. In the visible region (400-700 nm), reflectance increased compared to lower wavelengths, with the coating based on EP2 reaching the highest reflectance values at the transition from the UV to the visible spectrum. Coating based on IRP has significantly lower reflectance across the VIS region (30-40%), in the NIR region (700-2500 nm) reflectance continuously decreases with increasing wavelength. Unlike "cool" pigments designed for high NIR reflectivity to reduce urban heat (which can reach over 95% reflectance), IR-absorbing pigments are characterized by low reflection in their target IR range (Kuzman et al., 2025).

Coatings slightly increase with the peak at 880 nm, reaching R = 45% for EP1 and with the peak at 860 nm, reaching R = 47% for EP3. In the deeper NIR region (>1900 nm), reflectance for IRP drops below approximately 15%. IRP pigment reflects the sunlight's invisible heat radiation while allowing the majority of the visible light to pass through. It offers more light, less heat and higher UV absorption, allows diffusion of visible light while reducing UV and NIR transmission and exhibits properties similar to sun-protective filters on all transparent substrates (Susonity, 2025).

Figure 4 presents the transmittance (T, %) of different coatings across the entire solar spectrum.

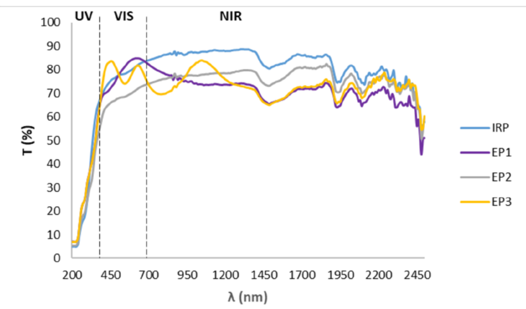

» **Figure 3:** *Transmittance spectra of various coatings in the UV-VIS-NIR regions*

Transmittance refers to how much light passes through a material compared to the amount of light that initially hits it. A material with high transmittance (close to 100%) lets most light through (like clear glass), while low transmittance means the material blocks or absorbs most light (like tinted glass or opaque objects) (Paschotta, 2019). All coatings exhibit very low transmittance below 260 nm (<20%) and rises sharply toward the VIS region for all coatings. Among all, the coating based on EP2 achieved the lowest transmittance in the visible region. The coating based on IRP shows the highest transmittance over most of the NIR (≈85-90% between ≈900-1800 nm) with several narrow features and modest depressions. In contrast, coatings based on EP1-EP3 show systematically lower T (≈70-85%), indicating reduced light transmission. A pronounced drop in T for all samples near ≈2400-2500 nm was observed.

Conclusions

The present study successfully evaluated the spectral absorbance, reflectance, and transmittance of coatings formulated with various functional pigments and cellulose nanocrystals (CNC) as a binder across the UV-VIS-NIR range (200 nm to 2500 nm), achieving the primary objective of the work. This research aimed to advance solutions for thermal control without deteriorating the optical properties of the coatings by combining functional pigments with a bio-based binder.

Four different pigments were used, with three being pearlescent pigments (EP1, EP2, EP3) and one being an infrared-absorbing pigment (IRP). Scanning Electron Microscope (SEM) analysis showed that the IRP pigment particles formed clusters with mainly rounded or polyhedral shapes. In contrast, the pearlescent pigments (EP1, EP2, EP3) displayed a characteristic "corn flake" morphology, appearing as thin, irregular flakes with sharp edges.

The optical property analysis showed significant differences based on pigment type. The coating containing the infrared-absorbing pigment (IRP) exibited the highest overall absorbance, which increased steadily across the Near-Infrared (NIR) region (700-2500 nm), peaking at 2100 nm. In contrast, the coatings with the pearlescent pigments (EP1-EP3) showe lower absorbance, remaining relatively constant across the spectrum. The IRP coating had the lowest reflectance across the entire solar spectrum, with its reflectance continuously decreasing in the NIR region. In contrast, the EP pigment coatings exhibited the highest reflectance in the visible (VIS) region.

Regarding transmittance, the IRP coating exhibited the highest values over most of the NIR range (approximately 85-90% between 900 and 1800 nm), indicating significant light transmission. This is consistent with the IRP pigment's property of allowing most visible light to pass through while absorbing invisible heat radiation. In contrast, coatings based on EP1-EP3 showed consistently lower transmittance in this range.

Overall, the combination of specific pigments and CNC as a binder offers a promising, sustainable pathway for developing functional coatings that provide effective thermal control and exhibit properties similar to sun-protective filters on transparent substrates.

Funding

The authors would like to acknowledge the financial support of Horizon Europe projects UPSTREAM (GA 101112877) and REMEDIES (GA 101093964).

References

Ahn, H.-S., Gasonoo, A., Lim, S.-M., Lee, J.-H. & Choi, Y. (2022) Fabrication of Color Glass with High Light Transmittance by Pearlescent Pigments and Optical Adhesive. *Materials*. 15 (7), 2627. Available from: doi: 10.3390/ma15072627

Chen, M., Zhang, H. & Wu, Y. (2023) Improving the decorative performance of UV-curable coatings with iridescent cellulose nanocrystal film. *RSC Advances.* 13 (32), 22569–22578. Available from: doi: 10.1039/d3ra03481j

Droguet, B. E., Liang, H.-L., Frka-Petesic, B., Parker, R. M., De Volder, M. F. L., Baumberg, J. J. & Vignolini, S. (2022) Large-scale fabrication of structurally coloured cellulose nanocrystal films and effect pigments. *Nature Materials.* 21 (3), 352–358. Available from: doi: 10.1038/s41563-021-01135-8

Frka-Petesic, B., Parton, T. G., Honorato-Rios, C., Narkevicius, A., Ballu, K., Shen, Q., Lu, Z., Ogawa, Y., Haataja, J. S., Droguet, B. E., Parker, R. M. & Vignolini, S. (2023) Structural Color from Cellulose Nanocrystals or Chitin Nanocrystals: Self-Assembly, Optics, and Applications. *Chemical Reviews.* 123 (23), 12595–12756. Available from: doi: 10.1021/acs.chemrev.2c00836

Greiler, L. C. & Mahltig, B. (2021) Pearlescent Effect Pigments for Coatings on Textiles-Part I: Protective Materials Against UV Light and IR Light. *World Journal of Textile Engineering and Technology*. 7, 73-83.

Jeon, H., Oh, K. K. & Kim, M. (2025) Cellulose Nanocrystals for Advanced Optics and Electronics: Current Status and Future Directions. *Micromachines.* 16 (8), 860. Available from: doi: 10.3390/mi16080860

Kuzman, S., Dramićanin, T., Popov, A. I., Brik, M. G. & Dramićanin, M. D. (2025) Pigments and Near-Infrared Phosphors Based on Mn5+. *Nanomaterials.* 15 (4), 275. Available from: doi: 10.3390/nano15040275

La Notte, L., Giordano, L., Calabrò, E., Bedini, R., Colla, G., Puglisi, G. & Reale, A. (2020) Hybrid and organic photovoltaics for greenhouse applications. *Applied Energy.* 278, 115582. Available from: doi: 10.1016/j.apenergy.2020.115582

Mansour, S. A. & Farha, A. H. (2025) A Review of Near-Infrared Reflective Nanopigments: Aesthetic and Cooling Properties. *Crystals.* 15 (3), 271. Available from: doi: 10.3390/cryst15030271

Mara, J., Bodnár, A.-E., Trif, L. & Telegdi, J. (2023) Development of Effective Infrared Reflective Coatings. *Applied Sciences.* 13 (23), 12903. Available from: doi: 10.3390/app132312903

Paschotta, R. (2019) Transmittance. In: *RP Photonics Encyclopedia*. Frauenfeld, RP Photonics AG. Available from: doi: 10.61835/vr5

Rossi, S., Russo, F. & Bouchakour Rahmani, L. (2020) Study of the Durability and Aesthetical Properties of Powder Coatings Admixed with Pearlescent Pigments. *Coatings.* 10 (3), 229. Available from: doi: 10.3390/coatings10030229

Ruberto, Y., Vivod, V., Grkman, J. J., Lavrič, G., Graiff, C. & Kokol, V. (2024) Slot-die coating of cellulose nanocrystals and chitosan for improved barrier properties of paper. *Cellulose.* 31 (6), 3589–3606. Available from: doi: 10.1007/s10570-024-05847-3

Sirviö, J. A., Visanko, M., Heiskanen, J. P. & Liimatainen, H. (2016) UV-absorbing cellulose nanocrystals as functional reinforcing fillers in polymer nanocomposite films. *Journal of Materials Chemistry A.* 4 (17), 6368–6375. Available from: doi: 10.1039/c6ta00900j

Specialchem (2026) *Coating Ingredients Master Catalog: all products from all suppliers*. Available from: https://www.specialchem.com/coatings [Accessed 14th April 2026].

Susonity (2025) *Sitemap - Surface Solutions*. Available from: https://www.susonity.com/SI/en/sitemap [Accessed 14th April 2026].

Tofanica, B.-M., Mikhailidi, A., Fortună, M. E., Rotaru, R., Ungureanu, O. C. & Ungureanu, E. (2025) Cellulose Nanomaterials: Characterization Methods, Isolation Techniques, and Strategies. *Crystals.* 15 (4), 352. Available from: doi: 10.3390/cryst15040352

Toy, E., Aslan, E., Yeşilci, E., Karaahmet, O., Grijalbo, A. & Çiçek, B. (2025) Effect of particle size on color and NIR reflectivity of (Fe,Cr)2O3 black pigment. *Inorganic Chemistry Communications.* 175, 114132. Available from: doi: 10.1016/j.inoche.2025.114132

Xu, M., Li, W., Ma, C., Yu, H., Wu, Y., Wang, Y., Chen, Z., Li, J. & Liu, S. (2018) Multifunctional chiral nematic cellulose nanocrystals/glycerol structural colored nanocomposites for intelligent responsive films, photonic inks and iridescent coatings. *Journal of Materials Chemistry C.* 6 (20), 5391–5400. Available from: doi: 10.1039/c8tc01321g

Yang, J., Zhang, H., Hong, X., Mu, B. & Ye, B. (2024) VO2 nano-rod coated mica composite pearlescent pigment for temperature control packaging. *Surfaces and Interfaces.* 48, 104157. Available from: doi: 10.1016/j.surfin.2024.104157

Original scientific paper
http://doi.org/10.24867/JGED-2026-3-011

Colour prediction in multilayer polymer systems under polarized light for packaging applications

ABSTRACT

Conventional colour measurement methods do not fully account for the optical properties of multilayer polymer systems in transmitted polarized light. This work presents a Mueller-calculus-based model that predicts the spectral radiance and perceived colour of multilayer anisotropic polymer film stacks viewed in polarized light, targeting design needs in packaging. The model accepts the light source spectrum, polarizer and analyser angles, film optical-axis orientations, polymer film birefringence, and the spectral transmittance of added colour filters. The model was implemented in Python using SymPy and Colour libraries. Validation experiments employed stacks 1–3 layers at a 45-degree angle of 25±5 μm thickness BOPP films between parallel and crossed polarizers with a measured LED light source and X-Rite i1Pro spectrophotometer, including stacks combined with three gel colour filters and three flexographically printed patches on BOPP; BOPP birefringence was retrieved as Δn 0.015 via spectral analysis and it is consistent with the literature. The model reproduced key spectral features and colour coordinates, yielding absolute spectral RMSEs of 0.34-1.01 mW/(m²·sr·nm) for stacks without colour filters and a mean RMSE of 0.27 mW/(m²·sr·nm) with colour filters. The mean colour difference ΔE_{76} across configurations with colour filters was 10.8. The model can be used for preview prototyping of polarized-light effects and security features in multilayer packaging and may provide a basis for an intelligent colour-management system.

Vladislav Vereshchagin [1]
Aleksandra Pogiba [2]
Alexander Kondratov [2]

[1] Moscow Polytechnic University, Department of Incognitive Technologies, Moscow, Russia
[2] Moscow Polytechnic University, Department of Innovative Materials of Printmedia Industry, Moscow, Russia

Corresponding author:
Vladislav Vereshchagin
e-mail:
slavaver@ya.ru

First received: 25.9.2025.
Revised: 11.1.2026.
Accepted: 21.1.2026.

KEY WORDS
colorimetry, birefringence, Mueller calculus, packaging, polarized light, polypropylene, BOPP

Introduction

Control of colour and visual effects in modern packaging materials is of major commercial and scientific interest (Tomiša & Vusić, 2019). Among the key factors influencing these visual properties are the optical characteristics of the materials. Some polymer films are anisotropic materials and have different refractive indices along the optical axis and the transverse direction. As a result, two light beams propagate through such a material at different speeds (Samadi-Dooki et al., 2024). When light passes sequentially through a polarizer, a film sample, and an analyser, the analyser recombines the two beams. Since these beams travel at different speeds within the film, they acquire optical path difference determined by difference in refractive indexes and film thickness. Therefore, the transmitted light is no longer a mixture of colours forming white light, but a single interference colour, arising from the recombination of two waves. This optical property of anisotropic materials is known as birefringence. Birefringence is widely used in photoelasticity to analyse stress distribution in solids. Another application is the creation of colourful images under polarized light. The author termed such images PFC (polarization-filtered coloration) images (Slepkov, 2022a), generated using a different number of polymer film layers and orientations. This concept can, to some extent, be adapted for packaging applications.

Further use lies in anti-counterfeiting technologies. By stacking polymer films with anisotropic properties with cutouts in one or more layers, readable barcodes can be designed to appear only in polarized light (Kondratov et al., 2023). Moreover, biobased cellulosic materials with birefringence enable eco-friendly anti-counterfeiting solutions (Li et al., 2024).

Polymer films are widely used for packaging in multilayer systems, where the industry demands both colour constancy and predictability. The visual appearance of packaging plays an important role in successful marketing and design significantly affects respondents' decision-making process (Febriant, Widodo & Faizin, 2023; Malešević & Stančić, 2021).

Therefore, predicting the resulting colour effect is essential for utilizing birefringent polymer films in colourful packaging.

Quantitative analysis of interference colours observed in samples with double refraction (birefringence) is usually carried out using the Michel-Levy diagram. This method correlates interference colours, observed in optical microscopy or recorded digitally, with the sample's retardation, thickness, and birefringence (Linge Johnsen et al., 2018). The Michel–Lévy chart is generally applied when the optical axis of the sample is oriented at 45° to the polarizers.

The aim of this study was to develop a model for predicting the colours generated by multiple anisotropic polymer films with the addition of colourful layer viewed in polarized light, with practical applications in the packaging industry. The model accounts for the following known conditions: the spectral characteristic of the light source, the rotation angles of the polarizer and analyser, the orientation of the polymer film's optical axis, the film thickness, the induced phase shift (dependent on film thickness, refractive indices and light wavelength) and spectral transmittance of the colourful layer.

To our knowledge, the application of Mueller calculus for colour prediction in multilayer anisotropic polymer systems for packaging industry under controlled polarization conditions is novel.

The practical use of the developed model is prototyping anti-counterfeiting designs in multilayer polymer labels in packaging. It helps to create readable barcodes that become visible only under polarized light, eliminating the need to physically test various material combinations and layer configurations and reduces costly trial-and-error processes. Later, the model can be integrated into soft-proofing and ink formulation software systems. This integration would enable designers to combine interference colours generated by birefringent polymer layers with ink layers to achieve target colour specifications.

Model

Mueller calculus provides a mathematical formalism for describing the transformation of the polarization state of light as it interacts with various optical elements. It describes fully polarized, partially polarized, and unpolarized light, which are common in experimental and natural conditions. This suitability for complex systems, where multiple polarization effects occur simultaneously, provides predictive power for interpreting experimental measurements (Bass, 1995; del Toro Iniesta, 2003).

In this formalism, the polarization of an electromagnetic wave is represented by the four-component Stokes vector, which captures both the intensity and polarization characteristics of the beam. In this study, the unpolarized beam radiating from the light source was described by a series of special-case Stokes vectors $\overrightarrow{S_\lambda}$ for each wavelength λ (1).

$$\overrightarrow{S_\lambda} = \begin{bmatrix} I_\lambda \\ 0 \\ 0 \\ 0 \end{bmatrix} \tag{1}$$

where, I_λ is intensity of the light at a given wavelength.

The optical element is described by a 4x4 real-valued Mueller matrix that operates linearly on the Stokes vector, thereby enabling a unified treatment of a wide range of optical effects, including birefringence. There are Mueller matrixes for linear polarizers M_P (ϕ) (2), a general linear retarder M_R (δ, θ) (3), a simple non-polarizing colour filter M_F (λ) (4) for a given wavelength λ and neutral density filter. Colour filters were described by an identity matrix scaled by the filter's transmittance and neutral density filter is based on a simple non-polarizing colour filter but have same value T for all wavelengths λ.

$$M_P(\phi) = \begin{bmatrix} \frac{1}{2} & \frac{\cos(2\phi)}{2} & \frac{\sin(2\phi)}{2} & 0 \\ \frac{\cos(2\phi)}{2} & \frac{\cos(4\phi)}{4} + \frac{1}{4} & \frac{\sin(4\phi)}{4} & 0 \\ \frac{\sin(2\phi)}{2} & \frac{\sin(4\phi)}{4} & \frac{1}{4} - \frac{\cos(4\phi)}{4} & 0 \\ 0 & 0 & 0 & 0 \end{bmatrix} \tag{2}$$

where, ϕ is the angle of the transmission axis relative to the horizontal plane.

$$M_R(\delta,\theta) = \begin{bmatrix} 1 & 0 & 0 & 0 \\ 0 & \cos^2(2\theta) + \sin^2(2\theta)\cos\delta & \cos(2\theta)\sin(2\theta)(1-\cos\delta) & -\sin(2\theta)\sin\delta \\ 0 & \cos(2\theta)\sin(2\theta)(1-\cos\delta) & \sin^2(2\theta) + \cos^2(2\theta)\cos\delta & \cos(2\theta)\sin\delta \\ 0 & \sin(2\theta)\sin\delta & -\cos(2\theta)\sin\delta & \cos\delta \end{bmatrix} \tag{3}$$

where, δ is the phase difference between the fast and slow axes of the transmitted light and θ is the angle of the fast axis relative to the horizontal plane.

$$M_F(\lambda) = I_4 T(\lambda) \tag{4}$$

where, I_4 is a 4x4 identity matrix, λ is wavelength, T (λ) is transmittance for wavelength λ.

The resulting Stokes vector, $\overrightarrow{S_O}$ (5), is then calculated via matrix multiplication.

$$\overrightarrow{S_O} = M_N \cdots M_2 M_1 \overrightarrow{S_\lambda} \tag{5}$$

where, $\overrightarrow{S_\lambda}$ is Stokes vector for unpolarized light, $M_N \cdots M_2 M_1$ is optical element M_1 followed by M_2 and till M_N.

This model was implemented in a program written in Python. The main libraries that were used in implementation: Sympy (Meurer et al., 2017) and Colour (Mansencal et al., 2024). Code for this project can be found on the GitHub repository (https://github.com/slavaver/birefringence-model).

Materials and equipment

A series of optical experiments was conducted to validate the predictions of the developed model. Polymer film samples, polarizers, colour filters, a LED-light source with a diffuser and a spectrophotometer were employed. The experimental setup is shown in figure 1.

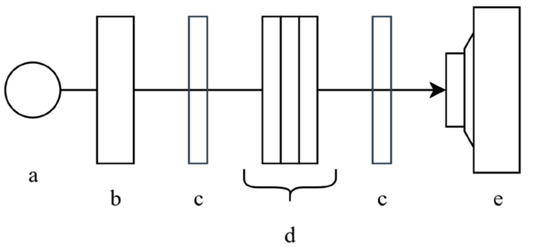

» **Figure 1:** *A diagram of the experimental setup used for taking spectral measurements, a – light source, b – diffusor, c – polarizer, d – stack of BOPP polymer films (1-3 layers), e – spectrophotometer*

All data were obtained with the spectrophotometer X-Rite i1Pro rev. D with spectral readings from 380 nm to 730 nm in 10 nm steps using ArgyllCMS utility “spotread” in emissive measurement mode (absolute results) resulting in spectral radiance in mW/(m²·sr·nm) data. Results represent single measurements only. The manufacturer's specification states short-term repeatability: x, y ±0.002 typ. (5000 K, 80 cd/m²). All measurements were conducted in a darkened room to eliminate ambient light interference. Spectrophotometer self-calibration was performed before measurements using the built-in white reference.

The X-Rite i1Pro was calibrated against the instrument's white reference standard (99% diffuse reflectance) in absolute radiance measurement mode. In one of the works authors used a similar spectrophotometer and have stated that relative standard deviations (RSD) of measurement vary from 0.1% to 1% (Apyari et al., 2011). In this case maximum relative expanded uncertainty for approximate 95% reference interval (RI) U(95%RI) = 2 × RSD = 2%.

The first component of the experimental setup is a LED-light source and a diffuser. Their measured spectral radiance (mW/(m²·sr·nm)) is shown in figure 2.

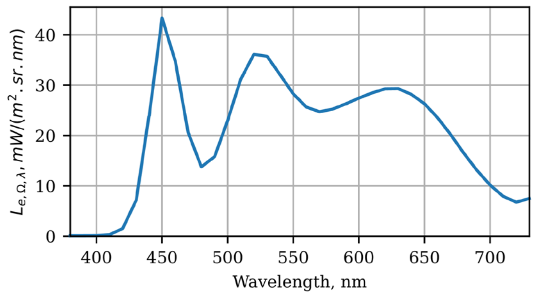

» **Figure 2:** *Measured spectral radiance in mW/(m²·sr·nm) of LED-lights emission after diffusor using spectrophotometer X-Rite i1Pro*

The linear polarizer from TAC and PVA declared characteristics are transmittance 0.41 when single and 0.05 when crossed (Fig. 3). Polarizing efficiency is 99.99%, wavelength range- 380~800nm, thickness- 0.25mm. To account for the difference between an ideal polarizer (transmittance 0.50) and the real polarizer used (transmittance 0.41), an additional coefficient of 0.82 was applied.

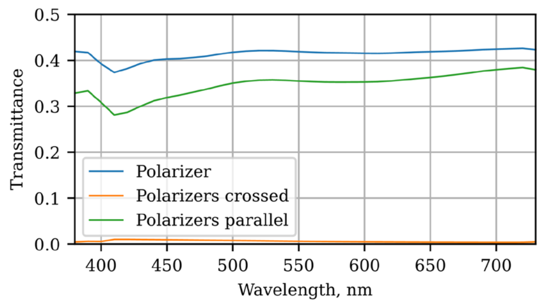

» **Figure 3:** *Spectral transmittance of one polariser and two polarisers with parallel and crossed transmission axes to compare declared and real transmittance*

Biaxially oriented isotactic polypropylene (BOPP) films with a thickness of 25±5 µm were used in experiments.

The mean spectral transmittance of 1 layer of BOPP film is 0.99. The birefringence of the BOPP film was obtained with spectral content analysis (SCA) method measuring spectral transmittance with crossed and parallel polarizers, but a costly polarimetric gate was replaced with the experimental setup using an X-Rite i1Pro (Slepkov, 2022b; Ajovalasit, Barone & Petrucci, 1998).

The retardance Γ produced by the birefringent sample depends on the distance d travelled by the light of wavelength λ in the sample (6).

From the literature it is known that under certain wavelength material can behave like a half-wave plate and this leads to the biggest difference in transmittance between parallel and crossed polarizers. One and two layers of BOPP films were used and two layers showed more visible difference in transmittance (Fig. 4) and based on the characteristics of film retardance is equal to 0.015.

$$\Gamma = \frac{2\pi\Delta n d}{\lambda} \tag{6}$$

where, Γ – retardance, Δn – birefringence, d – material thickness, λ – wavelength.

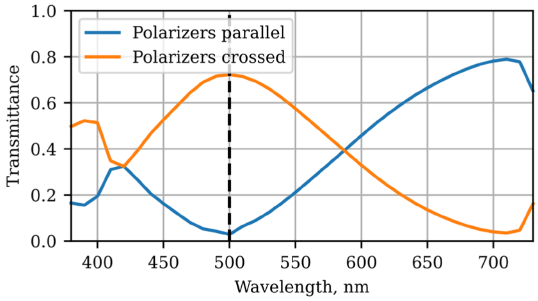

» **Figure 4:** *Spectral transmittance of two layers of BOPP films 25 µm between polarizers in parallel and crossed configurations. Polymer films oriented with their optical axis at 45° to the transmission axis of the input polarizer. Vertical dashed line at 500 nm marks where stack acts as half-wave plate*

Calculated birefringence matches with values in "Guideline for Using Light Microscopy in Forensic Examinations of Tape Components Scientific Working Group for Materials Analysis" in the range of 0.014- 0.016 and value in Table I of the article (Slepkov, 2022b).

Three gel colour filters red, green and blue were used in the experiment. Their spectral transmittance shown in figure 4.

These filters don't exhibit anisotropic properties as they don't show colour change in different angle between two polarisers. The other three filters are an ink layer on BOPP films of yellow, cyan and magenta colours printed by flexographic method (Fig. 5).

In the model they account as two optical elements one film layer and one colour filter.

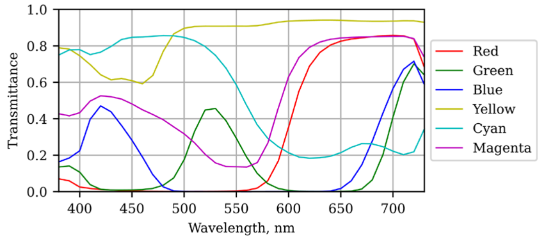

» **Figure 5:** *Spectral transmittance of gel colour filters (red, green, blue) and yellow, cyan, magenta colour patches on BOPP films 25 µm used in experiment*

Results

On this step the developed model was validated using stacks of BOPP films (25 µm thickness) 1-3 layers without additional colour layers in crossed and parallel polarizers. Stacks of BOPP films were oriented with their optical axis at 45° to the transmission axis of the input polarizer.

A comparison of the modelled and experimental spectral radiance is shown in Figure 6 and absolute root mean square errors (RMSE) values for the spectral radiance ranges from 0.34 to 1.01 for different layer configurations and polarizer orientations (Table 1). Maximum relative error is approximately 10%.

Table 1

Comparison of absolute RMSE in mW/(m²·sr·nm) between experimental and calculated spectral radiance for stacks of BOPP films with number of layers from 1 to 3 in parallel and crossed polarizers. Stacks of BOPP films were oriented with their optical axis at 45° to the transmission axis of the input polarizer

Layers	Polarizers	RMSE
1	Parallel	0.34
2		0.57
3		1.01
1	Crossed	0.50
2		0.66
3		0.95

The chromaticity diagram (Figure 7) illustrates the colour coordinates of samples with a varying number of BOPP layers under crossed and parallel polarizer configurations.

The experimental data points (circles) and model predictions (triangles) show reasonable correlation, particularly for single and double-layer configurations.

Colour difference ΔE_{76} in the CIELab colour space revealed values ranging from 3.2 to 22.5 between experimental and calculated data (Table 2).

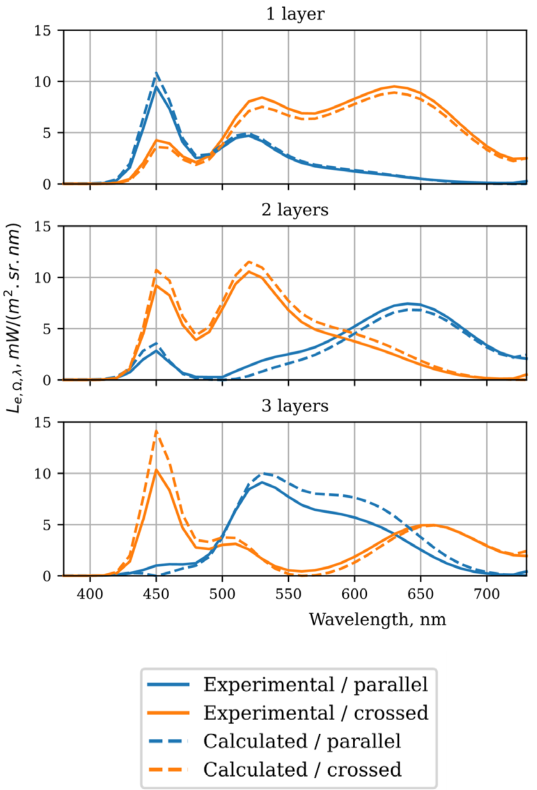

» **Figure 6:** *Spectral radiance comparison between experimental and calculated with the developed model for stacks of BOPP films with number of layers from 1 to 3 (25 µm per layer) under parallel and crossed linear polarizer configuration. Stacks of BOPP films were oriented with their optical axis at 45° to the transmission axis of the input polarizer*

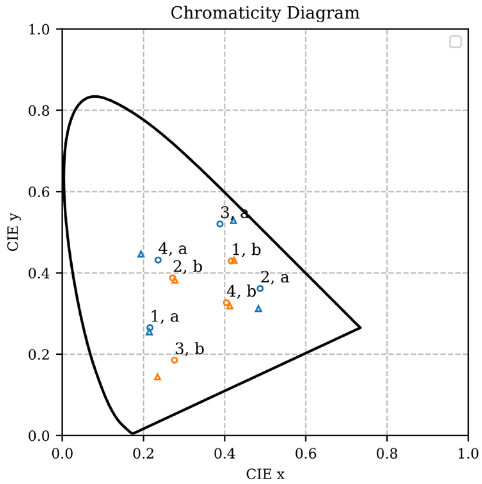

» **Figure 7:** *Chromaticity diagram with colours for 1-3 layer BOPP stacks (25 µm per layer) under parallel and crossed linear polarizer configuration. Stacks of BOPP films were oriented with their optical axis at 45° to the transmission axis of the input polarizer. Number on diagram specifies number of layers of BOPP, letter a is for parallel polarizers and b for crossed. Circles are for experimental data and triangles – calculated data*

The model showed agreement with experimental observations in reproducing the spectral features and overall radiance patterns. The lowest deviations were observed for single-layer samples, while increasing complexity with additional layers resulted in higher error values.

The model was also validated using stacks that included colour layers in crossed and parallel polarizers and stacks were placed at a 45° angle. Six different colour filters: yellow, cyan, magenta, red, green, and blue were tested in combination with 1-3 layers of BOPP films. Examples of two cases with green and cyan colour filters shown in Figure 8. They demonstrate the model's capability to predict the spectral shape and magnitude. The calculated data follow the experimental curves, capturing the characteristic features of the interference patterns.

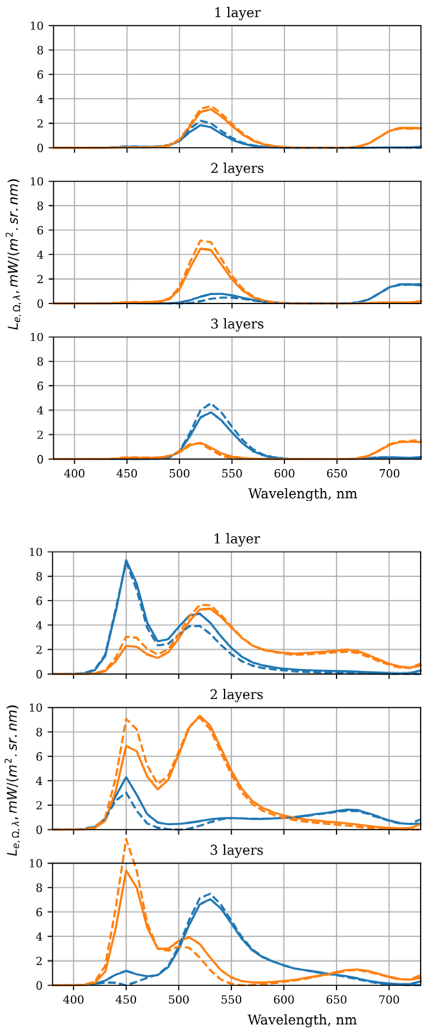

» **Figure 8:** *Spectral radiance comparison between experimental and calculated with the developed model for stacks of BOPP films with number of layers from 1 to 3 (25 µm per layer) under parallel and crossed linear polarizer configuration and green colour filter on the left and cyan filter on the right. Stacks of BOPP films were oriented with their optical axis at 45° to the transmission axis of the input polarizer*

Table 2
Comparison of CIELab coordinates for resulting colours for 1-3 layer BOPP stacks (25 µm per layer) under parallel and crossed linear polarizer configuration. Stacks of BOPP films were oriented with their optical axis at 45° to the transmission axis of the input polarizer and colour difference ΔE_{76} between experimental and calculated data

The mean absolute RMSE across all configurations was 0.27. Table 3 shows the absolute RMSE values for each colour filter and layer combination. The relative error is approximately 10%.

The colour prediction accuracy was evaluated using ΔE_{76} values in the CIELab colour space.

Layers	Polarizers	Experimental			Calculated			ΔE_{76}
		L	a	b	L	a	b	
1	Parallel	48.9	-14.0	-24.1	50.3	-11.5	-27.5	4.5
2		54.8	37.7	33.4	48.7	49.2	17.4	20.7
3		73.0	-29.7	70.0	78.3	-23.1	90.8	22.5
1	Crossed	77.4	2.7	49.7	74.7	4.3	50.5	3.2
2		71.3	-36.3	10.4	75.1	-33.9	10.3	4.5
3		42.1	40.5	-38.7	40.2	47.4	-56.3	19.0

Table 3
Comparison of absolute RMSE in mW/(m²·sr·nm) between experimental and calculated spectral radiance for stacks of BOPP films with number of layers from 1 to 3 in parallel and crossed polarizers and yellow, cyan, magenta, red, green and blue colour filters. Stacks of BOPP films were oriented with their optical axis at 45° to the transmission axis of the input polarizer

The overall mean colour difference across all tested configurations was 10.8 (Table 4).

Single-layer samples with crossed polarizers achieved the best performance (mean ΔE_{76} = 3.8), approaching the threshold for acceptable colour matching in many industrial applications.

Layers	Polarizers	RMSE						
		Yellow	Cyan	Magenta	Red	Green	Blue	Mean
1	Parallel	0.28	0.37	0.23	0.02	0.11	0.10	0.19
2		0.52	0.38	0.45	0.15	0.12	0.05	0.28
3		0.67	0.30	0.39	0.30	0.22	0.06	0.32
1	Crossed	0.35	0.25	0.34	0.10	0.09	0.06	0.20
2		0.44	0.57	0.15	0.17	0.20	0.13	0.28
3		0.58	0.67	0.41	0.17	0.07	0.33	0.37
Mean		0.47	0.42	0.33	0.15	0.13	0.12	**0.27**

Table 4
Comparison of colour difference ΔE_{76} for resulting colours for 1-3 layer BOPP stacks (25 µm per layer) under parallel and crossed linear polarizer configuration and 6 colour filters. Stacks of BOPP films were oriented with their optical axis at 45° to the transmission axis of the input polarizer. Mean values for each filter and layer combination are presented

The performance of the model can be contextualized using standard ΔE_{76} thresholds from colorimetry literature ΔE_{76} 2-4 is noticeable to most observers; and ΔE_{76} > 4 represents clear colour differences.

Layers	Polarizers	ΔE_{76}						
		Yellow	Cyan	Magenta	Red	Green	Blue	Mean
1	Parallel	3.0	12.2	7.3	0.8	6.5	9.3	6.5
2		16.5	9.6	12.4	3.8	20.7	6.5	11.6
3		19.1	17.1	24.1	9.1	9.4	23.5	17.0
1	Crossed	2.2	6.9	4.8	0.5	3.8	4.9	3.8
2		4.0	13.2	2.9	6.8	7.0	9.4	7.2
3		20.0	35.8	18.3	3.1	8.8	24.0	18.3
Mean		10.8	15.8	11.6	4.0	9.4	12.9	**10.8**

Discussion

The experimentally determined birefringence Δn of 0.015 for the BOPP films aligns well with published literature values. This result confirms the reliability of the measurement method, which utilizes a spectrophotometer commonly employed in the printing industry.

The model using Mueller calculus demonstrates predictive capability. With a mean absolute RMSE of 0.27 and mean colour difference ΔE_{76} of 10.8, the model's performance is sufficient for preview applications in packaging design. However, for critical colour matching applications requiring ΔE_{76} lower than 4, further optimization of the model is necessary.

A trend of decreasing accuracy was observed as the number of film layers increased. This can likely be attributed to the cumulative optical effects and increased complexity of interference patterns within multilayer systems. Single-layer samples under crossed polarizers showed the best ΔE_{76} of 3.8, while three-layer samples under parallel polarizers exhibited the largest difference ΔE_{76} of 18.3.

The model uses film thickness (d) as an explicit parameter in the phase retardance calculation (Equation 6). This allows accommodation of manufacturing thickness variations. However, the current measurement aperture of the used spectrophotometer is 4.5 mm and model validation reflects the averaged optical properties on plane. Direct comparison between model predictions and real BOPP films with spatially varying thickness requires an understanding of the rate of thickness change.

Future work should address several areas for model improvement. These include:
(1) investigating the effects of non-normal light incidence; (2) integrating the ink spectral collection system proposed by (Zhang et al., 2024); and (3) exploring neural network approaches to account for potential non-linear optical effects and improve predictive accuracy.

Conclusion

In this study, a Mueller calculus-based model was developed and validated for predicting the colour of multilayer BOPP systems. The model can predict spectral radiance and resultant colour for multilayer BOPP stacks under polarized light conditions with accuracy of an absolute mean RMSE of 0.27 mW/(m²·sr·nm) for spectral composition predictions and colour differences with mean ΔE_{76} of 10.8 across six chromatic filters.

While the theoretical framework is material-agnostic, all experimental validation and colour accuracy benchmarking reported herein are specific to BOPP films with 25 µm thickness.

This study demonstrates that birefringence in BOPP films can be determined using a standard spectrophotometer, thereby avoiding the need for a more costly polarimetric gate. The experimentally derived BOPP birefringence Δn of 0.015 is consistent with literature values for transparent films, indicating that the retrieval pipeline is physically grounded for anisotropic polymer films used for packaging.

The proposed model provides a practical basis for an intelligent colour-management system. Such a system would enable virtual prototyping of multilayer stacks under various conditions, reducing trial-and-error in product design and facilitating the development of security features visible only under polarized light.

While the current model shows promising results for BOPP films, future work should explore its applicability to other common packaging materials, such as PET and PE, and investigate the influence of different polymer orientation states.

Funding

This work was financially supported by the Moscow Polytechnic University within the framework of the grant named after Vladimir Fortov.

References

Ajovalasit, A., Barone, S. & Petrucci, G. (1998) A review of automated methods for the collection and analysis of photoelastic data. *The Journal of Strain Analysis for Engineering Design.* 33 (2), 75–91. Available from: doi: 10.1243/0309324981512832

Apyari, V. V., Dmitrienko, S. G., Batov, I. V. & Zolotov, Y. A. (2011) An Eye-One Pro mini-spectrophotometer as an alternative to diffuse reflectance spectrometer. *Journal of Analytical Chemistry.* 66 (2), 144–150. Available from: doi: 10.1134/S1061934811020043

Bass, M. (1995) *Handbook of optics*. 2nd ed. New York, McGraw-Hill.

Febriant, I. A., Widodo, A. S. & Faizin, A. (2023) The effectiveness of Canned Coffee packaging's graphic design elements in consumers' decision-making process. *Journal of Graphic Engineering and Design.* 14 (4), 5–12. Available from: doi: 10.24867/JGED-2023-4-005

Kondratov, A. P., Nikolaev, A. A., Nazarov, V. G., Vereshchagin, V. Y. & Volinsky, A. A. (2023) Design and multilevel structuring of shape memory polymers for pleochroism control. *Journal of Applied Polymer Science.* 140 (41). Available from: doi: 10.1002/app.54532

Li, X., Qiu, X., Yang, X., Zhou, P., Guo, Q. & Zhang, X. (2024) Multi-Modal Melt-Processing of Birefringent Cellulosic Materials for Eco-Friendly Anti-Counterfeiting. *Advanced Materials.* 36 (36). Available from: doi: 10.1002/adma.202407170

Linge Johnsen, S., Bollmann, J., Lee, H. & Zhou, Y. (2018) Accurate representation of interference colours (Michel–Lévy chart): from rendering to image colour correction. *Journal of Microscopy.* 269 (3), 321–337. Available from: doi: 10.1111/jmi.12641

Malešević, M. & Stančić, M. (2021) Influence of packaging design parameters on customers' decision-making process. *Journal of Graphic Engineering and Design.* 12 (4), 33–38. Available from: doi: 10.24867/JGED-2021-4-033

Mansencal, T., Mauderer, M., Parsons, M., Shaw, N., Wheatley, K., Cooper, S., Vandenberg, J. D., Canavan, L., Crowson, K., Lev, O., Leinweber, K., Sharma, S., Sobotka, T. J., Moritz, D., Pppp, M., Rane, C., Eswaramoorthy, P., Mertic, J., Pearlstine, B., Leonhardt, M., Niemitalo, O., Szymanski, M., Schambach, M., Huang, S., Wei, M., Joywardhan, N., Wagih, O., Redman, P., Goldstone, J., Hill, S., Smith, J., Savoir, F., Saxena, G., Chopra, S., Sibiryakov, I., Gates, T., Pal, G., Tessore, N., Pierre, A., Thomas, F.-X., Srinivasan, S., Downs, T., Rusching, K., Chen, X., Herb, B., Caswell, T. A., Collod, L. & Brummer, B. (2024) *Colour 0.4.6* [Software]. Available from: doi: 10.5281/zenodo.13917514

Meurer, A., Smith, C. P., Paprocki, M., Čertík, O., Kirpichev, S. B., Rocklin, M., Kumar, A., Ivanov, S., Moore, J. K., Singh, S., Rathnayake, T., Vig, S., Granger, B. E., Muller, R. P., Bonazzi, F., Gupta, H., Vats, S., Johansson, F., Pedregosa, F., Curry, M. J., Terrel, A. R., Roučka, Š., Saboo, A., Fernando, I., Kulal, S., Cimrman, R. & Scopatz, A. (2017) SymPy: symbolic computing in Python. *PeerJ Computer Science.* 3, e103. Available from: doi: 10.7717/peerj-cs.103

Samadi-Dooki, A., Lamontia, M. A., Londoño, J. D., Williamson, C., Burch, H. E., Yahyazadehfar, M., Carbajal, L. A. & Kourtakis, K. (2024) Effect of Chain Orientation on Coupling of Optical and Mechanical Anisotropies of Polymer Films. *Coatings.* 14 (6), 764. Available from: doi: 10.3390/coatings14060764

Slepkov, A. D. (2022a) Painting in polarization. *American Journal of Physics.* 90 (8), 617–624. Available from: doi: 10.1119/5.0087800

Slepkov, A. D. (2022b) Quantitative measurement of birefringence in transparent films across the visible spectrum. *American Journal of Physics.* 90 (8), 625–634. Available from: doi: 10.1119/5.0087798

Tomiša, M. & Vusić, D. (2019) Deviations of Spot Colorimetric Values on Multi-layered Flexible Packaging during the Graphic Reproduction and Sterilisation Process. *Technical Gazette.* 26 (2). Available from: doi: 10.17559/TV-20190119234822

del Toro Iniesta, J. C. (2003) *Introduction to Spectropolarimetry*. Cambridge, Cambridge University Press. Available from: doi: 10.1017/cbo9780511536250

Zhang, W., Liu, X., Zhang, R., Jiang, F., He, J. & Fang, S. (2024) Design of printing ink spectral collection system and research on ink proportion prediction method. *AIP Advances.* 14 (4). Available from: doi: 10.1063/5.0186340

Original scientific paper http://doi.org/10.24867/JGED-2026-3-019

Design recommendations and future prospects for text legibility in augmented reality

ABSTRACT

This paper provides a systematic review of the literature on text legibility in augmented reality (AR) using the PRISMA methodology, with an emphasis on head-mounted displays (HMD) and screen devices. Based on the literature review, we propose design recommendations for legibility in AR. The analysis was carried out using the 10 most important parameters: font type, text style, color and contrast, font size, text anchoring, text segmentation and organization, environmental illumination, background influence, perception depth, and text display in dynamic environments. The analysis shows that billboard and outline styles and light fonts on a dark background ensure the most reliable legibility. For static information, world-anchoring is recommended, and for dynamic information, screen-anchoring is advised. Level-of-Detail (LOD) approaches are shown to reduce cognitive load. Specialized fonts (e.g. SharpView) and adaptive algorithms that adjust the contrast, size and position of text in real time are also examined. The results indicate a marked dominance of research on HMD devices, although screen AR has great practical importance and requires more research. Regarding other research directions, the review noted hybrid approaches (HMD + smartphone), projection AR, and hardware/software upgrades such as colorimetric compensation and text position stabilization. Research on text legibility in AR for 3D text, text segmentation, and dynamic real-world scenarios remains underdeveloped. Future advances in text legibility in AR are related to the integration of typographical, perceptual and technical solutions, and reporting harmonization.

Ana Jović
Ivana Žiljak Stanimirović
Miroslav Mikota
Lidija Mandić

University of Zagreb,
Faculty of Graphic Arts,
Zagreb, Croatia

Corresponding author:
Ana Jović
e-mail:
ajovic@grf.hr

First received: 2.10.2025.
Revised: 25.12.2025.
Accepted: 4.2.2026.

KEY WORDS
text legiblity, legibility parameters, augmented reality, mixed reality, design recommendations

Introduction

The purpose of the written word is to convey information, and this is only made possible by legible letters. Legibility refers to the reader's ability to recognize individual letters and the word that certain letters make up, while readibility or reading comfort has different meanings for researchers, but most often refers to how easily the text is understood and how pleasant it is to read (Richardson, 2022; Mills & Weldon, 1987). This ability depends on various factors such as letter shape, size, word letter spacing, line spacing, contrast, and lighting.

In this work, the focus in on legibility, but we also consider literature that involves readability in cases where the authors actually refer to legibility.

The advent of augmented reality (AR) in the early 2000s marked the beginning of a new type of technology, with its advantages and disadvantages. New research questions about text legibility were raised as soon as certain devices that enable AR became openly available. Augmented reality combines the real and virtual worlds by adding digital elements such as image, sound, video, and touch to the real environment in real time.

Unlike virtual reality (VR), which fully immerses the user in the virtual world, AR complements reality without complete replacement (Rampolla & Kipper, 2013). AR mainly uses head-mounted displays (HMDs) (such as smart glasses), but also smartphones and tablets to display information that integrates with the user's environment. The main challenge in an AR environment is to ensure the legibility of text despite changing conditions such as ambient light, complex backgrounds, and the user's distance from virtual elements.

In recent research, the term mixed reality (MR) is increasingly accepted as a more precise framework for describing digital systems that connect the real and virtual worlds. Although AR and MR are often used interchangeably, the term MR has a broader meaning that includes positioning virtual content in a space, interacting with the user in real-time, and adjusting the display according to the user's perspective.

The reality-virtuality taxonomy was introduced by Paul Milgram and his associates back in 1994 (Milgram & Kishino, 1994), and it was explained in detail by Dörner (Dörner et al., 2022). According to this approach, AR and augmented virtuality (AV) represent two extremes within a single continuum, while MR encompasses all forms in which virtual and real content mix and interact with each other, as shown in Figure 1. However, as the vast majority of related research uses the term AR in the context of MR, this one will also use the term AR, implying that AR actually encompasses the MR terminology.

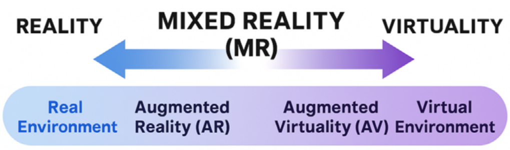

» **Figure 1:** *Mixed reality continuum, modified from Ko, Chang & Ji (2013)*

This paper includes the study of readability parameters for AR/MR when using mostly optically see-through (OST) HMD devices and screen devices. The paper does not consider readability in VR.

Based on the search of the Scopus database, Figure 2 shows how the number of research papers on AR and research papers on AR together with legibility have been increasing over the last 15 years. This clearly suggests that the field of AR and text legibility is still evolving and requires careful consideration.

The AR environment extends the methods of assessing the legibility of text used for text on paper and text on the screen. Large number of methods of assessing the legibility remains the same, such as measurements of the speed and accuracy of reading text and subjective assessments through a questionnaire (Richardson, 2022). However, some of the methods require adjustments. For example, the eye-tracking method is influenced by the depth factor in relation to the placement of the text. The eye dynamically adjusts to the difference in depth between the representation of text and objects in the scene, causing eye fatigue (Gabbard, Mehra & Swan, 2019). Also, the experimental manipulation of typographic elements must take into account the additional dimension of the display, which is reflected in the choice of text anchoring and the location of the text.

For this reason, new fonts and algorithms adapted to AR technologies are being tested, such as the SharpView font that optimizes legibility with unfocused text displays in AR systems (Arefin et al., 2024).

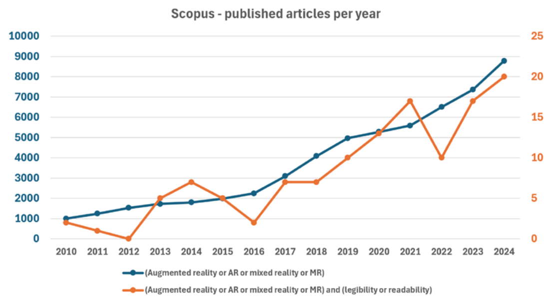

» **Figure 2:** *Search results of the Scopus database for scientific articles dealing with AR (blue) and AR with legibility or readability of text (orange)*

In this paper, we bring an overview of the literature on the topic of legibility of text in AR. This paper is an extension of the conference work (Jović, Mikota & Mandić, 2025). Instead of five, this paper examines ten legibility parameters using the PRISMA methodology for literature review (Page et al., 2021) and details design recommendations for HMDs and also for screen devices.

We note that other relevant review papers in this area are Erickson et al. (2020), Gattullo et al. (2022), and Cauz, Clarinval & Dumas (2024). In their work, Erickson et al. (2020) conducted a systematic review of visual perception in OST HMDs, analyzing 14 key papers with a focus on textual enhancements (billboard, outline, shadow), color and contrast, ambient lighting, color mixing, text location and size, and user demographics. Their paper provides an overview of research gaps and recommendations for the design of user interface (UI) elements on OST HMDs, but in the broader context of visual perception.

Our paper specializes in the legibility of the text and provides systematic design guidelines for legibility based on the PRISMA methodology. Gattullo et al. (2022) conducted a systematic review of visual assets in industrial AR applications for maintenance, installation, and staff training.

Their work classifies visual elements according to what they depict (text, photograph, video, sign, auxiliary model, drawing, technical drawing, product model), how they convey information (frame of reference, color coding, animation) and why they are used (locating, operating, checking, warning). Their work confirms the growth of AR adoption in industry, but Gattullo et al. (2022) primarily analyze the broader taxonomy of visual elements in industrial AR, while our work focuses on a detailed analysis of text legibility on HMDs and screen devices.

Cauz, Clarinval & Dumas (2024) conducted a comprehensive multivocal review of text legibility in AR and VR, including gray literature. In their study, they focused on seven legibility parameters: color and contrast, text drawing style, font type, font size, anchor, position, and text layout and segmentation. They offered two decision tree models for selecting the right text drawing style, text color, anchor and position for a text.

However, unlike them, our work excludes VR displays, focuses on HMD devices and screens, and brings a more systematic overview based on the PRISMA methodology with an analysis of ten key parameters of text legibility.

The contributions of this paper include:

1. systematic review of the literature on text legiblity in AR based on the PRISMA methodology,
2. design recommendations for ten most commonly studied parameters of text legibility on HMDs and screen devices,
3. an overview of other observed research directions that are related to legibility.

Section 2 presents the PRISMA guidelines applied to the literature review on legibility in AR. Section 3 provides a literature review and highlights design recommendations for the studied legibility parameters. Section 4 discusses the results and provides an overview of other research directions. Section 5 presents the conclusions of the study.

Methodology

A review of the Web of Science (WoS) and Scopus databases was conducted systematically using the PRISMA methodology (Page et al., 2021). The review was conducted in three phases: Identification, Screening, and Include, as shown in Figure 3.

The criteria used to exclude and include articles are listed in Table 1.

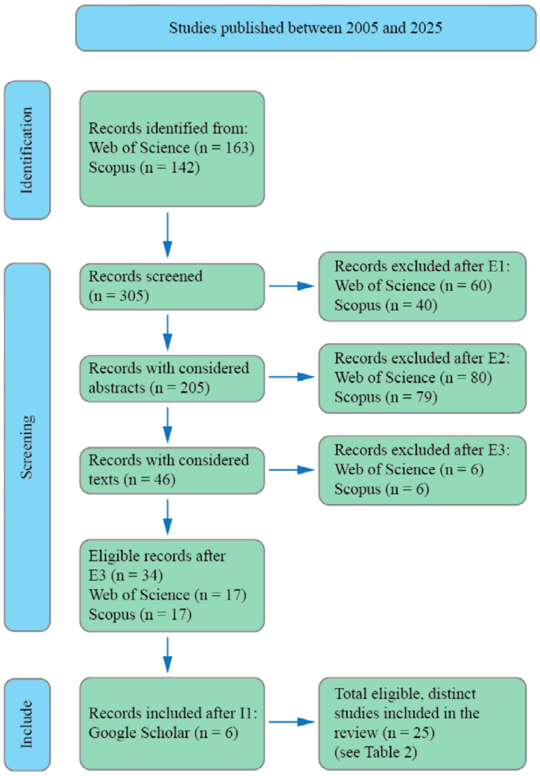

» **Figure 3:** *PRISMA methodology for the systematic review of related work*

Table 1

Exclusion and inclusion criteria for the related work

No.	Exclusion and inclusion criteria
E1	Papers with unrelated research areas (e.g. medicine, chemistry, cartography, electrical engineering), retracted papers, papers dealing with AR hardware
E2	Papers not directly related to text legibility (including only text readability related papers), VR only papers, head-up display (HUD) only papers, papers in which text legibility is only a secondary topic, papers related to methods for contrast enhancements and occlusion reduction
E3	Papers with specific text legibility applications (e.g. non-Latin characters legibility, legibility on lunar surface), conference papers with the same topic later published in a scientific journal
I1	Papers cited in review papers from related work (see Section 1) that are indexed in Google Scholar, with the topic of text legibility and which may not be excluded based on E1, E2 or E3 criteria

At the beginning of the identification phase, the Query string "(augmented reality or AR or mixed reality or MR) and (legibility or readability)" was used in the WoS and Scopus databases.

The studies are limited to English and include original scientific and review articles. Studies ranging from 01/01/2005 to 01/09/2025 were included. 163 articles have been identified in the WoS database, and 142 in the Scopus database.

In the screening phase, in the first elimination step (E1), which included an overview of titles and keywords, articles were removed from those areas of research that are not related to the legibility of text in mixed reality, such as medicine and chemistry; articles that have been retracted and articles that deal exclusively with hardware topics in mixed reality. This eliminated 60 articles in WoS and 40 articles in Scopus.

Then, the summaries of the remaining abstracts were reviewed, and in the next step E2, those papers that were not directly related to legibility or included VR, HUD and other related but not direct topics for legibility in mixed reality were eliminated.

In the last step of exclusion (E3), the entire texts of the papers were considered and those papers that have a specific application for legibility and are therefore not widely applicable were removed. Also, the conference versions of the papers that were later published in the journal were removed.

In the last phase of inclusion, the review papers mentioned in Section 1 (Erickson et al., 2020; Gattullo et al., 2022; Cauz, Clarinval & Dumas, 2024) were additionally considered and the papers cited in them underwent the same review with the same elimination criteria (E1 – E3) and the final list of papers included those indexed in the Google Scholar database.

Since the Google Scholar database does not allow searching for multiple keywords with logical conditions as the WoS and Scopus databases allow, it was not possible to conduct the same detailed search for the entire Google Scholar database.

However, by considering the WoS and Scopus databases and additional consideration of the papers cited in the reviews, all studies relevant to this topic were taken into account.

The final list includes 25 studies, 15 of them common to WoS and Scopus, 2 different ones for these two databases WoS: Kruijff et al. (2019), Erickson et al. (2021); Scopus: Gabbard et al. (2007), Jankowski et al. (2010) and 6 studies from Google Scholar.

We note that all articles considered in the screening phase after the first elimination (E1) were considered for other research directions (Section 4), including the articles cited in review papers.

Literature review on augmented reality legibility

Introduction to the considered literature

The evolution of augmented reality text rendering shows that legibility is the result of the interaction of optics, environmental conditions, and typographic decisions. Systematic reviews and experimental work suggest that most research is still conducted under controlled, static conditions, although environmental dynamics (user movement, background and light changes) significantly alter perception (Cauz, Clarinval & Dumas, 2024). In newer approaches, adaptive algorithms and eye perspective control to maintain contrast and avoid occlusion are increasingly prominent (Emsenhuber et al., 2023). Since AR is becoming more and more present in various fields such as industry, education, medicine and entertainment (Mekni & Lemieux, 2014), research dealing with the legibility of a text and its accompanying concept of readability is becoming more common (Gattullo et al., 2022).

The ten most frequently investigated parameters of legibility according to literature, which we analyze in this work are: font type, text style, color and contrast, font size, text anchoring, text segmentation and organization, environmental illumination, background influence, perception depth, and text display in dynamic environments. This review summarizes the consensus and divergence on these legibility dimensions and derives practical design guidelines.

In Table 2, we present 25 studies that were selected based on the PRISMA metodology. The field is dominated by HMD studies: 20 out of 25 (~80%) are focused on OST/VST HMD, while 5 out of 25 (~20%) are focused on screen. This imbalance is expected because AR-specific phenomena (e.g., additive color mixing in OST, vergence-accomodation (VA) conflict) require testing on HMD. However, given the prevalence of handheld/screen AR, it makes sense to encourage more systematic research on screen as well, especially in dynamic scenarios.

Table 2 (part 1)
Prevalence of HMD and screen methodologies in the included studies

HMD	Screen	Author
x		Cauz, Clarinval & Dumas (2024)
x		Arefin et al. (2024)
x		Emsenhuber et al. (2023)
x		Wysopal et al. (2023)
x		Erickson et al. (2021)
x		Falk et al. (2021)

Table 2 (part 2)
Prevalence of HMD and screen methodologies in the included studies

HMD	Screen	Author
	x	Cardenas et al. (2021)
x		Fukushima, Hamada & Hautasaari (2020)
x		Erickson et al. (2020)
	x	Sawyer et al. (2020)
x		Kruijff et al. (2019)
x		Kim et al. (2019)
	x	Sonderegger et al. (2019)
x		Gabbard, Mehra & Swan (2019)
x		Merino, Bergel & Nierstrasz (2018)
x		Manghisi et al. (2017)
x		Vairinhos, Almeida & Dias (2016)
x		Gattullo et al. (2015a)
x		Gattullo et al. (2015b)
x		Debernardis et al. (2014)
	x	Dao & Gabbard (2013)
x		Fiorentino et al. (2013)
	x	Jankowski et al. (2010)
x		Gabbard et al. (2007)
x		Gabbard, Swan & Hix (2006)

In the forthcoming subsection we present an overview of the research on legibility by the key parameters.

Overview of legibility research by parameters

The ten legibility parameters considered in this review represent recurring dimensions through which text perception in augmented reality has been empirically studied. Each parameter captures a specific aspect of how virtual text is rendered, perceived, and interpreted within real-world environments. In continuation, we first define the ten legibility parameters considered in this work.

Font type refers to the typographic design of letterforms, including serif and sans-serif distinctions as well as purpose-designed AR fonts. In AR contexts, font type primarily affects character recognizability under conditions of limited resolution, reduced contrast, and variable focus, rather than aesthetic preference alone. Text style describes the graphical treatment used to separate text from the background, such as plain text, billboard, outline, or drop shadow, as well as 2D versus 3D representations. This parameter is used for improving background interference and maintaining sufficient contrast in visually complex environments. Color and contrast address the relationship between text color and text background, including polarity (light-on-dark vs. dark-on-light) and color selection. In AR, this parameter is influenced by display technology (OST vs. VST) and ambient illumination, directly affecting visibility, visual fatigue, and reading accuracy. Font size defines the physical or angular dimensions of text as perceived by the user. In AR, font size interacts with viewing distance, field of view, and device resolution, and is often dynamically adjusted to preserve legibility across spatial contexts. Text anchoring specifies the spatial reference frame of text placement, such as world-anchored, screen-anchored, or body-anchored positioning. Anchoring influences reading stability, cognitive load, and naturalness of interaction, particularly during user movement.

Text segmentation and organization encompass line length, line spacing, hierarchical structuring, and progressive disclosure of information. These properties affect reading speed and cognitive effort and are especially relevant when presenting multi-line or task-related information in AR. Environmental illumination refers to the level and distribution of ambient light in the physical environment. Illumination affects perceived contrast, particularly in OST displays, where virtual content competes with real-world luminance. Background influence captures the visual complexity, texture, and color variability of real-world surfaces behind the text. Uncontrolled or highly textured backgrounds may degrade legibility. Perception depth relates to the spatial distance at which text is rendered relative to the user and surrounding objects. Depth differences between virtual text and real content can induce VA conflict, affecting visual comfort and reading performance. Text display in dynamic environments addresses changes in text presentation under conditions of user movement, background motion, or varying lighting.

An overview of research on the legibility of font types in augmented reality

The choice of typeface is one of the first typographic factors considered in the AR context. Early work focused on comparing serif and sans-serif typefaces, but the findings in AR suggest that the simplicity of form and the avoidance of overly elaborate details may be more crucial than the typeface itself, especially under conditions of variable focus and contrast. In addition, specialized AR fonts appear that target reading outside of optimal focus. Cardenas et al. (2021) showed that no significant difference in readability was found between Arial, Times New Roman, Georgia, and Verdana fonts in the older population. Cauz, Clarinval & Dumas (2024) point out that fonts with too much detail should be avoided and that there is no consensus about the superiority of serif or sans-serif; in practice, Arial (sans-serif) is often used as the standard. Arefin et al. (2024) developed a specialized SharpView font for out-of-focus reading, which shows 24–44% better sharpness results compared to Arial; the findings suggest the benefit of purpose-designed AR fonts, with the need for further empirical verification.

An overview of research on the text style legibility in augmented reality

The text display style (plain, billboard, outline, drop shadow; 2D or 3D) directly determines the visibility of letters on changing, often complex AR backgrounds. Most works record gains in legibility when the text is separated from the background by a billboard or outline/drop shadow, with caution due to potential occlusion and loss of context. In practice, the parameters of opaque (opaque vs. transparent), polarity (light on dark vs. dark on light) and adaptive approaches (e.g. LOD) are also examined, while 3D variants of text are under-researched.

Gabbard, Swan & Hix (2006) showed that the billboard performed best on different backgrounds compared to plain text, while Gabbard et al. (2007) showed that drop shadow and outline improve legibility and the billboard was not the most effective due to poor color contrast control. Jankowski et al. (2010) found that negative polarity speeds up reading. The best results were obtained for billboard, medium for anti-interference (contrast outline) and drop shadow, while the weakest results were obtained for plain text.

According to Fiorentino et al. (2013), a billboard is the best option for legibility (black text on a white background), but shows the problem of occlusion. In the context of this paper, plain text, outline, and a combination of outline and billboard were also tested. In a short review study, Dao & Gabbard (2013) found that a high-contrast billboard is most commonly used on handheld displays, whereas in some studies drop shadow is used for text emphasis. Debernardis et al. (2014) found that a billboard significantly outperforms plain text, and the recommendation is blue billboard and white text with good contrast (for OST and VST HMD devices). Gattullo et al. (2015b) showed that in OST at lighting that is ≤1,000 lux plain white text is the most legible on a dark background, while billboard is most legible on a light background. At 4,000 lux OST is unusable; for VST 1,000–4,000 lux black plain text on a light background is the most legible, optionally 1 px white outline may be used (the billboard is also good, but increases occlusion).

Vairinhos, Almeida & Dias (2016) indirectly established that 2D text is subjectively more legible than 3D (embossed, wireframe), using the Arial font. Research by Kruijff et al. (2019) showed that along with black text, blue billboard is most often preferred for OST and VST, while for VST, the next preferred billboard color is green. Sawyer et al. (2020) showed that on complex backgrounds, drop shadow gives the best results; outline is effective when the text is bold (tested on screen, transferable to AR). According to Erickson et al. (2020), a billboard generally improves legibility, however, dynamically matching the billboard's colors to its surroundings can degrade reading performance.

Falk et al. (2021) found that an opaque (solid) billboard is more readable than a transparent one (50%). This was tested on OST HMD devices. Wysopal et al. (2023) used a LOD system that dynamically adjusts the display according to angle/distance. The billboard was dominantly used for the display of text. According to Cauz, Clarinval & Dumas (2024), billboard and outline most often increase legibility, while there is no need to combine them at the same time.

An overview of research on text color and contrast in augmented reality

Color and contrast determine the visibility and visual pleasingness of text in AR, especially due to the differences between OST and VST systems and changing lighting conditions. In the literature, the polarity of the display (the relationship between the color of the text and the background), the choice of text/background color and the effect of dark mode on sharpness and fatigue are most often examined. The findings suggest that brighter, cooler colors and high, stable contrast generally make it easier to read, but the optimal combinations depend on the type of device and lighting.

According to Gabbard, Swan & Hix (2006), green gives the best legibility results for plain text and they recommended avoiding red. Later, Gabbard et al. (2007) found that white, cyan, and green are more effective than red on OST HMDs. Similarly, Fiorentino et al. (2013) showed that, in industrial settings, plain red text is weaker than black, white and green and that the combination of white billboard and black text gives the best legibility results in industrial conditions. On handheld displays, according to Dao & Gabbard (2013), saturated, high-contrast colors (red, neon green, yellow) are recommended for plain text to make it stand out over unpredictable backgrounds. According to Debernardis et al. (2014), white text on a blue billboard, with good contrast, shows the best legibility in most situations. Similar results were obtained by Kim et al. (2019), who showed that dark background and light letters increase accuracy and reduce fatigue while reading. Erickson et al. (2020) found that using red color usually leads to unfavorable results on OST devices, while blue, green, and white are more reliable. They also showed that, for OST HMDs, negative contrast (dark background, light letters) is more favorable than the positive contrast. Likewise, Erickson et al. (2021) found that dark mode (dark background, light letters) on the HoloLens device increases sharpness and subjectively positive reading experience in low light (10–12 lux). Falk et al. (2021) showed that for OST HMDs, higher reading accuracy is given by the positive polarity of the text (blue text on a white background). Lastly, Cauz, Clarinval & Dumas (2024) found that bright colors (white, cyan, green) are more visible on the OST HMD devices, while black loses visibility. On the VST HMDs, high contrast helps, but too strong constrast can cause discomfort.

An overview of font size research in augmented reality

The font size directly determines the threshold for the visibility of letters in AR, especially when the contrast is low and/or read at greater distances. In the literature, the size is expressed in different units (mm/dmm, pt, visual angle, "Unity units"), and the common pattern is: larger font = better legibility, with the need for dynamic scaling according to distance and position of text in the field of view (central vs. peripheral).

Kruijff et al. (2019) found that larger fonts are preferable in the peripheral field of view, with size expressed in degrees of field of view (small/medium/large). Erickson et al. (2020) recommended using a sign height of approximately 2 inches (~50 mm) at a distance of about 2 m, with further increase for longer distances. Cardenas et al. (2021) reported that sizes of 8/10/12/14 pt on the screen significantly affected legibility, with 14 pt being the most preferred size. According to Falk et al. (2021), in a three-level test (20/30/40 "Unity" units) on the Vuzix device, the smallest size resulted in the fastest reading, while on the Moverio device, the size had no significant effect. Wysopal et al. (2023) showed that autoscaling (LOD) by distance increases legibility and reduces display clutter. According to Cauz, Clarinval & Dumas (2024), font size recommendations in AR are quite diverse, approximately 5–17 dmm for OST and 26–40 dmm for VST, and increasing the size is particularly helpful in low-contrast conditions.

An overview of research on text anchoring in augmented reality

Anchoring determines how the text is placed in relation to the user and the environment. It directly affects legibility, cognitive load, and naturalness of movement. In practice, anchoring is chosen according to the type of information and context: stable, "spatial" messages seek a peaceful reference in the world, while status/HUD information needs constant availability in the field of view.

Merino, Bergel & Nierstrasz (2018) warned that an insufficiently stabilized (non-fixed) world-anchored text can cause legibility problems, which highlights the importance of quality displacement tracking and filtering. Fukushima, Hamada & Hautasaari (2020) show that world-anchored text leads to faster reading, fewer errors and lower mental effort, while screen-anchored text increases cognitive load, slows down reading and promotes unnatural head posture. The research showed that participants walked more naturally when using world anchor. According to Cauz, Clarinval & Dumas (2024), a screen-anchored text is recommended for dynamic information, while a world-anchored text is more suitable for static content. When walking, a body-anchored text often proves to be more suitable than the screen-anchored text.

An overview of research on text segmentation and organization in augmented reality

Segmentation (line length) and typographic organization (line spacing, hierarchy of information) of text directly affect reading speed and cognitive load in AR. The general pattern from the literature suggests that shorter lines and clear inter-line spacing make it easier to track, while progressive content detection and depiction (Level-of-Detail, LOD) helps to dose information according to context – distance and task.

Sonderegger et al. (2019) showed that a modular (LOD) structure on screens increases the flexibility of access to information and makes it easier to focus attention on the requested data. According to Falk et al. (2021), a comparison of one, two, and three lines confirms that a multiline layout (fewer words per line, up to three lines) is faster to read, while a single-line, long text display is the most inefficient one. Wysopal et al. (2023) showed that an LOD organization hides less important information over longer distances and displays details when the user is closer, thereby reducing clutter and maintaining legibility. According to Cauz, Clarinval & Dumas (2024), shorter lines of text and sufficient line spacing are recommended for better legibility, noting that these parameters are still poorly researched in AR and require additional validation.

An overview of research on the impact of environmental illumination on text legibility in augmented reality

Enivornmental illumination (lighting) directly determines the perceived contrast between text and background in AR and therefore affects OST and VST systems differently. On the OST, stronger ambient light easily "washes out" the virtual display, while VST uses auto exposure, and therefore maintains contrast at higher light levels better, but loses quality in the dark. The optimal combinations of color/polarity and text styles change with the lighting level.

Gabbard, Swan & Hix (2006) showed that in the range of ~2,000–20,000 lux, the differences in legibility between the text styles are small at lower lighting, but increase with the increase in light above ~3,000 lux where the billboard is best, followed by green plain text, while red plain text is the weakest. Gattullo et al. (2015b) stated that for OST HMDs up to ~1,000 lux it is better to use light text on a dark background or a billboard on a light background, while at ~4,000 lux the OST devices become practically unusable due to very high errors. For VST, the usability for text legibility is similar at ~1,000 and ~4,000 lux. Gattullo et al. (2015a) found that at ~400 lux (indoor conditions) white text on a blue billboard is the most legible, with the results for 1,000 and 4,000 lux coincide with the previous work. Kim et al. (2019) found that there is a strong influence of lighting on the OST HMDs and that there is a dark mode preference in darker conditions. Erickson et al. (2020) point out that on the OST HMDs, the increase in ambient lighting negatively affects legibility as it reduces the contrast between virtual elements and the physical background. According to Erickson et al. (2021), there are fewer errors at 200–270 lux than at 10–12 lux (narrowed pupil increases sharpness) and, in the dark, users prefer dark mode. Falk et al. (2021) showed that at approximately 500–1075 lux (office/cloudy day conditions), legibility is better than at 20–50 lux, with low light making it difficult to search for and read text. According to Cauz, Clarinval & Dumas (2024), on OST HMD devices, a brighter environment reduces legibility due to a drop in contrast, while on VST HMDs, automatic brightness adjustment helps maintain visibility, although low light degrades the display.

An overview of research on the influence of background on text legibility in augmented reality

The background in AR is often unpredictable and textured, which directly affects the perceived contrast and reading speed. The literature shows that monochrome/neutral surfaces and consistent lighting make it easier to read, while complex, colorful or wooded backgrounds reduce legibility. When the background cannot be controlled, background treatments (e.g., solid billboard) and filters to mitigate complexity (blur/scrim) are helpful.

Gabbard, Swan & Hix (2006) showed that in the best reading options (billboard, green plain text), the influence of the background is largely neutralized. Gabbard et al. (2007) stated that a brick background produces the most errors, while a monotonous bright building (consistent lighting) is the most favorable for text legibility. Jankowski et al. (2010) found no difference in legibility between a city video and a 3D video game, suggesting that the type of dynamic background is less important than text treatment or contrast. Fiorentino et al. (2013) pointed out that a neutral background (e.g., a motorblock) allows for the fastest processing of information. Debernardis et al. (2014) showed that, on OST HMD devices, a dark background improves legibility, while on VST HMDs, the contrast is crucial, not the color itself. Manghisi et al. (2017) confirmed that textured backgrounds reduce legibility even with optimal contrast. Sawyer et al. (2020) reported that Gaussian blur and scrim ≥ 30% have the best effect on complex backgrounds (findings from screen devices, transferable to AR). Falk et al. (2021) found that monochrome backgrounds have better legibility than abstract/colorful ones. Erickson et al. (2021) show that dark mode is preferred on both uniform and noisy, gray backgrounds, with noise further distorting the results, especially at higher illumination. According to Cauz, Clarinval & Dumas (2024), complex texture and low contrast impair legibility.

An overview of research on the impact of perception depth problems in augmented reality

Depth perception in AR is closely related to vergence–accommodation conflict: the user often reads virtual text at one optical depth while simultaneously observing physical objects at another. Such separation of focus can increase effort, slow down reading and increase eye fatigue. Therefore, the choice of text depth and display format (2D vs. 3D) have direct consequences on legibility and comfort.

Gabbard, Swan & Hix (2006) showed that varying text distances of 1, 2, and 4 m with uniform size did not significantly affect legibility, suggesting that moderate depth shifts alone may not degrade reading when the text size is adequately scaled. Vairinhos, Almeida & Dias (2016) found that distance estimation for 3D text (embossed/wireframe) is somewhat weaker than for 2D text, suggesting the advantage of 2D text display for precisely positioned information. Gabbard, Mehra & Swan (2019) showed that switching focus between real and AR-displayed text accelerates eye fatigue and degrades reading performance, especially when the differences in distance are greater. According to Cauz, Clarinval & Dumas (2024), vergence–accommodation conflict was highlighted as a central problem when reading in AR; the recommended text depths in the literature are in range of 1–10 m, with the optimal depth depending on the type of text and the usage scenario.

An overview of research on text display in dynamic augmented reality environments

In dynamic AR scenarios (user movement, background and lighting changes), legibility depends on the system's ability to adjust the display – color, contrast, size, and position of text in real time, and to avoid overlapping with the background. Although many studies were conducted in static conditions, the studies that address dynamics show clear guidelines for adaptive representation.

Gabbard et al. (2007) showed that a system that samples the background and selects the accent style (billboard/outline/drop shadow) can help, but it is necessary to ensure a sufficiently strong contrast between the text and the selected style to avoid color similarity and consequently poorer legibility. Kruijff et al. (2019) reported that for text highlighting, blinking is the most effective motion type for OST HMD displays, while circular motion is optimal in VST HMD environments. They also showed that background motion is not crucial for the choice of motion type. Emsenhuber et al. (2023) showed that eye-perspective view management (EPR-VM) outperforms static display and camera-guided repositioning (Baseline, HMD-VM) because it reduces overlap, double vision, and contrast loss, thereby improving legibility on OST HMDs.

Wysopal et al. (2023) introduced a LOD approach that dynamically doses/scales text according to distance and viewing angle, thereby maintaining legibility without display clutter. According to Cauz, Clarinval & Dumas (2024), real-time adjustment of color and contrast in relation to changing lighting and background is necessary, as many earlier studies were performed under static conditions, while dynamic scenarios significantly alter perception.

Recommendations for parameter design based on the considered literature

From the reviewed articles, design recommendations that ensure the best text legibility in AR can be established. Table 3 shows the recommendations, specifically divided depending on whether an HMD or a screen device is used.

Table 3 (part 1)

Design recommendations for font type, text style, color and contrast, font size, text anchoring, text segmentation and organization, environmental illumination, background influence, perception depth, and text display in dynamic environments

Parameter	Design recommendations	Used literature
Font type	HMD: For optimal legibility, use simple sans-serif fonts (e.g., Arial, Verdana) and avoid decorative ones; when the text is out of focus, apply specialized AR fonts (e.g., SharpView). SCREEN: On classic screens, there is no clear advantage of serif or sans-serif; Arial is a safe standard, and Arial, Times New Roman, Georgia, and Verdana offer comparable legibility, including for older users.	Cardenas et al. (2021) Cauz, Clarinval & Dumas (2024) Arefin et al. (2024)
Text style	HMD: A billboard with an opaque background and high, stable contrast is recommended; the use of a single style (billboard or outline/drop shadow), without dynamic color matching is advisable. The LOD view helps to change the angle and distance. When occlusion is a problem, give preference to a drop shadow or a thin outline; prefer 2D text. Cool backgrounds (e.g., blue; in VST devices, green) are often preferred.	Gabbard, Swan & Hix (2006) Gabbard et al. (2007) Jankowski et al. (2010) Fiorentino et al. (2013) Dao & Gabbard (2013) Debernardis et al. (2014) Gattullo et al. (2015b) Vairinhos, Almeida & Dias (2016)

Table 3 (part 2)

Design recommendations for font type, text style, color and contrast, font size, text anchoring, text segmentation and organization, environmental illumination, background influence, perception depth, and text display in dynamic environments

Parameter	Design recommendations	Used literature
Text style	SCREEN: On complex backgrounds, billboard gives the best results, and drop shadow can also be used. If you use an outline, it will give you better results with bold text. Plain text is the weakest option. Prefer negative polarity and high contrast.	Kruijff et al. (2019) Sawyer et al. (2020) Erickson et al. (2020) Falk et al. (2021) Wysopal et al. (2023) Cauz, Clarinval & Dumas (2024)
Color and contrast	HMD: High, stable contrast with opaque backgrounds is recommended; on OST devices, light colors (white, cyan, green) are more visible, black loses visibility or is reproduced as transparent, while red should be avoided. Blue color of the billboard and white text on a dark background proved to be the most effective. Dark mode (light letters on a dark background) increases sharpness and comfort, especially in low light. High contrast between text and background is key to improving legibility, but too strong contrast, especially with VST, can cause discomfort and increased effort. When changing focus frequently, it is useful to increase the edge contrast (SharpView-approach). SCREEN: High contrast is recommended with a slight preference for dark backgrounds and light text for higher accuracy and less fatigue. On unpredictable backgrounds, saturated, high-contrast colors (e.g., neon green, yellow, red) are used for highlighting plain text.	Gabbard, Swan & Hix (2006) Gabbard et al. (2007) Fiorentino et al. (2013) Dao & Gabbard (2013) Debernardis et al. (2014) Kim et al. (2019) Erickson et al. (2020) Erickson et al. (2021) Falk et al. (2021) Cauz, Clarinval & Dumas (2024)

Table 3 (part 3)

Design recommendations for font type, text style, color and contrast, font size, text anchoring, text segmentation and organization, environmental illumination, background influence, perception depth, and text display in dynamic environments

Parameter	Design recommendations	Used literature
Font size	HMD: Font size has a significant impact on legibility, especially at low contrast, longer distances, and in peripheral vision. Units vary (pt, Unity units, dmm, arc minutes, mm); converted to pt typical recommendations are approximately ~14–48 pt (OST) and ~74–113 pt (VST), while at ~2 m it is about ~142 pt. Because of the differences between devices and scenes, automatic size adjustment (LOD) is the most efficient approach, with the validation of the minimum readable size per device. SCREEN: Larger size directly improves legibility. In the tested range, 14 pt was the most desirable. For the general and older population, ≥14 pt is recommended, and ≤10 pt should be avoided.	Kruijff et al. (2019) Erickson et al. (2020) Cardenas et al. (2021) Falk et al. (2021) Wysopal et al. (2023) Cauz, Clarinval & Dumas (2024)
Text anchoring	HMD: A world-anchored text for static information is recommended for better legibility and less mental effort. Screen-anchored text can be used for dynamic conditions. When walking, a body-anchored text is more suitable than a screen-anchored text. With world anchor, it is necessary to ensure the stable position of the text in space. SCREEN: A screen anchor with a consistent position of the elements is applied; anchoring to the environment or body is not applicable.	Merino, Bergel & Nierstrasz (2018) Fukushima, Hamada & Hautasaari (2020) Cauz, Clarinval & Dumas (2024)

Table 3 (part 4)

Design recommendations for font type, text style, color and contrast, font size, text anchoring, text segmentation and organization, environmental illumination, background influence, perception depth, and text display in dynamic environments

Parameter	Design recommendations	Used literature
Text segmentation and organization	HMD: Short lines of text and clear line spacing improve legibility. Apply LOD (hide less important information at greater distances, gradually reveal details when approaching). The parameters of line spacing and length have so far been poorly researched. SCREEN: Organize content modularly/progressively (quick access to the required data), with short lines and adequate line spacing; multi-row blocks are typically read faster than a single long line.	Sonderegger et al. (2019) Falk et al. (2021) Wysopal et al. (2023) Cauz, Clarinval & Dumas (2024)
Environmental illumination	HMD: Legibility is most stable in medium to strong indoor lighting (~200–1,000 lux); very low light (≤50 lux) slows down reading, and very high (≥3,000–4,000 lux) degrades the OST due to a drop in contrast (often unusable). For OST, use high contrast/solid billboard and bright colors; In darker conditions, dark mode is preferred because it reduces visual fatigue. VST maintains legibility even at 1,000–4,000 lux (VST devices control contrast by automatically adjusting the brightness), but in low light the quality decreases. Too strong a contrast can cause discomfort. Controlled lighting in industrial settings (around 400 lux) ensures consistent results, while natural light can vary and affect legibility. The optimal solution is to maintain moderate lighting and use adaptive lighting systems, which is enabled by VST devices. SCREEN: There are no specific studies.	Gabbard, Swan & Hix (2006) Gattullo et al. (2015a) Gattullo et al. (2015b) Kim et al. (2019) Erickson et al. (2020) Erickson et al. (2021) Falk et al. (2021) Cauz, Clarinval & Dumas (2024)

Table 3 (part 5)
Design recommendations for font type, text style, color and contrast, font size, text anchoring, text segmentation and organization, environmental illumination, background influence, perception depth, and text display in dynamic environments

Parameter	Design recommendations	Used literature
Background influence	HMD: Prefer monochrome/neutral backgrounds with consistent lighting; textured and colorful backgrounds reduce legibility. On OST devices, a dark background is preferred and it is more important than the color of the background. When the background cannot be controlled, apply a solid billboard. SCREEN: Complex backgrounds make it difficult to read. Prefer uniform/neutral backgrounds. A possible solution is to use a background filter such as scrim or blur to neutralize the impact of background noise. There are no differences between the types of dynamic backgrounds if you use text that is clearly highlighted by one of the proven methods such as text on a billboard.	Gabbard, Swan & Hix (2006) Gabbard et al. (2007) Jankowski et al. (2010) Fiorentino et al. (2013) Debernardis et al. (2014) Manghisi et al. (2017) Sawyer et al. (2020) Erickson et al. (2021) Falk et al. (2021) Cauz, Clarinval & Dumas (2024)
Perception depth	HMD: Place the text at a depth close to the task in order to reduce effort and vergence–accommodation conflict. Avoid large depth jumps between text and real objects. In the practical range of ~1–10 m, choose the depth according to the scenario. The distance itself does not impair legibility if the size is proportionally scaled. Prefer 2D text for reading as 3D (embossed/wireframe) makes it difficult to estimate distances. SCREEN: Not applicable (no change in depth); focus should be on text size and contrast.	Gabbard, Swan & Hix (2006) Vairinhos, Almeida & Dias (2016) Gabbard, Mehra & Swan (2019) Cauz, Clarinval & Dumas (2024)

Table 3 (part 6)
Design recommendations for font type, text style, color and contrast, font size, text anchoring, text segmentation and organization, environmental illumination, background influence, perception depth, and text display in dynamic environments

Parameter	Design recommendations	Used literature
Text display in dynamic environments	HMD: The use of Eye-Perspective Repositioning (EPR-VM), which reduces overlap and contrast loss and improves legibility compared to static or camera-guided approaches, is recommended. To highlight content, text animations in sparing amounts are recommended, with blinking being more effective on OST and circular motion on VST. The movement of the background is not decisive. It is necessary to maintain a high contrast of text and background (text style) when applying billboard/outline/shadow. It is recommended to use systems that automatically change the display of text based on environmental conditions to reduce the cognitive effort of the user and improve perception. Algorithms for automatic, real-time, adjustment of color, contrast and text size would be ideal for maintaining good legibility during the user's movement or changing environment. SCREEN: There are no direct findings in the literature.	Gabbard et al. (2007) Kruijff et al. (2019) Emsenhuber et al. (2023) Wysopal et al. (2023) Cauz, Clarinval & Dumas (2024)

Discussion and other research directions

While the reviewed studies provide evidence for several legibility-enhancing strategies, the generalizability of these findings is constrained by variations in experimental conditions and hardware configurations. Namely, a large proportion of the literature is based on controlled laboratory settings with static users, stable illumination, and simplified backgrounds, which only partially reflect real-world AR usage scenarios. In this context, lighting conditions represent a major source of variability. Studies usually report results obtained under specific illuminance ranges (e.g., indoor office lighting), whereas outdoor or rapidly changing lighting environments can significantly alter contrast perception, particularly on OST HMDs. Consequently, recommendations related to color, polarity, and text style may not transfer uniformly across lighting contexts. Similarly, user movement is often limited or excluded in experimental designs, despite evidence that walking, head motion, and changing viewpoints introduce additional challenges such as reduced text stabilization and increased cognitive load.

Findings obtained from static reading studies may therefore overestimate legibility performance in dynamic environments. Optical hardware differences further limit cross-study comparability. Results obtained on specific OST or VST devices depend on factors such as display brightness, focal distance, field of view, resolution, and color reproduction. As a result, parameter thresholds (e.g., optimal font size, contrast levels, or depth placement) reported for one device cannot be assumed to generalize directly to others without validation.

Regarding the frequency of examined parameters in the considered literature, it is evident (see Table 3) that the most commonly examined parameters are the style of text display (billboard/outline/shadow), color and contrast, environmental illumination, and background influence. Somewhat less frequently, but consistently, font size and text display in dynamic environments are examined, while segmentation and organization of text, depth perception, text anchoring, and font type remain less covered. At the same time, research on HMD devices is considerably more prevalent than research on screen-based devices, largely because HMDs enable hands-free interaction. Nevertheless, persistent technological challenges affect current HMDs, including additive color mixing and limited contrast on OST displays, VA conflict with fixed-focus optics, sensitivity to ambient/environmental illumination (especially outdoors), and limited battery life with associated thermal constraints. These limitations partially explain why screen-based AR continues to offer advantages for detailed reading tasks, particularly in dynamic or visually demanding environments. Due to the scarcity of research, it is recommended to conduct more systematic studies on legibility in AR on screens, with more proposed harmonized metrics and field testing in dynamic scenarios.

In order to achieve improved legibility/readability, hybrid systems that combine HMD and screen devices have been explored. Recent research highlights the complementarity of these technologies: smartphones are better suited for detailed reading and precise 2D input, while HMDs provide spatial context and hands-free viewing.

Bang & Woo (2023) showed that using a mobile phone as an auxiliary display alongside an HMD reduces subjective load and visual fatigue and improves perceived readability/comfort, although objective metrics may not always show significant progress. Grubert et al. (2024) examined text input via a smartphone keyboard with the display of information on different devices (smartphone, HUD, OST HMD), under static and dynamic conditions. Using only smartphones achieved the best performance and the lowest cognitive load when reading, while today's common OST HMD with a single focal plane reduces the speed (and in some places accuracy) of reading, especially during movement.

Bang et al. (2025) further demonstrated that the benefit of hybrid systems depends on the spatial proximity of its components. Specifically, when AR content and smartphone are located in the near zone, reading on the smartphone is more accurate and comfortable. As the distance increases, the cost of switching (looking, holding the device) decreases the benefit, so the phone needs to be switched to the input role or the AR text should be drawn closer. This indicates that there is the need for smart coordination based on the spatial relationships between the text and the device (HMD/phone) in order to choose the best reading device on which the text content will be displayed. From the perspective of foundational legibility parameters, the hybrid systems primarily address limitations related to contrast stability, background interference, and illumination sensitivity on OST HMDs by leaving detailed reading tasks to screens, where contrast, polarity, and background control are inherently more stable.

Beyond hybrid systems, projection-based AR, where text is projected directly onto a surface, has been investigated as an alternative display modality. Di Donato et al. (2015) showed that, under typical industrial settings (~500 lx, color controlled, different materials), projected text can achieve legibility comparable to monitors when surfaces with a pronounced 3D texture (grooves/relief) that deform the outlines of the letters are avoided. The research showed that wood and steel surfaces are efficient for text display, while blue text color is systematically weaker on all surfaces due to lower lighting in sum with the background. The practical implications of this work include the preference for uniform surfaces, the avoidance of blue color for key text, and software contrast enhancement (outline/billboard) when projection is unavoidable. Thus, projection AR can be seen as a modality that is particularly sensitive to environmental illumination and background influence, where surface material, texture, and color directly determine effective contrast and outline visibility, often necessitating stronger text styles. Future work should relate material selection, lighting and text style into predictive models of legibility and explore multimodal scenarios (HMD + projection) in dynamic environments.

In the context of mobile AR in interiors, 3D typography (using 3D instead of 2D text to display content) does not inherently guarantee improved legibility over 2D text. Instead, control of the thickness and depth (extrusion) of letters, local contrast (including "volumetric" shadows) and thoughtful positioning in the scene are crucial. Palm (2018) reported a slight preference for lighter text variants, but without the consistent advantage of color alone. In addition, thickness/depth and contrast have a greater impact on legibility than the choice of serif/sans-serif typeface. The recommendations of this study are: limit extrusion, explicitly test the contrast of edges/depths against the actual background, use sans-serif in visually rich environments, and plan the placement of text according to purpose instead of aesthetic preferences. Rather than introducing new legibility principles, 3D typography primarily amplifies existing challenges related to contrast control, background complexity, and depth perception. Further research is needed to determine the optimal parameters of legibility of 3D text in functional AR tasks and to propose consistent 3D text evaluation methods.

In addition to typographic guidelines, some of the newer works deal with hardware/software upgrades of devices that directly improve legibility in AR. Colorimetric compensation for OST HMDs using screen profiling can reduce additive color mixing errors and stabilize contrast, especially on darker backgrounds, although dark colors remain a challenge (Sridharan et al., 2013). Under dynamic conditions, when a person moves while wearing an OST HMD, the text on the display also moves. Text movement reduces its legibility, as it makes it impossible to use the vestibular-ocular reflex (VOR) of the eye. The use of VOR-inspired text stabilization during walking reduces text movement, increases forward gaze, and reduces discomfort, with the greatest gain over shorter distances (Koide, Kanari & Sato, 2022). On the optical hardware side, using an electrically operated attenuator to transmit light on liquid crystal (LC) lenses allows contrast to be maintained even under bright ambient light, thereby improving legibility, with current limitations such as chromatic aberration and small aperture (Wang et al., 2017).

At the level of available technology, Mekni & Lemieux (2014) emphasized the need for continued improvement of HMD devices, particularly toward multifocal, multiplanar and other solutions (Matsuda, Fix & Lanman, 2017) that address VA conflict. Until such display technologies mature, screen-based AR is likely to remain dominant for everyday reading tasks due to the prevalence, reliability and habitual use of mobile devices.

Lastly, we enumerate significant research gaps in underexplored areas. 1) 3D text legibility: There is a lack of systematic evaluation of 3D text legibility parameters in functional AR tasks and across different display technologies.

2) Screen-based and handheld AR: Environmental illumination and text display in dynamic environments are well studied in HMD-based AR but remain largely unexplored in screen-based AR, despite fundamental device differences. 3) Text segmentation and organization: There is a lack of systematic investigation into how segmentation parameters, such as line length, line spacing, hierarchical structuring, and LOD interact with dynamic viewing conditions, user movement, and background complexity. 4) Dynamic, real-world usage scenarios: Many findings are derived from laboratory-based, static conditions. Field studies that incorporate natural user movement, changing lighting, and complex backgrounds are still relatively rare, despite their importance for real-world AR applications. Addressing these gaps would enable more robust design guidelines and facilitate the transfer of research findings into practical systems across devices and application domains.

Conclusion

In this review, based on a systematic literature search following the PRISMA methodology, we have shown that legibility in AR is most reliably achieved by a combination of: 1) simple typographic solutions (opaque billboard or moderate outline, high and stable contrast, short lines in multiple rows, and LOD scaling), 2) controlled background and lighting conditions (neutral surfaces, dark-mode background in low-light conditions, avoidance of red text color on OST devices), and 3) proper anchoring (world anchor for static, screen anchor for dynamic information). The effects of font size and depth perception depend on the device, distance, and context of the task.

Therefore, the minimum readable settings must be validated on the target hardware and in the target environment. Legibility studies in AR were found to be strongly focused on HMDs (OST/VST), while screen/handheld-based usage scenarios were less frequently or only indirectly investigated. This review provides clear design recommendations for the 10 most commonly considered parameters of text legibility in AR, both for the use of HMDs and for screens.

When considering other directions of research, hybrid HMD+screen approaches have been shown to provide benefits primarily when AR content and smartphone are in the near zone, where reading on a screen device is preferred. When the distance between the devices increases, more advanced solutions are sought for the choice of devices for displaying or for adapting the proximity of text. Projection AR is confirmed as a viable alternative to screen and HMD on uniform surfaces under controlled conditions, while there is room for further research into 3D text and its legibility. Various hardware and software improvements for text display suggest that the way to improve legibility in AR lies in the integration of multiple aspects of the technology: simultaneous color compensation, display stabilization, and contrast/text size adjustments depending on conditions.

Future work should prioritize dynamic trials in real-world settings and systematically bridge findings across HMD, smartphone/screen, and projection-based AR, with stratified analyses by user populations and application domains. From a practical standpoint, given the diversity of devices and reporting practices observed in the literature, full methodological standardization is unlikely in the near term. Instead, a feasible step toward improved comparability would be the inclusion of supplementary conversion tables in legibility studies, translating key parameters, most notably font size, viewing distance, luminance, and visual angle, across commonly used units (e.g., pt, mm, dmm, degrees, arcminutes), based on explicitly reported experimental conditions.

In parallel, the community would benefit from greater transparency and partial alignment in the reporting of both objective and subjective legibility metrics, including illuminance (lux), luminance and contrast (Weber or Michelson), type size (dmm/mm/pt/angular size/arcmin), color difference (ΔE), and minimum reporting items such as device class (OST/VST), viewing distance, text depth and anchoring, and background characteristics.

Funding

This research did not receive any specific grant from funding agencies in the public, commercial, or not-for-profit sectors.

References

Arefin, M. S., Montalto, C., Plopski, A. & Swan, J. E. (2024) A SharpView Font with Enhanced Out-of-Focus Text Legibility for Augmented Reality Systems. In: *The 31st IEEE Conference on Virtual Reality and 3D User Interfaces, IEEE VR 2024, 16–21 March 2024, Orlando, Florida*. Piscataway, IEEE. pp. 31–41. Available from: doi: 10.1109/VR58804.2024.00027

Bang, S., Lee, H., Oh, S. Y. & Woo, W. (2025) AReading with Smartphones: Understanding the Trade-offs between Enhanced Legibility and Display Switching Costs in Hybrid AR Interfaces. In: *Proceedings of the 2025 CHI Conference on Human Factors in Computing Systems, CHI '25, 26 April - 1 May 2025, Yokohama, Japan*. New York, Associaton for Computing Machinery. pp. 1–20. Available from: doi: 10.1145/3706598.3713879

Bang, S. & Woo, W. (2023) Enhancing the Reading Experience on AR HMDs by Using Smartphones as Assistive Displays. In: *The 30th IEEE Conference on Virtual Reality and 3D User Interfaces, IEEE VR 2023, 25 - 29 March 2023, Shanghai, China*. Piscataway, IEEE. pp. 378–386. Available from: doi: 10.1109/VR55154.2023.00053

Cauz, M., Clarinval, A. & Dumas, B. (2024) Text readability in augmented reality: a multivocal literature review. *Virtual Reality.* 28 (1). Available from: doi: 10.1007/s10055-024-00949-6

Cardenas, D. G., Ginters, E., del Rio, M. S. & Martin-Gutierrez, J. (2021) Determining the Legibility of Fonts Displayed in Augmented Reality Apps for Senior Citizens. In: *2021 62nd International Scientific Conference on Information Technology and Management Science of Riga Technical University, ITMS 2021, 14 - 15 October 2021, Riga, Latvia*. Piscataway, IEEE. pp. 1–8. Available from: doi: 10.1109/ITMS52826.2021.9615329

Dao, B. & Gabbard, J. L. (2013) Early steps towards understanding text legibility in handheld augmented reality. In: *2013 IEEE Virtual Reality, VR 2013, 18 - 20 March 2013, Lake Buena Vista, Forida*. Piscataway, IEEE. pp. 159–160. Available from: doi: 10.1109/VR.2013.6549411

Debernardis, S., Fiorentino, M., Gattullo, M., Monno, G. & Uva, A. E. (2014) Text Readability in Head-Worn Displays: Color and Style Optimization in Video versus Optical See-Through Devices. *IEEE Transactions on Visualization and Computer Graphics.* 20 (1), 125–139. Available from: doi: 10.1109/TVCG.2013.86

Di Donato, M., Fiorentino, M., Uva, A. E., Gattullo, M. & Monno, G. (2015) Text legibility for projected Augmented Reality on industrial workbenches. *Computers in Industry.* 70, 70–78. Available from: doi: 10.1016/j.compind.2015.02.008

Dörner, R., Broll, W., Grimm, P. & Jung, B. (2022) *Virtual and Augmented Reality (VR/AR)*. Cham, Springer. Available from: doi: 10.1007/978-3-030-79062-2

Emsenhuber, G., Langlotz, T., Kalkofen, D., Sutton, J. & Tatzgern, M. (2023) Eye-Perspective View Management for Optical See-Through Head-Mounted Displays. In: *Proceedings of the 2023 CHI Conference on Human Factors in Computing Systems, CHI '23, 23 - 28 April 2023, Hamburg, Germany*. New York, Association for Computing Machinery. pp. 1–16. Available from: doi: 10.1145/3544548.3581059

Erickson, A., Kim, K., Bruder, G. & Welch, G. F. (2020) A Review of Visual Perception Research in Optical See-Through Augmented Reality. In: Argelaguet, F., McMahan, R. and Sugimoto, M. (eds.) *International Conference on Artificial Reality, ICAT-EGVE 2020, 2 - 4 December 2020*. Available from: doi: 10.2312/egve.20201256

Erickson, A., Kim, K., Lambert, A., Bruder, G., Browne, M. P. & Welch, G. F. (2021) An Extended Analysis on the Benefits of Dark Mode User Interfaces in Optical See-Through Head-Mounted Displays. *ACM Transactions on Applied Perception.* 18 (3), 1–22. Available from: doi: 10.1145/3456874

Falk, J., Eksvard, S., Schenkman, B., Andren, B. & Brunnstrom, K. (2021) Legibility and readability in Augmented Reality. In: *2021 13th International Conference on Quality of Multimedia Experi-*

ence, QoMEX 2021, 14 - 17 June 2021, Montreal, Canada*. Piscataway, IEEE. pp. 231–236. Available from: doi: 10.1109/QoMEX51781.2021.9465455

Fiorentino, M., Debernardis, S., Uva, A. E. & Monno, G. (2013) Augmented Reality Text Style Readability with See-Through Head-Mounted Displays in Industrial Context. *Presence: Teleoperators and Virtual Environments.* 22 (2), 171–190. Available from: doi: 10.1162/PRES_a_00146

Fukushima, S., Hamada, T. & Hautasaari, A. (2020) Comparing world and screen coordinate systems in optical see-through head-mounted displays for text readability while walking. In: *2020 IEEE International Symposium on Mixed and Augmented Reality, ISMAR 2020, 9 - 13 November 2020, Porto de Galinhas, Brazil*. Piscataway, IEEE. pp. 649–658. Available from: doi: 10.1109/ISMAR50242.2020.00093

Gabbard, J. L., Swan, J. E. & Hix, D. (2006) The Effects of Text Drawing Styles, Background Textures, and Natural Lighting on Text Legibility in Outdoor Augmented Reality. *Presence: Teleoperators and Virtual Environments.* 15 (1), 16–32. Available from: doi: 10.1162/pres.2006.15.1.16

Gabbard, J. L., Swan, J. E., Hix, D., Kim, S.-J. & Fitch, G. (2007) Active Text Drawing Styles for Outdoor Augmented Reality: A User-Based Study and Design Implications. In: *2007 IEEE Virtual Reality Conference, VR 2007, 10 - 14 March 2007, Charlotte, North Carolina*. Piscataway, IEEE. pp. 35–42. Available from: doi: 10.1109/VR.2007.352461

Gabbard, J. L., Mehra, D. G. & Swan, J. E. (2019) Effects of AR Display Context Switching and Focal Distance Switching on Human Performance. *IEEE Transactions on Visualization and Computer Graphics.* 25 (6), 2228–2241. Available from: doi: 10.1109/TVCG.2018.2832633

Gattullo, M., Uva, A. E., Fiorentino, M. & Gabbard, J. L. (2015a) Legibility in Industrial AR: Text Style, Color Coding, and Illuminance. *IEEE Computer Graphics and Applications.* 35 (2), 52–61. Available from: doi: 10.1109/MCG.2015.36

Gattullo, M., Uva, A. E., Fiorentino, M. & Monno, G. (2015b) Effect of Text Outline and Contrast Polarity on AR Text Readability in Industrial Lighting. *IEEE Transactions on Visualization and Computer Graphics.* 21 (5). 638-651. Available from: doi: 10.1109/TVCG.2014.2385056

Gattullo, M., Evangelista, A., Uva, A. E., Fiorentino, M. & Gabbard, J. L. (2022) What, How, and Why are Visual Assets Used in Industrial Augmented Reality? A Systematic Review and Classification in Maintenance, Assembly, and Training (From 1997 to 2019). *IEEE Transactions on Visualization and Computer Graphics.* 28 (2), 1443–1456. Available from: doi: 10.1109/TVCG.2020.3014614

Grubert, J., Witzani, L., Otte, A., Gesslein, T., Kranz, M. & Kristensson, P. O. (2024) Text Entry Performance and Situation Awareness of a Joint Optical See-Through Head-Mounted Display and Smartphone System. *IEEE Transactions on Visualization and Computer Graphics.* 30 (8), 5830–5846. Available from: doi: 10.1109/TVCG.2023.3309316

Jankowski, J., Samp, K., Irzynska, I., Jozwowicz, M. & Decker, S. (2010) Integrating Text with Video and 3D Graphics. In: *Proceedings of the SIGCHI Conference on Human Factors in Computing Systems, CHI '10, 10 - 15 April 2010, Atlanta, Georgia*. New York, Association for Computing Machinery. pp. 1321–1330. Available from: doi: 10.1145/1753326.1753524

Jović, A., Mikota, M. & Mandić, L. (2025) Enhancing Text Legibility in Augmented Reality: Challenges and Design Recommendations. In: *28th International Conference on Printing, Design and Graphic Communication BLAŽ BAROMIĆ 2025, Zagreb, Croatia*. Zagreb, pp. 161-169. Available from: https://www.croris.hr/crosbi/publikacija/prilog-skup/900018

Kim, K., Erickson, A., Lambert, A., Bruder, G. & Welch, G. (2019) Effects of Dark Mode on Visual Fatigue and Acuity in Optical See-Through Head-Mounted Displays. In: *Symposium on Spatial User Interaction, SUI '19, 19 - 20 October 2019, New Orleans, Louisiana*. New York, Association for Computing Machinery. pp. 1–9. Available from: doi: 10.1145/3357251.3357584

Ko, S. M., Chang, W. S. & Ji, Y. G. (2013) Usability Principles for Augmented Reality Applications in a Smartphone Environment. *International Journal of Human-Computer Interaction.* 29 (8), 501–515. Available from: doi: 10.1080/10447318.2012.72246

Koide, H., Kanari, K. & Sato, M. (2022) An Examination on Reduction of Displayed Character Shake while Walking in Place with AR Glasses. In: *2022 IEEE Conference on Virtual Reality and 3D User Interfaces Abstracts and Workshops, VRW 2022, 12 - 16 March 2022, Christchurch, New Zealand*. Piscataway, IEEE. pp. 786–787. Available from: doi: 10.1109/VRW55335.2022.00244

Kruijff, E., Orlosky, J., Kishishita, N., Trepkowski, C. & Kiyokawa, K. (2019) The Influence of Label Design on Search Performance and Noticeability in Wide Field of View Augmented Reality Displays. *IEEE Transactions on Visualization and Computer Graphics.* 25 (9), 2821–2837. Available from: doi: 10.1109/TVCG.2018.2854737

Manghisi, V. M., Gattullo, M., Fiorentino, M., Uva, A. E., Marino, F., Bevilacqua, V. & Monno, G. (2017) Predicting Text Legibility over Textured Digital Backgrounds for a Monocular Optical See-Through Display. *Presence: Teleoperators and Virtual Environments.* 26 (1), 1–15. Available from: doi: 10.1162/PRES_a_00285

Matsuda, N., Fix, A. & Lanman, D. (2017) Focal surface displays. *ACM Transactions on Graphics.* 36 (4), 1–14. Available from: doi: 10.1145/3072959.3073590

Mekni, M. & Lemieux, A. (2014) Augmented Reality: Applications, Challenges, and Future Trends. In: *Applied Computational Science: Proceedings of the 13th International Conference on Applied Computer and Applied Computational Science, ACACOS '14, 23 – 25 April 2014, Kuala Lumpur, Malaysia*. Athens, WSEAS Press. pp. 205–214.

Merino, L., Bergel, A. & Nierstrasz, O. (2018) Overcoming Issues of 3D Software Visualization through Immersive Augmented Reality. In: *2018 IEEE Working Conference on Software Visualization, VISSOFT 2018, 24 - 25 September 2018, Madrid, Spain.* Piscataway, IEEE. pp. 54–64. Available from: doi: 10.1109/VISSOFT.2018.00014

Milgram, P. & Kishino, F. (1994) A taxonomy of mixed reality visual displays. *IEICE Transactions on Information and Systems*. E77–D (12), 1321–1329.

Mills, C. B. & Weldon, L. J. (1987) Reading text from computer screens. *ACM Computing Surveys.* 19 (4), 329–357. Available from: doi: 10.1145/45075.46162

Page, M. J., McKenzie, J. E., Bossuyt, P. M., Boutron, I., Hoffmann, T. C., Mulrow, C. D., Shamseer, L., Tetzlaff, J. M., Akl, E. A., Brennan, S. E., Chou, R., Glanville, J., Grimshaw, J. M., Hróbjartsson, A., Lalu, M. M., Li, T., Loder, E. W., Mayo-Wilson, E., McDonald, S., McGuinness, L. A., Stewart, L. A., Thomas, J., Tricco, A. C., Welch, V. A., Whiting, P. & Moher, D. (2021) The PRISMA 2020 statement: an updated guideline for reporting systematic reviews. *BMJ.* 372 (71). Available from: doi: 10.1136/bmj.n71

Palm, K. (2018) *Design and use of 3D typography for indoor augmented reality mobile applications*. Master's thesis. Umeå University.

Rampolla, J. & Kipper, G. (2013) *Augmented Reality: An Emerging Technologies Guide to AR*. Rockland, Syngress.

Richardson, J. T. E. (2022) *The Legibility of Serif and Sans Serif Typefaces: Reading from Paper and Reading from Screens*. Cham, Springer.

Sawyer, B. D., Wolfe, B., Dobres, J., Chahine, N., Mehler, B. & Reimer, B. (2020) Glanceable, legible typography over complex backgrounds. *Ergonomics.* 63 (7), 864–883. Available from: doi: 10.1080/00140139.2020.1758348

Sonderegger, A., Ribes, D., Henchoz, N. & Groves, E. (2019) Food Talks: Visual and interaction principles for representing environmental and nutritional food information in augmented reality. In: *2019 IEEE International Symposium on Mixed and Augmented Reality Adjunct, ISMAR-Adjunct, 10 - 18 October 2019, Beijing, China*. Piscataway, IEEE. pp. 98–103. Available from: doi: 10.1109/ISMAR-Adjunct.2019.00040

Sridharan, S. K., Hincapié-Ramos, J. D., Flatla, D. R. & Irani, P. (2013) Color correction for optical see-through displays using display color profiles. In: *Proceedings of the 19th ACM Symposium on Virtual Reality Software and Technology, VRST '13, 6 - 9 October 2013, Singapore*. New York, Association for Computing Machinery. pp. 231–240. Available from: doi: 10.1145/2503713.2503716

Vairinhos, M., Almeida, S. & Dias, L. N. (2016) Typographic Features on Distance Estimation with Head-Mounted Displays. In: *Proceedings of the 1st International Workshop on Multimedia Alternate Realities, MM '16, 16 October 2016, Amsterdam, Netherlands*. New York, Association for Computing Mahinery. pp. 15–20. Available from: doi: 10.1145/2983298.2983300

Wang, Y.-J., Chen, P.-J., Liang, X. & Lin, Y.-H. (2017) Augmented reality with image registration, vision correction and sunlight readability via liquid crystal devices. *Scientific Reports.* 7 (1). Available from: doi: 10.1038/s41598-017-00492-2

Wysopal, A., Ross, V., Passananti, J., Yu, K., Huynh, B. & Höllerer, T. (2023) Level-of-Detail AR: Dynamically Adjusting Augmented Reality Level of Detail Based on Visual Angle. In: *2023 IEEE Conference Virtual Reality and 3D User Interfaces, VR, 25 - 29 March 2023, Shanghai, China*. Piscataway, IEEE. pp. 63–71. Available from: doi: 10.1109/VR55154.2023.00022

Original scientific paper http://doi.org/10.24867/JGED-2026-3-035

Exploration of biodegradable materials for a digitally printed fashion embellishments

ABSTRACT

Initially utilized in aerospace and medical industries, 3D printing has emerged as revolutionary technology with significant potential in transforming garment creation that previously unattainable through traditional manufacturing. The integration of biodegradable materials in 3D printing represents a promising approach in addressing the environmental challenges posed by conventional plastic-based printing technologies. This study explores biodegradable materials—Polyterra PLA, Esun PLA+, and bio resin—for producing digitally printed sustainable fashion embellishments. Through a mixed method approach involving practical experimentations, a flower-shaped embellishment prototype was made and painted for application on garment. By addressing the limitations of biodegradable materials and demonstrating their potential in high-fashion applications, this study contributes to the advancement of 3D printing by optimising biodegradable materials for a more sustainable and creative design potential for the fashion industry.

KEY WORDS

3D printing, fashion embellishments, biodegradable material, sustainable

Grasheli Kusuma Andhini
Tashannie Abigail Loekman

Binus University International, Jakarta, Indonesia

Corresponding author:
Grasheli Kusuma Andhini
e-mail:
grasheli.andhini@binus.edu

First received: 31.7.2025.
Revised: 11.1.2026.
Accepted: 25.2.2026.

Introduction

Technological advancements have continuously shaped various industries, with the fashion sector being no exception. Over the past few decades, innovations such as computer-aided design (CAD), augmented reality (AR), and smart textiles have revolutionized the industry, enabling new creative possibilities, efficiency, and consumer engagement. CAD software has streamlined the design process by enabling the creation of precise digital prototypes, reducing the time and cost associated with physical mock-ups (Adediran et al., 2024; RS Design Spark, n.d.). Introduced in 1987, CAD is widely used for creating garment components, patterns, and simulations, significantly enhancing efficiency and accuracy (Singh, 2021).

Smart textiles, another breakthrough, incorporate sensors and adaptive materials that interact dynamically with the wearer, offering functionalities like temperature regulation and health monitoring (Ruckdashel, Venkataraman & Park, 2021).

Among these breakthroughs, three-dimensional (3D) printing stands out as a revolutionary technology with immense potential to redefine garment creation.

Initially utilized in aerospace and medical industries, 3D printing is now gaining prominence in fashion, offering designers the ability to create intricate, customized pieces previously unattainable through traditional manufacturing.

Despite its benefits of allowing for flexible designs with high precision (Gudaitiene, Minkus & Darulis, 2025), 3D printing faces challenges especially in fashion industry. High production costs, long printing times, and material limitations, such as brittleness and lack of flexibility, hinder its widespread adoption (Xiao & Kan, 2022).

Moreover, the environmental sustainability of 3D printing materials, typically plastic-based, raises concerns (Jandyal et al., 2022). Figure 1 below shows the 3D printing iteration process.

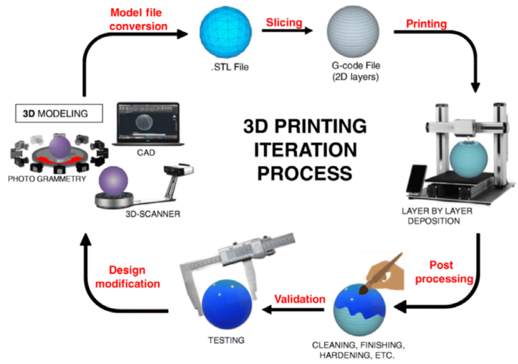

» **Figure 1:** *3D printing iteration process (Ambrosi & Bonanni, 2021)*

3D printing has emerged as a revolutionary technology in fashion, enabling intricate designs, new innovative fabrications, personalized products, and for high fashion applications (Olawumi et al., 2023; Sheikh et al., 2020; Sun & Zhao, 2017). By constructing objects layer by layer, 3D printing facilitates the creation of complex geometries and reduces material waste (Shahrubudin, Lee & Ramlan, 2019). This technology, initially commercialized in 1980, has expanded across industries, with the global market for 3D printing expected to grow by 25% annually until 2030 (Yoo, 2025).

Fashion applications range from haute couture to accessories, with designers like Iris Van Herpen and Daniel Peleg pioneering its use. Van Herpen's experimental designs and Peleg's fully 3D-printed garments highlight the potential of this technology to push creative boundaries (Deabler, 2017; Holgate, 2016). Similarly, Koerner's innovative use of 3D printing in films like Black Panther highlighted the medium's versatility and aesthetic appeal (Guimapang, 2019).

In Indonesia, 3D printing is still in its early stages due to limited access to advanced machines. Designers like Tex Saverio and DIBBA have showcased its potential by combining 3D-printed elements with traditional techniques (Idea3D, 2015; Kuswanto et al., 2017). Technological advancements like CAD, smart textiles, and 3D printing are reshaping fashion, offering new possibilities for design and production. While challenges remain, ongoing research into sustainable materials and innovative applications promises a more efficient and environmentally conscious future for the industry.

While 3D printing has enabled rapid prototyping, customization, and waste reduction (Olawumi et al., 2023), its reliance on non-biodegradable materials, such as thermoplastics and resins, presents significant environmental challenges. Plastics, the primary materials for 3D printing, contribute substantially to global waste, with over 400 million tons generated annually and projections indicating continued growth (Dueñas-Moreno et al., 2023; IUCN, 2024; Rodríguez-Hernández et al., 2020). Improper disposal exacerbates this issue, polluting ecosystems and posing risks to biodiversity and human health (Filamatrix Staff, 2024; Oladapo et al., 2023). The rise of sustainability in fashion demands alternatives that align with environmentally conscious practices.

Biodegradable materials, such as polylactic acid (PLA) and bio-resins, have emerged as promising substitutes, capable of decomposing under certain conditions and reducing the ecological footprint of 3D-printed products (Byjus, 2018; Oladapo et al., 2023). These materials are derived from renewable resources and have a lower environmental impact compared to non-biodegradable materials, such as petroleum-based plastics (Subramani et al., 2024). However, their integration into fashion faces significant hurdles, including brittleness, limited heat resistance, and higher costs. Additionally, existing research on the use of biodegradable materials in 3D printing for fashion remains sparse, with most studies focusing on technical applications rather than fashion, leaving critical questions about their viability and optimization unanswered. Despite these advancements, the industry's reliance on non-biodegradable materials limits its sustainability. Efforts to recycle 3D printing waste have also been hindered by inconsistent material quality and the complexities of multi-material recycling. This study addresses these gaps by exploring how biodegradable materials can be leveraged to create durable, aesthetically appealing, and sustainable fashion garments.

To tackle the challenges of using biodegradable materials in 3D-printed fashion, this research adopts a multidisciplinary methodology combining material science, design experimentation, and environmental assessment. The approach begins with a comprehensive evaluation of biodegradable filaments and bio-resins, focusing on their mechanical properties, thermal stability, and biodegradability. Laboratory testing will identify the limitations and opportunities of these materials, providing insights into their suitability for high-fashion applications.

3D Printing Materials

The selection of materials for 3D printing plays a pivotal role in determining the quality, sustainability, and functionality of printed objects. Among the various materials used in 3D printing, filaments such as PLA and ABS, as well as liquid resins, stand out. PLA, or polylactic acid, is a biodegradable polymer derived from renewable resources like corn starch and sugarcane. It is favoured for its affordability, ease of use, and environmental benefits (Conniff & Tewolde, 2022). PLA is especially relevant to this research as it aligns with the focus on sustainability and biodegradability. While PLA's properties include a low melting point and user-friendly printing characteristics, its brittleness and limited thermal resistance pose challenges for applications requiring durability (Polygenis, 2023).

In contrast, ABS is a petroleum-based thermoplastic known for its strength, impact resistance, and suitability for high-performance applications. However, its environmental drawbacks, such as non-biodegradability and the release of toxic fumes during printing, make it less desirable for sustainable initiatives (Khosravani & Reinicke, 2020; Printerra, 2023). Liquid resins, used primarily in SLA machines, offer high resolution and smooth surface finishes but are not biodegradable and pose environmental and health risks due to their toxic nature (Madeline, 2023).

The Fused Deposition Modelling (FDM) machine is widely used for 3D printing for its affordability, user friendliness, and compatibility with thermoplastic filaments like PLA (Xiao & Kan, 2022). It is one of the widely used additive technology using digital 3D CAD model for the creation of prototype. The FDM process involves heating the filament to its melting point and extruding it through a nozzle to build objects layer by layer (Warnier et al., 2014), where printing accuracy is influenced by key parameters such as raster width, nozzle diameter (typically 0.2–0.6 mm), print speed, temperature, raster angle, and layer thickness (Žarko et al., 2017). The standard workflow beginning with CAD modelling, followed by STL export, slicing, printing, and finishing aligns well with the design-to-prototype sequence required in this project. However, these same parameters also introduce technical limitations, particularly when printing intricate forms or thin decorative elements (Gudaitiene, Minkus & Darulis, 2025).

Fine details below 2 mm, for example, are susceptible to deformation, uneven edges, or surface inconsistencies depending on the selected print settings. While FDM machines are not capable of achieving the high resolution of SLA or SLS machines, their low cost and accessibility make them ideal for exploratory research and prototyping in fashion applications.

Moreover, the simplicity of FDM technology allows experimentation with material modifications and the development of innovative designs. Despite its relatively rough surface finishes and slower printing speeds compared to other technologies, the FDM machine's ability to produce functional and cost-effective prototypes supports its selection for this study. The method used in this study is grounded in recognized additive manufacturing practices while acknowledging limitations that influenced the final prototype quality.

The success of an FDM print relies not only on the design of the model but also on the careful selection of printing parameters that directly influence structural accuracy and surface quality. Poorly prepared models or inappropriate parameter choices can result in defects such as uneven surfaces, tearing during printing, or dimensional inaccuracies caused by internal stresses in the material. Similarly, layer thickness and raster width significantly affect the smoothness and resolution of the printed surface; thinner layers and narrower raster widths produce finer, more detailed finishes, whereas thicker layers create visible stepping and rougher textures (Gudaitiene, Minkus & Darulis, 2025). Incorporating these considerations is essential for ensuring the reliability and reproducibility of 3D-printed fashion embellishments.

Biodegradable materials, particularly PLA, are gaining traction as an eco-friendly alternative to traditional 3D printing materials. PLA's biodegradability stems from its composition of renewable sources and its ability to decompose under industrial composting conditions (EDI, n.d.). However, PLA's mechanical properties, such as low tensile strength and brittleness, limit its use in applications requiring high durability (Subramani et al., 2024). Additionally, PLA's low melting point restricts its suitability for high-temperature environments.

Although biodegradable films have a high potential as a sustainable approach to 3D Printing, they have several challenges that need to be addressed to identify the full potential of the materials. There must be deeper research and development to improve the cost, strength, and properties. Despite the challenges in using biodegradable materials, the demand for sustainable materials and 3D Printing technology has risen in recent years (Subramani et al., 2024). The flexibility of the design and high customization of biodegradable materials create new possibilities for sustainable production and design processes while addressing the rising issue of plastic pollution. The adoption of biodegradable materials in 3D printing also addresses the growing concern of plastic pollution. Failed prints and support structures contribute significantly to 3D printing waste. PLA's biodegradability allows for reduced environmental impact, as it can decompose more efficiently compared to non-biodegradable plastics (Subramani et al., 2024).

However, the process of composting PLA requires specific conditions, such as high temperatures and controlled environments, which are not always accessible (European Bioplastics, 2024). In contrast to the PLA, PLA+ is widely used as an enhanced version for its biodegradability and with a better thermal stability and improved tensile strength, making it more suitable for a more complex application with its better flexibility (Anaç, Koçar & Altuok, 2024; Goryl et al., 2024; Hong, Choi & Han, 2009).

PLA is an eco-friendly variant and designed to be biodegradable, but it has less tensile strength as compared to the PLA+. In contrast, PLA+ focuses rather on the performance while PLA emphasises on the environmentally sustainable appeal (Pratama & Hasdiansah, 2021).

This research proposes a comprehensive framework for optimizing biodegradable materials in 3D printed fashion.

By addressing existing challenges and exploring innovative solutions, it aims to contribute to a more sustainable and creative future for the fashion industry. Sustainability is approached through responsible material selection and circular design strategies, with a particular focus on PLA+ as the primary biodegradable material due to its balance of printability, performance, and alignment with environmentally conscious practices, despite its inherent limitations. To address the issues on brittleness and thermal instability, this study explored innovative modifications and post-processing techniques aimed at enhancing the performance of PLA+ for fashion embellishments.

Method

A mixed-methods approach is used in this study, combining material experimentation, design prototyping, and qualitative interview with purposive sampling to explore the potential of biodegradable filaments for 3D-printed fashion garments. Illustrated in Figure 2, the methodology is structured into several interrelated stages to ensure a comprehensive understanding of material performance, design possibilities, and the practical application of biodegradable materials in fashion. It began with the initial research that involved reviewing literatures and interviews, then material analysis where three materials were examined and compared in terms of its properties and suitability for fashion embellishment creations. A standardized production workflow was followed for all samples, including design modelling, slicing, printing, and post-processing. Each material (Polyterra PLA, PLA+, bio resin) was printed in three repeated samples of equal size to ensure comparability. The results were then carried to post-processing stage that involved surface refinement, colouring, and finishing to enhance the visual appeal.

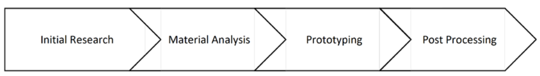

» **Figure 2:** *Research Framework*

The data collection process in the interviews involves purposive sampling to ensure five interviewees possessed relevant expertise aligned with the study's objectives. They were selected based on their professional experience, technical knowledge, and familiarity with processes related to 3D printing, material development, sustainable practices, and high-fashion garment construction. Two fashion designers with extensive experience in eveningwear and advanced draping techniques were included to provide insights into aesthetic expectations, garment integration, and practical considerations in wearable design. To address the technical aspects of additive manufacturing, the sample incorporated 3D printing practitioners and engineering specialists with several years of hands-on experience working with different filament types, printer settings, and production workflows. Additionally, a sustainability expert from plastic recycling organizations and the waste management industry with a background in biodegradable plastic manufacturing contributed knowledge on material properties, environmental implications, and end-of-life considerations. These professionals provide broad perspectives from both fashion and engineering that guide the research process.

In addition to expert input, a survey was conducted with 56 respondents aged 25–40 who expressed interest in fashion, providing user-oriented perspectives on design appeal and sustainability values. This combined qualitative sampling approach ensured a comprehensive understanding of both technical and experiential factors relevant to developing biodegradable 3D printed fashion embellishments.

The obtained qualitative data is applied during the prototyping and experimentation phases. This includes prototyping 3D model designs, material experimentation, and design exploration. Desktop sculpting software Nomad Sculpt was used for developing the 3D designs. It was chosen as it is a lightweight application that can be done directly on mobile/tablet for faster prototyping and experimentation. The app offers a wide variety of functions and usage that allows a detailed rendering or 3D model. The good UI/UX allows user to easily sculpt and modify shapes into an intricate design. The features support rapid prototyping while offering a high-quality printing resolution. The application offers various textures, colors, background lighting to allow user in visualizing the final product or mock up with high similarity as the real size product design. Fashion embellishment prototypes were created in this study using PLA+ that can be applied for the creation of demi couture womenswear.

The design process began with initial sketching, followed by building the digital model in Nomad Sculpt using a basic sphere or cube as the starting form, illustrated in Figure 3. This base shape was then sculpted using various tools such as crease, clay, smooth, and drag brushes to define the structure, add depth, and refine surface details. Additional features, including creases, textures, and dimensional accents, were incorporated to enhance the visual complexity of the embellishment.

Throughout the process, the model's thickness was adjusted to maintain a 3D-printable minimum of 1.2–1.5 mm to ensure both durability and printability. Once the shape was finalized, smoothing and mesh retopology were applied to simplify the polygon count while maintaining the surface detail, resulting in a cleaner, a more detailed, and stronger print quality. The completed design was then exported as an STL file and prepared for fabrication through slicing software before the final 3D printing stage.

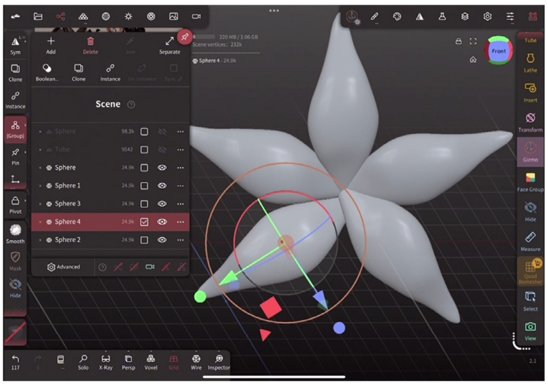

» **Figure 3:** *Sketching in Nomad Sculpt*

To strengthen the methodological rigor of the study, several step-by-step experimental procedures and basic material tests were incorporated. Each sample was produced using controlled settings, with melting temperatures ranging from 160–200°C and heating durations between 10–30 minutes, depending on the trial.

Tools such as silicone moulds, shredders, and digital thermometers were used to ensure consistency across samples, and all test pieces were created in similar sizes to allow fair comparison. After fabrication, a series of simple technical tests were conducted to evaluate the material performance. A flexibility test was performed by manually bending the samples to a 90° angle, where slight surface cracking indicated limited flexibility and low tolerance for bending stress. A drop test was also carried out to observe durability under impact. Surface smoothness was assessed visually on both the top and bottom sides of the samples, documenting irregularities such as bubbling, unevenness, or textural variations.

Colour consistency was examined after painting to identify how evenly pigments adhered across different material bases. Finally, heat exposure tests were conducted by placing samples under elevated temperature to observe deformation, brittleness, or texture changes. These basic yet systematic tests provided practical insights into the material behaviour and informed the selection of the most suitable biodegradable base for fashion embellishments.

Discussion

Biodegradable material is environmentally friendlier compared to conventional plastics making it a sustainable option. It offers less carbon emissions, lower levels of volatile organic compounds, and reduces air pollution during the printing process. Since it is made from renewable resources that can be composted, it decreases the carbon footprint, and the plastic waste issues as well. However, due to the limited infrastructure and government intervention that has been ongoing in Indonesia, experts mentioned that the end-of-life for biodegradable materials commonly ends up in sanitary landfills. It is a controlled landfill coated with plastic or geomembrane to prevent environmental pollution from the landfill. In fact, currently there is no industrial composting site available in Indonesia that requires high microbial activity, sufficient water content (at least 60%), sufficient air content, and adequate temperature, and high constant heat up to 60-degree Celsius. Consequently, most of the waste is handled by waste management services and some companies that produce biodegradable plastic. The waste is organised and processed, and if recyclable it is recycled; if not, then it is given to black soldier maggot to compost it, and if composting is not suitable, it is sent to the landfill.

There is another type of biodegradable plastic that is fully biodegradable, for instance PHA. However, due to its limited availability, it is very costly and requires specific printer and settings for it to be printed. For now, it is unavailable in Indonesia since it requires more infrastructure to have the specific machine that can print the PHA and the access to import the PHA filament.

Recycling could be another alternative aside from composting, but it is not recommended by some sustainable and 3D printing experts. The main challenge is that recycling the 3D printed waste decreases the quality in one or two cycles and not all plastic can be recycled. For instance, biodegradable plastic is meant to be compost not recycled. Furthermore, since it would lose its quality, experts and previous research noted that biodegradable plastic or plastic needs to be combined with virgin plastic.

There was already an attempt in Indonesia to use plastic bottle waste recycled as a filament however, there are still many issues encountered on the material consistency of various plastic bottles and still need more development. One alternative can be done is by assembling a machine to recycle used filament but there is still a shortage of spare parts and is still hard to find them especially in Indonesia. Due to the limited availability and inaccessibility of the spare parts, having to privately get it from abroad, most Indonesian 3D printing companies do not do and sell recycled filaments yet.

PLA may act as a good bio-based plastic, some of the most common are Polyterra and Esun. Based on the interview with experts, PLA is good for indoor use that are not directly exposed to sunlight with a quite food strength up to 100mph and it can withstand pressure. Even though it is not water resistant, it is still fine to be worn on body with sweat, only if it is regularly wiped for any water or liquid to prevent damage on the shape. Originally, PLA is not 100% pure plastic, it is a mixture of corn or wood fibre, making it not too strong as it absorbs moisture in humid temperatures. 28 – 30 to 33- 35 degrees Celsius is a good temperature for PLA.

It is fine to be worn in the daylight if it is not exposed for long hours and the heat does not reach to 60 degrees Celsius before PLA deflates or bends. Therefore, for long-term use, experts recommend covering the 3D printed PLA with resin for a more durable and water and heat resistant. Another alternative is to create a higher infill in the design model since thinner surface may cause the PLA to break easily; the infill needs to be around 80 – 100% to offer more durability.

Prototype making

To ensure the printed embellishments achieved the required durability, strength, and usability, the 3D printer was configured with optimized settings tailored for wearable applications. The table 1 below summarizes the key specifications and printing parameters used in this study for producing the prototypes.

Table 1
Printer Setting

Model	Creality Ender 3 V2 Neo
Nozzle Size	0.4mm standard nozzle
Layer Height	0.12 – 0.20mm
Build Chamber Dimensions	220 x 220 x 250mm
Nozzle Temperature	200 – 210°C
Bed Temperature	55 – 60°C
Print Speed	50 – 60mm/s
Infill Percentage	100% for strength and support
Retraction	5mm / 45mm/s to reduce stringing

A corset prototype was developed in this study by assembling multiple 3D printed flower embellishments. The 3D modelling design was created imitating daffodil's flower structure and arranged onto the scanned 3D mannequin replicating the real-size body. The model was printed in different sizes, density and rotated to fit the body. By printing the flower singularly, the embellishment can potentially be applied for many arrangements or garments, for instance as accessories, tops, or as decorations. Also, it allows future alterations to fit on the different body proportions and sizing. Tiny loops were printed at the back of each flower to serve as attachment points for easy application on to garments. The current available 3D printer chamber has an average of 35cm x 35cm x 35cm in size, as a result, for large volumes printing, designs need to be divided and later assembled after printing for a larger scale. Lace, rope, or a chainmail can be used to assemble the small pieces for a larger scale application.

Prior deciding on the PLA+ as the primary material, the initial flower embellishment prototypes were produced using three different bases: bio resin, Polyterra PLA, and Esun PLA+ on an FDM printer. As shown in Figure 4, bio resin produced the most defined and detailed shapes, consistent with resin-based additive manufacturing research; however, its brittleness and higher cost made it less suitable for wearable embellishments. Although it easy to print using PLA, it showed visible cracking in the flexibility test and limited impact resistance in the drop test. This is aligned with prior literature describing standard PLA's low elongation and rigidity (Subramani et al., 2024; Xiao & Kan, 2022), confirming its unsuitability for embellishments that undergo even minor bending or handling.

In contrast, PLA+ demonstrated smoother surface finishes and greater resilience during testing, reflecting findings that modified PLA formulations offer improved toughness and interlayer adhesion (Li & Lee, 2022). Both PLA and PLA+ were printed using white filament to allow easier colouring during the post processing stage and to better see the shaping quality and appropriateness of the chosen material for an intricate shape. While bio resin was printed in grey instead of clear filament to allow easier external colouring. It would be harder to achieve the desired colour if clear filament was used.

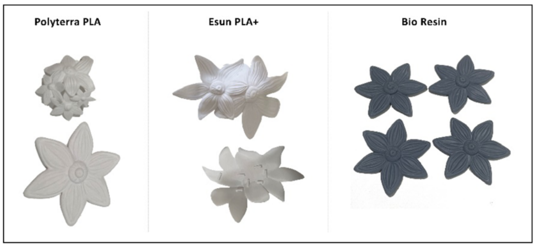

» **Figure 4:** *Initial prototype making*

Post Processing

For the post processing, nail buffer and sandpaper were used for preparation before the colouring as well as perfecting the printed samples for a shinier and more polished finish. By doing so it helped in smoothing visible surface imperfections as well as impacting the overall finish quality (Alzyod, Takacs & Ficzere, 2024; Sawant, Shinde & Raykar, 2023). The final prototypes were made using PLA+ and best coloured using Tamiya Acrylic with additional topcoat using Acrylo water based.

It gave a smoother finish and enough shine for the colour silver. Prior this, trials were conducted using different colourants and colourants combination using Tamiya Acrylic, Tamiya Enamel, Acrylo, Mr. Hobby water based, and Mr. Hobby lacquer. These paints were hand painted, and air brushed during the trials. Table 2 summarises the comparative evaluation on different colourants used for PLA and Bio Resin.

Table 2

Comparative Evaluation on Different Colourants

Colourant	PLA, PLA+	Bio Resin
Tamiya Acrylic	Silver very glossy and shiny, lightest silver than the other paints	Shinier and glossier than using enamel paint
Tamiya Enamel	Very opaque finish, high shine, good consistency	Shinier finish than PLA base; has a lighter shade
Tamiya Acrylic + Acrylo water based	Has slightly more shine, smoother finish, lighter silver	
Mr. Hobby: water based	Not adhere well, paint to is watery; sheer gloss	Like Tamiya Acrylic but not that ‘wet’; lighter shine
Mr. Color: lacquer	Very dull in colour, no shine	Very dull but since it is smoother, it has more shine compared to PLA base
Mr. Color: lacquer + Acrylo silver		More shine

To evaluate the functional performance of the 3D-printed fashion embellishment prototypes, several basic technical tests were conducted to assess flexibility, durability, surface quality, colour stability, and heat resistance. Prior studies noted that standard PLA tends to be brittle with low elongation (Subramani et al., 2024; Xiao & Kan, 2022), and this was confirmed through the technical tests conducted in this research. The flexibility test, which involved manually bending the embellishments to a 90° angle, resulted in fine surface cracks, demonstrating limited flexibility and reinforcing existing findings about PLA’s inherent rigidity. Durability assessments further supported this, as the prototypes remained intact when dropped from heights up to 1.5 meters but developed cracks and slight deformation when dropped from 2 meters, indicating moderate impact resistance. These behaviours are consistent with previous research describing PLA’s mechanical limitations and fragility under stress (Li & Lee, 2022).

Visual inspection of surface quality revealed a smooth and even top surface, while the underside exhibited a more textured, uneven finish, which is acceptable for embellishments since this area is not visible when attached to garments.

Previous studies have noted that heat and humidity exposure could degrade the results (Manoj & Panda, 2022; Goetjes, Zarges & Heim, 2024; Nugraha et al., 2023; Quader et al., 2024), this is in line with the colour consistency tests showing that prolonged exposure to heat caused noticeable yellowing, with higher temperatures intensifying the discoloration.

Heat-resistance testing further confirmed deformation above 160°C, reflecting the thermal sensitivity typical of PLA-based materials. These findings offer valuable insights into the prototypes' advantages and shortcomings, facilitating the assessment of their appropriateness for fashion embellishment applications where aesthetic appeal takes highest priority over high mechanical flexibility. Results from the mechanical and visual tests showed that PLA+ offered the best balance of flexibility, surface quality, and durability compared to Polyterra PLA and bio resin. While standard PLA was too rigid and bio resin too brittle, PLA+ withstood impact better and produced smoother printed surfaces, making it the most suitable material for the fashion embellishment.

To support the experimental findings, a questionnaire survey was conducted to assess public perceptions of 3D printing in fashion, their awareness and efficiency belief. The statistical results presented in Table 3 provide insight into how these technologies are perceived beyond the experimental context.

Table 3

Questionnaire results

Heard-before	Not sure	Yes, but only high fashion	Yes, reduces waste/ time	Row total
No	1	5	26	32
Yes	0	3	21	24
Column total	1	8	47	56

A chi-square test showed no significant association between prior awareness of 3D printing in fashion and respondents’ beliefs that 3D printing improves fashion production efficiency, $\chi^2(2)=0.91$, $p=0.64$, Cramer's $V=0.13$. The χ^2 and p is used to address the question whether there is evidence of a relationship or not, while Cramer’s V used to measure how strong the relationship is. The results show that the respondents largely believed 3D printing improves efficiency, with 83.9% selecting ‘Yes, by reducing waste and production time,’ 14.3% selecting ‘Yes, but only for high fashion or experimental designs,’ and 1.8% reporting uncertainty. This suggests that perceived efficiency benefits of 3D printing are broadly accepted within our respondents and do not differ meaningfully between respondents who had prior awareness and those who did not. In the context of this study, these findings reinforce the potential for biodegradable 3D-printed embellishments to be accepted as part of future fashion production, provided that material limitations and practical performance considerations are addressed. Furthermore, it highlights the value of exploring sustainable 3D-printing practices in relation to perceived benefits such as waste reduction.

Conclusion

By addressing material challenges and limitations, this study explored biodegradable materials for the creation of 3D printed fashion embellishments through a design-led and exploratory experimental approach. Evaluation was conducted through visual inspection and comparative qualitative analysis, focusing on surface smoothness, colour consistency, and overall aesthetic finish of the printed samples. While this approach is appropriate for early-stage material and design exploration, the absence of standardized instrumental measurements is acknowledged as a limitation. Future studies are therefore recommended to incorporate quantitative testing methods to further validate and extend the findings.

Table 4 summarizes the comparative evaluation of biodegradable options – Polyterra PLA, Esun PLA+, and bio resin – highlighting key characteristics, performance, and its suitability for garment embellishments. All three materials are suitable for making 3D printed embellishments however, their optimal use depends on the application requirements. While bio resin offers the highest level of detail for intricate and complex applications, its brittleness and cost make it less suitable for wearable components.

In contrast, standard PLA such as Polyterra PLA, with its lower elongation and rigidity, is better suited for decorative pieces or detachable elements that experience minimal physical stress. Modified PLA such as Esun PLA+ provides higher elongation and greater flexibility, making it more suitable for structural embellishments and wearable components that require both movement and durability.

Polyterra PLA is a biomass filled material blended with wood flour or corn starch, resulting in a matte surface texture, low odour, and a relatively low melting point. While it is easy to print and environmentally conscious, its mechanical performance is moderate, with noticeable brittleness under stress. This makes Polyterra PLA suitable for decorative or detachable eco conscious embellishments that experience low physical stress. On the other hand, Esun PLA+ is a modified PLA with strength additives like corn flour. From the experiment results, it shows that Esun PLA+ has a better flexibility that supports structural embellishments aligned with previous research. From a cost perspective, Polyterra PLA is the most affordable option, followed by PLA+, while bio resin remains the most expensive.

In this study, PLA+ emerged as the most appropriate material due to its balanced combination of strength, flexibility, and printability, producing prototypes that held their form while demonstrating better resilience and smoother surface finishes compared to Polyterra PLA and bio resin.

These combined findings particularly the improved surface quality, stronger impact resistance, and moderate flexibility offer clear empirical justification for selecting PLA+ as the primary material for the final embellishment prototype. This supports informed material selection and strengthens the integration of sustainable, functional 3D-printing practices within fashion design and production.

Across all materials, surface roughness could be minimized through sanding; however, the use of colorants, while improving aesthetics may negatively affect tensile strength. For a smoother surface finish can be achieved through airbrush painting, with the application of primer further enhancing gloss and surface uniformity.

Figure 5 depicts the making process of the 3D printed fashion embellishment while Figure 6 shows the various sizes and colour finishes of the 3D printed fashion embellishments that were created in this study. It began from the inspiration image that was taken as reference for visual and structural for the design model. Then digital model was created and sculpted using Nomad Sculpt with consideration to the scales, sizes, and arrangement for its application on the garment. It facilitated in conceptualising, refining the embellishment, and playing with scales and arrangement prior to the printing.

Once the design was achieved, it was 3D printed using PLA+ filament to create physical prototype. In the post-processing phase, the prototype was cleaned, sanded, and painted. Sanding is needed prior colouring to smoothen any rough edge and imperfections because of the printing. It was then hand painted using Tamiya Acrylic and top painted with same colour Acrylo water-based paint. The embellishments then were attached on to garment by stitching the loops to the fabric using sewing thread.

While the experimental results demonstrate aesthetic promise and sustainable design potential, further studies are needed to enhance the quality and functional performance of 3D printed embellishments. It would benefit from testing on a wider range of colouring techniques to better explore on the colorants, combinations, the application of top or base coat and colouring techniques to expand design possibilities.

Practical considerations on the aftercare in terms of cleaning and washing and embellishment attachment methods to garment must also be assessed. In addition, further study on material resistance to environmental factors namely heat, UV, and humidity is highly recommended to ensure long term wearability. Overall, this study contributes to the advancement of 3D printing by optimising biodegradable materials for a more sustainable and creative design potential for the fashion industry.

Table 4

Comparative Evaluation on Biodegradable Materials

<table>
<tr><th></th><th>Polyterra PLA</th><th>Esun PLA+</th><th>Bio Resin</th><th>Source</th></tr>
<tr><td>Material Composition</td><td>Biomass filled; blended with wood flour / corn starch</td><td>Modified PLA with strength additives like corn flour</td><td>Plant based: soybean oil, lactic acid, or castor oil</td><td>(Byjus, 2018; Khosravani & Reinicke, 2020; Conniff & Tewolde, 2022)</td></tr>
<tr><td rowspan="2">Key Characteristic</td><td>Matte texture, low odour, low melting point</td><td>Glossy finish, better layer adhesion, more flexible, stronger</td><td>Strong, high-detail finish, UV curable</td><td>(Cisneros-López et al., 2020)</td></tr>
<tr><td>Printing result just okay</td><td>Smoother finish</td><td>Shapes & lines are more defined</td><td>Based on experimentation</td></tr>
<tr><td>Durability</td><td>Moderate, somewhat brittle but improved; best for decorative – low stress embellishment</td><td>Better flexibility and strength for structural embellishments</td><td>For high detail embellishment, very intricate</td><td>Based on experimentation; (Li & Lee, 2022)</td></tr>
<tr><td>Resolution / Surface Quality</td><td>Achieve surface roughness 7-8 µm</td><td>Offers enhanced tensile strength with a better resolution</td><td>Can achieve as fine as 25-30 µm</td><td>(Lim et al., 2018; Mushtaq et al., 2024)</td></tr>
<tr><td>Heat / Water Resistance</td><td colspan="3">Environmental conditions like humidity and heat reduces the hardness and tensile strength with notable physical degradation and cracks</td><td>(Manoj & Panda, 2022; Goetjes, Zarges & Heim, 2024; Nugraha et al., 2023; Quader et al., 2024)</td></tr>
<tr><td rowspan="3">Post Processing</td><td colspan="3">Sanding is needed to improve surface roughness; colorants may enhance the visual appeal but may reduce tensile strength</td><td>(Alzyod, Takacs & Ficzere, 2024; Sawant, Shinde & Raykar, 2023; Son & Lee, 2020)</td></tr>
<tr><td>Best to colour using Tamiya Acrylic hand painted and top it off with same colour Acrylo water-based paint</td><td colspan="2">Hand painted for higher resolution of the lines; use Tamiya Enamel</td><td rowspan="2">Based on experimentation</td></tr>
<tr><td colspan="3">For smoother surface: air brush painting gives smoother finish; results are glossier, smoother, and shinier if primer is used</td></tr>
<tr><td>Price</td><td>Cheapest</td><td>Moderate</td><td>More expensive</td><td></td></tr>
<tr><td>Suitability for Garment Embellishment</td><td>Eco conscious embellishments; for detachable elements; with low physical stress</td><td>Good for structural and complex embellishments</td><td>Best for intricate and more complex application</td><td>Based on experimentation</td></tr>
</table>

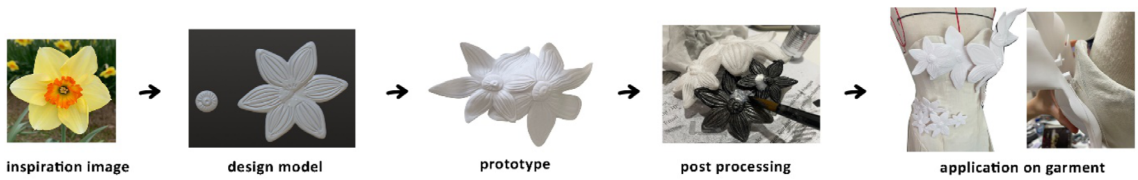

» **Figure 5:** *The making process of the 3D printed fashion embellishment*

» **Figure 6:** *The final 3D printed fashion embellishments*

Funding

This research did not receive any specific grant from funding agencies in the public, commercial, or not-for-profit sectors.

References

Adediran, A. A., Erinle, T. J., Ajewole, J. B. & Aliyu, S. J. (2024) Revolutionizing Mechanical Engineering: CAD'S Evolution, Cloud Impact And Future Trends. In: *2024 International Conference on Science, Engineering and Business for Driving Sustainable Development Goals, SEB4SDG, 2 - 4 April 2024, Omu-Aran, Nigeria*. New Jersey, IEEE. pp. 1–8. Available from: doi: 10.1109/SEB4SDG60871.2024.10630090

Alzyod, H., Takacs, J. & Ficzere, P. (2024) Improving surface smoothness in FDM parts through ironing post-processing. *Journal of Reinforced Plastics and Composites.* 43 (11-12), 671–681. Available from: doi: 10.1177/07316844231173059

Ambrosi, A. & Bonanni, A. (2021) How 3D printing can boost advances in analytical and bioanalytical chemistry. *Microchimica Acta.* 188 (8). Available from: doi: 10.1007/S00604-021-04901-2

Anaç, N., Koçar, O. & Altuok, C. (2024) Investigation of The Weldability of PLA Plus Sheets with Different Infill Ratios by Friction Stir Welding. *Gazi University Journal of Science Part C: Design and Technology.* 12 (1), 282–296. Available from: doi: 10.29109/gujsc.1399512

Byjus (2018) *Biodegradable and non-biodegradable - Definition & examples of biodegradable and non-biodegradable*. Available from: https://byjus.com/chemistry/biodegradable-and-non-biodegradable/ [Accessed 23rd March 2026].

Cisneros-López, E. O., Pal, A. K., Rodriguez, A. U., Wu, F., Misra, M., Mielewski, D. F., Kiziltas, A. & Mohanty, A. K. (2020) Recycled poly(lactic acid)–based 3D printed sustainable biocomposites: a comparative study with injection molding. *Materials Today Sustainability.* 7-8, 100027. Available from: doi: 10.1016/j.mtsust.2019.100027

Conniff, M. & Tewolde, M. (2022) *26 Types of 3D Printer Filament*. Xometry. Available from: https://www.xometry.com/resources/3d-printing/types-of-3d-printer-filaments/ [Accessed 23rd March 2026].

Deabler, A. (2017) *World's first 3D printed jacket costs $1,500*. New York Post. Available from: https://nypost.com/2017/07/28/worlds-first-3d-printed-jacket-costs-1500/ [Accessed 23rd March 2026].

Dueñas-Moreno, J., Mora, A., Kumar, M., Meng, X. Z. & Mahlknecht, J. (2023) Worldwide risk assessment of phthalates and bisphenol A in humans: The need for updating guidelines. *Environment International.* 181, 108294. Available from: doi: 10.1016/j.envint.2023.108294

EDI (n.d.) *The State of Biodegradable Materials in Additive Manufacturing: Facts, Developments and Use Cases*. EDI. Available from: https://www.ediweekly.com/the-state-of-biodegradable-materials-in-additive-manufacturing-facts-developments-and-use-cases/#:~:text=One%20significant%20challenge%20with%20biodegradable,and%20flexibility%20of%20traditional%20plastics [Accessed 23rd March 2026].

European Bioplastics (2024) *BIOPLASTICS MARKET DEVELOPMENT UPDATE 2025.* Available from: https://www.european-bioplastics.org/market/ [Accessed 23rd March 2026].

Filamatrix Staff (2024) *The Eco-Friendly Traits of PLA 3D Printing Filament*. Filamatrix. Available from: https://filamatrix.com/blogs/blogs/the-eco-friendly-traits-of-pla-3d-printing-filament [Accessed 23rd March 2026].

Goetjes, V., Zarges, J. & Heim, H. (2024) Resistance of poly(lactic acid)/starch composites to weathering effects. *Journal of Applied Polymer Science.* 141 (2). Available from: doi: 10.1002/app.54768

Goryl, K., Pollák, M., Kočiško, M. & Korol', M. (2024) Comparison of PLA and PLA Carbon Fiber Materials on Tensile Test. In: Gapiński, B., Ciszak, O., Ivanov, V. and Machado, J. M. (eds.) *International Scientific-Technical Conference MANUFACTURING 2024, Advances in Manufacturing IV, Volume 1 - Mechanical Engineering: Digitalization, Sustainability and Industry Application, 14 – 16 May 2024, Poznan, Poland*. Cham, Springer. pp. 73–82. Available from: doi: 10.1007/978-3-031-56463-5_6

Gudaitiene, R., Minkus, V. & Darulis, A. (2025) Calibration of the printing process for 3D models using Vat polymerisation and investigation of the mechanical properties of TGM-7 resin. *Journal of Graphic Engineering and Design.* 16 (3), 29–40. Available from: doi: 10.24867/JGED-2025-3-029

Guimapang, K. (2019) *A Conversation With Julia Koerner, Architecture's Queen of 3D Fabrication*. Archinect. Available from: https://archinect.com/features/article/150132998/a-conversation-with-julia-koerner-architecture-s-queen-of-3d-fabrication [Accessed 23rd March 2026].

Holgate, M. (2016) *Dutch Designer Iris van Herpen on 3-D Printing and the Future of Fashion*. Vogue. Available from: https://www.vogue.com/article/iris-van-herpen-dutch-designer-interview-3d-printing [Accessed 23rd March 2026].

Hong, C., Choi, C. & Han, D. (2009) Development of Bio-Polylactic Acid Materials for Eco-friendly Automotive Parts. *The Korean Society Of Automotive Engineers*, 2622–2627.

Idea3D (2015) *Koleksi Tex Saverio menggunakan teknik 3D printing*. Idea3D 3D Maker & Printing Service. Available from: https://www.idea3d.id/2015/04/koleksi-tex-saverio-menggunakan-teknik.html [Accessed 23rd March 2026].

IUCN (2024) *Plastic pollution*. IUCN. Available from: https://iucn.org/resources/issues-brief/plastic-pollution [Accessed 23rd March 2026].

Jandyal, A., Chaturvedi, I., Wazir, I., Raina, A. & Ul Haq, M. I. (2022) 3D printing – A review of processes, materials and applications in industry 4.0. *Sustainable Operations and Computers.* 3, 33–42. Available from: doi: 10.1016/j.susoc.2021.09.004

Khosravani, M. R. & Reinicke, T. (2020) On the environmental impacts of 3D printing technology. *Applied Materials Today.* 20, 100689. Available from: doi: 10.1016/j.apmt.2020.100689

Kuswanto, D., Hapinesa, O. M., Prihandana, D. B., Iftira, N. J., Wariswantika, I. & Kumalasari, A. I. (2017) Indonesian Pattern for 3D Printing Fashion Development. In: *The 4th International Conference on Creative Industry, 11 - 12 October 2017, Surabaya, Indonesia*.

Li, Y. & Lee, Y.-A. (2022) The Potential Use of PLA and Soft PLA in 3D Printing for Sustainable Wearables. In: *International Textile and Apparel Association Annual Conference Proceedings, ITAA, Virtual Conference*. Ames, Iowa State University Digital Press. Available from: doi: 10.31274/ITAA.13455

Lim, K. S., Levato, R., Costa, P. F., Castilho, M. D., Alcala-Orozco, C. R., van Dorenmalen, K. M. A., Melchels, F. P. W., Gawlitta, D., Hooper, G. J., Malda, J. & Woodfield, T. B. F. (2018) Bio-resin for high resolution lithography-based biofabrication of complex cell-laden constructs. *Biofabrication.* 10 (3), 034101. Available from: doi: 10.1088/1758-5090/aac00c

Madeline, P. (2023) *The different types of resins available for 3D printing*. 3Dnatives. Available from: https://www.3dnatives.com/en/different-types-of-resins-3d-printing-281220225/# [Accessed 23rd March 2026].

Manoj, A. A. & Panda, R. C. (2022) Biodegradable Filament for 3D Printing Process: A Review. *Engineered Science.* 18, 11-19. Available from: doi: 10.30919/ES8D616

Mushtaq, R. T., Wang, Y., Bao, C., Rehman, M., Sharma, S., Khan, A. M., Eldin, E. M.-T. & Abbas, M. (2024) Maximizing performance and efficiency in 3D printing of polylactic acid biomaterials: Unveiling of microstructural morphology, and implications of process parameters and modeling of the mechanical strength, surface roughness, print time, and print energy for fused filament fabricated (FFF) bioparts. *International Journal of Biological Macromolecules.* 259, 129201. Available from: doi: 10.1016/j.ijbiomac.2024.129201

Nugraha, A. D., Mamba'udin, A., Susanto, B., Kusni, M., Darmanto, S., Santos, G. N. & Akhsin Muflikhun, M. (2023) The influence of long-term hydrothermal and physical ageing on the characteristics of additively manufactured bio-based photopolymer resin. *Results in Materials.* 20, 100499. Available from: doi: 10.1016/j.rinma.2023.100499

Oladapo, B. I., Bowoto, O. K., Adebiyi, V. A. & Ikumapayi, O. M. (2023) Net zero on 3D printing filament recycling: A sustainable analysis. *Science of The Total Environment.* 894, 165046. Available from: doi: 10.1016/j.scitotenv.2023.165046

Olawumi, M. A., Oladapo, B. I., Ikumapayi, O. M. & Akinyoola, J. O. (2023) Waste to wonder to explore possibilities with recycled materials in 3D printing. *Science of The Total Environment.* 905, 167109. Available from: doi: 10.1016/j.scitotenv.2023.167109

Polygenis, T. (2023) *PLA vs PLA+: A Comprehensive Comparison*. Wevolver. Available from: https://www.wevolver.com/article/pla-vs-pla-plus [Accessed 23rd March 2026].

Pratama, W. H. & Hasdiansah. (2021) Pengaruh parameter proses terhadap kuat tarik spesimen uji astm d638 type iv menggunakan filamen esun pla. In: *Prosiding Seminar Nasional Inovasi Teknologi Terapan, SNITT 2021, 2 August 2021, Sungai Liat, Indonesia*. Sungai Liat, Politeknik Manufaktur Negeri Bangka Belitung. pp. 210-215. Available from: https://snitt.polman-babel.ac.id/index.php/snitt/article/view/72/36 [Accessed 23rd March 2026].

Printerra (2023) *The Environmental Impact of 3D House Printing*. Available from: https://printerra.ca/environmental-impact-of-3d-house-printing/ [Accessed 23rd March 2026].

Quader, R., Dramko, E., Grewell, D., Randall, J. & Narayanan, L. K. (2024) Characterizing the Effect of Filament Moisture on Tensile Properties and Morphology of Fused Deposition Modeled Polylactic Acid/Polybutylene Succinate Parts. *3D Printing and Additive Manufacturing.* 11 (3), 1151–1161. Available from: doi: 10.1089/3dp.2022.0222

Rodríguez-Hernández, A. G., Chiodoni, A., Bocchini, S. & Vazquez-Duhalt, R. (2020) 3D printer waste, a new source of nanoplastic pollutants. *Environmental Pollution.* 267, 115609. Available from: doi: 10.1016/j.envpol.2020.115609

RS Design Spark (n.d.) *DesignSpark CAD Design & 3D Modelling Software*. Available from: https://www.rs-online.com/designspark/mechanical-software [Accessed 23rd March 2026].

Ruckdashel, R. R., Venkataraman, D. & Park, J. H. (2021) Smart textiles: A toolkit to fashion the future. *Journal of Applied Physics.* 129 (13). Available from: doi: 10.1063/5.0024006

Sawant, D. A., Shinde, B. M. & Raykar, S. J. (2023) Post processing techniques used to improve the quality of 3D printed parts using FDM: State of art review and experimental work. *Materials Today: Proceedings.* Available from: doi: 10.1016/j.matpr.2023.09.202

Shahrubudin, N., Lee, T. C. & Ramlan, R. (2019) An Overview on 3D Printing Technology: Technological, Materials, and Applications. *Procedia Manufacturing.* 35, 1286–1296. Available from: doi: 10.1016/j.promfg.2019.06.089

Sheikh, J. A., Waheed, M. F., Khalid, A. M. & Qureshi, I. A. (2020) Use of 3D Printing and Nano Materials in Fashion: From Revolution to Evolution. In: Di Bucchianico, G. (ed.) *Advances in Design for Inclusion - Proceedings of the AHFE 2019 International Conference on Design for Inclusion and the AHFE*

2019 International Conference on Human Factors for Apparel and Textile Engineering, 24 – 28 July 2019, Washington D.C. Cham, Springer. pp. 422–429. Available from: doi: 10.1007/978-3-030-20444-0_43

Singh, S. (2021) *HISTORY OF CAD TOOLS IN GARMENT DESIGNING: A REVIEW*. Available from: https://www.researchgate.net/publication/349686476_HISTORY_OF_CAD_TOOLS_IN_GARMENT_DESIGNING_A_REVIEW [Accessed 23rd March 2026].

Son, J. & Lee, H. (2020) Preliminary Study on Polishing SLA 3D-Printed ABS-Like Resins for Surface Roughness and Glossiness Reduction. *Micromachines.* 11 (9), 843. Available from: doi: 10.3390/MI11090843

Subramani, R., Mustafa M. A., Ghadir, G. K., Al-Tmimi, H. M., Alani, Z. K., Rusho, M. A., Rajeswari, N., Haridas, D., Rajan, A. J. & Kumar, A. P. (2024) Exploring the use of Biodegradable Polymer Materials in Sustainable 3D Printing. *Applied Chemical Engineering.* 7 (2), 3870. Available from: doi: 10.59429/ace.v7i2.3870

Sun, L. & Zhao, L. (2017) Envisioning the era of 3D printing: a conceptual model for the fashion industry. *Fashion and Textiles.* 4 (1). Available from: doi: 10.1186/S40691-017-0110-4

Warnier, C. (ed.), Verbruggen, D. (ed.), Ehmann, S. (ed.) & Klanten, R. (ed.) (2014) *Printing things : visions and essentials for 3D printing*. Berlin, Gestalten.

Xiao, Y. Q. & Kan, C. W. (2022) Review on Development and Application of 3D-Printing Technology in Textile and Fashion Design. *Coatings.* 12 (2), 267. Available from: doi: 10.3390/COATINGS12020267

Yoo, H. (2025) *Additive manufacturing and 3D printing - statistics & facts*. Statista. Available from: https://www.statista.com/topics/1969/additive-manufacturing-and-3d-printing/#topicOverview [Accessed 23rd March 2026].

Žarko, J., Vladić, G., Pál, M. & Dedijer, S. (2017) Influence of printing speed on production of embossing tools using fdM 3d printing technology. *Journal of Graphic Engineering and Design.* 8 (1), 19–27. Available from: doi: 10.24867/JGED-2017-1-01

 http://doi.org/10.24867/JGED-2026-3-047

Effects of image form and model body shape in healthy eating advertisements on health perceptions and emotional responses

ABSTRACT

Mass media has become an essential channel for promoting healthy eating while preventing non-communicable diseases. However, the design forms of advertisement health messages can affect consumers' attitudes toward advertising and their health perceptions. This study adopted an experimental design to explore the effects of fruit and vegetable image design forms (anthropomorphic, photographic, and geometric) and model body shapes (no model, obese, overweight, normal, and thin) on health perceptions and emotional responses. The findings indicate that when the model's body shape was "normal," anthropomorphic fruit and vegetable designs significantly improved health perceptions; when the model's body shape deviated from health standards (e.g., thin or obese), photographic and geometric designs may weaken health perceptions. The body shape of the advertisements' models was the main factor affecting emotional responses. Advertisements with thin or obese models were more likely to cause negative emotions, while normal body shapes can maintain emotional stability. When designing healthy eating advertisements, selecting anthropomorphic fruit and vegetable images and models with normal body shapes can strengthen health perceptions while reducing negative emotional responses, improving advertising effectiveness.

Shy-Peih Huarng

National Chin-Yi University of Technology, Taichung, Taiwan

Corresponding author:
Shy-Peih Huarng
e-mail:
paandko@gmail.com

First received: 13.3.2025.
Revised: 31.8.2025.
Accepted: 22.9.2025.

KEY WORDS
image form, model body shape, health perception

Introduction

With increasingly severe obesity and chronic diseases caused by unbalanced diets in recent years, advertisements for healthy eating have attracted significant attention from consumers and public health departments (Chrysochou & Grunert, 2014).

In Taiwan, obesity among young people is severe. Taiwan's Nutrition and Health Survey 2020 showed that the amount of physical activity among young people is generally low, and high-intensity exercise further declines as people age, increasing the risk of developing non-infectious and chronic inflammatory diseases.

Thus, effectively conveying the importance of a balanced diet and exercise has become a core issue in current health advocacy.

Fruit and vegetable images are common visual elements in healthy eating advertisements, symbolizing "nature" and "health."

However, there is a lack of in-depth discussion on the impact of fruit and vegetable image design forms (e.g., anthropomorphic, photographic, geometric) on consumers' perceptions and emotional responses. Furthermore, research suggests that adding sports images to dietary advertisements can enhance positive emotions and behavioral intentions (Chrysochou & Grunert, 2014; Dixon et al., 2015); dynamic images attract attention more than static images, evoke positive emotions (Cian, Krishna & Elder, 2014), and give products a sense of vitality (Ruiter, 2019). Sports images can also help reduce negative emotions caused by dietary warnings (Horn & Jongenelis, 2022), further influencing consumers' dietary attitudes and behaviors (Rosenblatt et al., 2019).

Therefore, this study aims to examine the design form of fruit and vegetable images, including sports elements, to analyze their impact on advertising effectiveness.

The body shape of models, as an essential visual message in advertising, also impacts consumers' perceptions of and attitudes toward the advertising content. Past advertisements often used thin models to enhance appeal, which may lead to consumers developing misunderstandings surrounding healthy body shape (Garner et al., 1980), leading to eating imbalances and psychological anxiety (Bower, 2001; Halliwell & Dittmar, 2004). Thin female models are often regarded as a negative idealized stereotype (Stephens, Hill & Hanson, 1994). Although men are less affected by this stereotype, their attitudes toward advertisements are still affected by models' body shapes (Janssen & Paas, 2014).

Based on the above, this study aims to explore the impact of fruit and vegetable image design forms and model body shapes on the effectiveness of healthy eating advertisements to analyze their effects on health perceptions and emotional responses. The findings provide specific suggestions for the visual design of healthy eating advertisements, improving advertising while providing social benefits.

Literature Review

Message Design for Healthy Eating

Increasing rates of obesity and chronic diseases caused by unbalanced diets in countries worldwide have prompted governments and companies to actively promote healthy eating (Chrysochou & Grunert, 2014). Common message design methods can be divided into health and nutritional statements (Ippolito & Pappalardo, 2002).

The former emphasizes a product's benefits on a specific body part (e.g., promoting heart health). The latter focuses on nutrients (e.g., being rich in vitamin A). Such text-based messages have been shown to promote consumers' positive feelings and purchase intentions towards a product while reducing perceptions of disease risk (Kozup, Creyer & Burton, 2003).

However, Chrysochou and Grunert (2014) found that graphical messages can attract greater attention, evoking emotional responses more effectively than simple text.

Their study divided health information into functional statements (e.g., being rich in calcium to strengthen bones), process statements (e.g., local production), and health images (e.g., sports scenes). The results indicated that health images significantly impacted consumers' health perceptions and purchase intentions.

This is because images have associative and emotional triggering power, which can evoke emotional reactions from different consumers, further enhancing advertising effectiveness.

Emotional responses are essential in advertising effectiveness. Although negative warning messages (e.g., the risk of obesity) can attract attention, they can easily stimulate consumers' shame and anxiety (Horn & Jongenelis, 2022). In contrast, positive encouragement messages (e.g., sports scenes) can induce positive emotions, such as hope and humor, enhancing consumers' willingness to engage in healthy behaviors. Horn and Jongenelis (2022) showed that health advertisements with hope and power encouraged consumers to change behaviors most effectively; animation-style encouraging advertisements can also reduce negative emotions and physical humiliation.

Although existing research has confirmed the importance of image forms in the effectiveness of healthy eating (Chu, Hetherington & Tang, 2024) and the ability of advertisements with fruit and vegetable images to increase fruit and vegetable consumption (Oke & Tan, 2022), in-depth discussions on fruit and vegetable image design forms (e.g., photos vs. illustrations) and the combination of sports images are limited. This study further analyzed the combination of graphic design forms for fruit and vegetables with sports elements to understand consumers' health perceptions and emotional responses.

Advertisement Models’ Body Shape

In the visual design of advertisements, a model's body shape is not only a representative image of the product but also carries societal expectations regarding an “ideal body” (Messaris & Humphreys, 2006). Many healthy eating advertisements opt for slim models because they are considered more attractive, increasing sales (Antioco, Smeesters & Le Boedec, 2012). However, images with thin models have long been found to negatively impact consumers, especially women. An earlier study by Garner et al. (1980) indicated that thin models create unrealistic body standards, leading women to have negative evaluations of their body shapes, increasing the risk of anorexia and eating disorders (Bower, 2001; Halliwell & Dittmar, 2004).

The Social Comparison Theory, proposed by Festinger (1954) states that consumers tend to compare themselves with models in advertisements. When a model's appearance or figure is regarded as an “ideal standard,” it may easily lead to consumer dissatisfaction and anxiety. Studies suggest that approximately 50% to 75% of women of normal weight believe they are overweight, while only 25% of men of normal weight feel the same (Stephens, Hill & Hanson, 1994). This gender difference reflects that women are more subject to the influence of media images.

Furthermore, the preference for a slim body size has extended to Asia, including countries and regions such as Taiwan, China, Singapore, and India (D'Alessandro & Chitty, 2011). Therefore, long-term negative perceptions of the body shapes and self-deprecation from social pressure have become risk factors for women's health (Saunders, Nutter & Russell-Mayhew, 2022).

Recent research advocates using normal and plus-size models in advertising to help consumers resonate with “a sense of closeness to themselves” (Halliwell & Dittmar, 2004; Yu, Damhorst & Russell, 2011). While this can reduce negative emotions and competitive psychology (Janssen & Paas, 2014), improve consumers’ appreciation of the models' body shapes, brand attitudes and brand/product memories (Wallhead, Furnham & McClelland, 2025), slim models are still more mainstream (Halliwell & Dittmar, 2004). While current research has focused on the impact of model body shape on consumer attitudes, exploring its interaction with fruit and vegetable graphic design forms is limited. Thus, this study examined how models' body shapes affect consumers' health perceptions and emotional responses while proposing more effective advertisement design strategies.

Based on the above, this study proposed the following hypotheses. Hypothesis A: In healthy eating advertisements, the graphic design form of fruits and vegetables and the body shape of running models interact to affect consumers' health perceptions. Hypothesis B: In healthy eating advertisements, the graphic design form of fruits and vegetables and the body shape of the running models interact to affect consumers' emotional responses.

Research Method

This study adopted an experimental design. The design form and the models’ body shape were taken as the variables to examine the subjects' health perceptions and emotional responses.

Sample Selection

The method for collecting healthy eating samples was based on Google's search engine. We extensively collected designs with healthy eating images without limiting the types of commercial and public welfare advertisements or the presentation of advertisements and general illustrations. A total of 91 samples were collected.

Next, a literature review related to advertisement design was conducted. Two design experts were invited to classify graphic design forms, including one teacher with more than 15 years of graphic design teaching experience and one designer with 15 years of design experience. It was learned that healthy eating is most commonly presented by fruits and vegetables. The most common design forms are as follows: realistic (78%), geometric (20%), and anthropomorphic (18%).

Therefore, regarding fruit and vegetable image design, we selected three categories of realistic photos, and anthropomorphic and geometric illustrations for design. Three designers were asked to design images based on fruit and vegetable shapes. Next, the two design experts from the initial market survey were invited to evaluate and determine whether the image types matched (Figure 1).

The advertising layout design was simulated based on the graphic advertisement design by the Health Promotion Administration (MOHW) to promote healthy eating.

About two-thirds of the layout was dedicated to the three vegetable and fruit design forms, with the title and text placed in the center. The main headline was Healthy Eating Movement, and the subtitle, in both Chinese and English, read “Replenish Your Body's Energy.” The nutritional information for each vegetable and fruit was placed below its respective image; a health attribute logo was positioned in the lower center. Three samples were created (Figure 1).

Three categories | Photographs | Anthropomorphism | Geometric

» **Figure 1:** *Three design forms*

The body shape design of the running model was based on the profile of male and female characters, with a black and white illustrative design (Figure 3). Stunkard's (1983) nine types of body design were adopted for the male and female models' body design (Lancki et al., 2018). The Stunkard Scale exhibits a silhouette character rating scale comprising nine men and nine women. Models increase in size, with weight indicated by numbers: 1 = underweight; 2 to 4 = healthy weight; 5 to 6 = overweight; 7 to 9 = obese/seriously overweight, as a perception of body image (Cachelin et al., 2002; Lancki et al., 2018), as shown in Figure 2.

This study used numbers 2, 4, 6, and 8 to represent four types (thin, normal, overweight, and obese) as the basis for differences in model body design (Figure 3). The questionnaire was designed to ask subjects to assess their weight perception based on four body shapes (1 = extremely underweight to 7 = extremely overweight). The results showed that there were significant differences between the four model body shapes ($F=713.63$, $p=.00<.05$) of thin ($M=2.79$), normal ($M=4.10$), overweight ($M=5.62$), and obese ($M=6.60$). Regarding advertising layout, the healthy eating advertisements were the basis (Figure 1) to include running images in the middle of the text (Figure 4). This study used four body shapes for both male and female models, comprising eight model samples. Three samples featured only vegetable and fruit images, and 24 samples combined these images with model figures, totaling 27 samples.

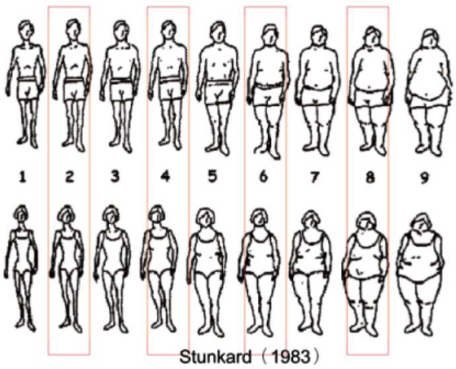

» **Figure 2:** *Stunkard (1983)'s Nine Model Body Shape*

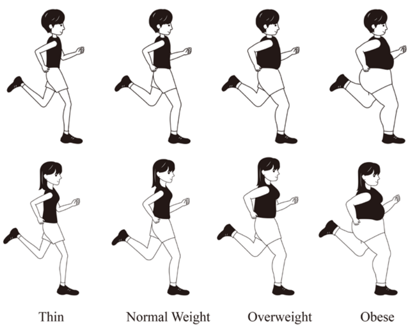

» **Figure 3:** *Model Body Samples Design*

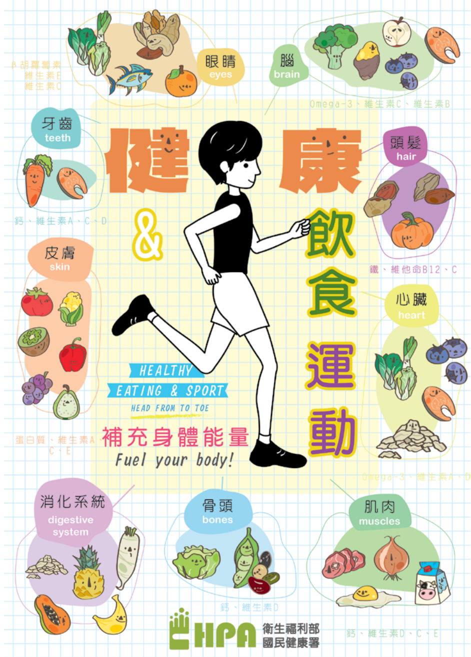

» **Figure 4:** *Sample Design*

Questionnaire Design

In the questionnaire design, at the beginning, subjects were asked to evaluate their weight perception based on four body shapes (1 = extremely underweight to 7 = extremely overweight) to determine whether there were differences regarding the four model body shapes.

Next, subjects watched 27 advertisement samples. The questionnaire items were designed based on the evaluation by Rosenblatt et al. (2019) regarding the impact of messages and images on the perception of food health warnings. It focused on the three aspects of health perception effectiveness, negative emotional responses, and changes in behavioral motivation. The items were modified to fit this study, leading to nine items.

This study used negative emotional responses for emotional design. This is primarily because consumers' emotional responses would be affected by warning messages about healthy eating, models' appearance and body shape, and related messages with weight loss implications (Bower, 2001; Horn & Jongenelis, 2022). Therefore, this study used negative emotions to design the emotional response items. The health perception effectiveness items were designed as: "This advertisement encourages people to buy healthier food," "This advertisement makes me worry about my weight/eating habits," and "This advertisement makes me confident in my ability to maintain a healthy weight/healthy diet." The negative emotional response items were: "This advertisement makes me feel anxious," "This advertisement makes me feel sad," and "This advertisement makes me feel uncomfortable."

The items for changes in behavioral motivation were: “This advertisement makes me feel motivated to maintain a healthy weight/healthy diet,” “This advertisement makes me feel inspired,” and “This advertisement makes me feel full of hope.” The above items were measured on a 7-point scale (1 = strongly disagree and 7 = strongly agree). The subjects' assessment of self-perceived weight was based on Horn and Jongenelis (2022). The subjects were also asked to conduct a weight assessment based on their own feelings, evaluated on a 5-point Likert scale (1 = extremely underweight and 5 = extremely overweight).

Research Subjects

The study subjects were college students. Voluntary college students were recruited online to participate in an online survey questionnaire. A total of 86 subjects (including nine males) were recruited. Each subject was instructed to complete the survey based on their feelings regarding healthy eating advertisements without knowing the research hypotheses. Subjects were asked to respond according to their perceptions.

Upon completing the survey, a 7-Eleven gift card worth NTD 100 was mailed to each subject as compensation. Personal information was not disclosed to others during the experiment, and all information regarding the subjects was deleted upon completion of the experiment.

Result

The study focused on healthy eating advertisement designs tailored to consumers with different self-perceived body weights. The actual distribution of self-reported body weight among the recruited participants was as follows: underweight ($n = 7$), normal weight ($n = 41$), overweight ($n = 33$), and obese ($n = 5$). Statistical analysis revealed no significant differences in health perception ($p =.69 >.05$), emotional response ($p =.83 >.05$), or behavioral change ($p =.65 >.05$) among these groups.

Therefore, this study did not further discuss the impact of self-perceived body weight on the effectiveness of healthy eating advertisements.

A correlation analysis was conducted to examine the relationships among health perception, emotional response, and behavioral change. The Pearson correlation analysis results indicate a significant positive correlation between health perception ($M = 3.47$, $SD =.74$) and behavioral change ($M = 3.54$, $SD =.90$) ($r =.72$, $p =.00 <.05$), suggesting that higher health perception is associated with greater behavioral change. Emotional response ($M = 2.84$, $SD =.99$) demonstrated a moderate correlation with health perception ($r =.47$, $p =.00 <.05$) and behavioral change ($r =.30^*$, $p =.00 <.05$).

Given these relationships, the discussion of results in the following focuses on the correlation between health perception and behavioral change.

Effects of Image Form and Model Body Shape in Health Perception

This study employed a two-way repeated measures ANOVA to examine the effects of different design forms (photographic, anthropomorphic, and geometric) and model body shapes (no model, overweight, obese, normal, and thin) on health perception. Table 1 presents the means and standard deviations for each condition. Overall, participants assigned the highest ratings to the “photographic-normal” ($M = 3.901$, $SD = 1.021$) and “anthropomorphic-normal” ($M = 3.971$, $SD = 1.037$) conditions, whereas the “geometric-obese” condition received the lowest rating ($M = 2.958$, $SD = 1.117$).

Multivariate tests indicated a significant main effect of design forms (Pillai’s Trace = .094, $F(2, 84) = 4.347$, $p = .016$, $\eta p^2 = .063$; see Table 2). The corresponding repeated-measures ANOVA also showed a significant main effect of design form, $F(2, 170) = 5.677$, $p = .004$, $\eta p^2 = .063$ (see Table 3). Mean comparisons revealed that the anthropomorphic design ($M = 3.623$, $SD = 0.084$) was associated with slightly higher health perception ratings than the photographic ($M = 3.501$, $SD = 0.085$) and geometric designs ($M = 3.494$, $SD = 0.090$). These findings suggest that anthropomorphic representations may enhance participants’ health perception more effectively than other formats, see Table 2.

The main effect of model body shapes was also significant (Pillai’s Trace = .394, $F(4, 82) = 13.316$, $p < .001$, $\eta p^2 = .221$; see Table 2). The repeated-measures ANOVA likewise revealed a significant main effect of model body shape, $F(4, 340) = 24.074$, $p < .001$, $\eta p^2 = .221$ (see Table 3). Further analysis revealed that models with a “normal” body shape ($M = 3.879$, $SD = 0.108$) and the “no model” condition ($M = 3.868$, $SD = 0.109$) received the highest health perception ratings, with no significant difference between them ($p = 0.909$). Conversely, the “obese” ($M = 3.065$, $SD = 0.109$) and “thin” ($M = 3.440$, $SD = 0.093$) conditions were rated lowest, with significantly lower scores than other body shapes ($p < 0.001$). These results indicate that models with a moderate body shape (i.e., “normal”) enhance health perception, whereas models at either extreme (overweight or underweight) may negatively affect participants’ health-related evaluations, see Table 3.

Additionally, the interaction effect between design forms and model body shapes was significant (Pillai’s Trace = .301, $F(8, 78) = 4.198$, $p < .001$, $\eta p^2 = .040$; see Table 2). The repeated-measures ANOVA also indicated a significant interaction effect, $F(8, 680) = 3.514$, $p = .001$, $\eta p^2 = .040$ (see Table 3), suggesting that the combination of design forms and model body shapes jointly influences health perception. When the model had a normal body shape, the anthropomorphic design condition (M = 3.971, SD = 0.112) received the highest health perception ratings, significantly higher than the geometric design condition (M = 3.766, SD = 0.124, p = 0.009). On the other hand, when the model was obese, both the photographic and geometric designs resulted in lower health perception ratings, whereas the anthropomorphic design demonstrated a relatively smaller negative impact (M = 3.137, SD = 0.107).

These findings suggest that when the model's body shape aligns with ideal health standards (e.g., "normal"), anthropomorphic design can further enhance health perception. However, when the model's body shape deviates from health norms (e.g., "obese"), photographic and geometric designs may further diminish health perception.

Figure 5a illustrates health perception ratings across different model body shapes for each design form, showing that models with a "normal" body shape consistently received higher ratings, regardless of

Table 1

Descriptive Statistics

		Model body shapes					
		No model (M±SD)	**Obese (M±SD)**	**Overweight (M±SD)**	**Normal (M±SD)**	**Thin (M±SD)**	**Total (M±SD)**
Design Forms	Photographs	3.93±1.15	3.10±1.12	3.37±1.03	3.90±1.02	3.21±.92	3.50±.09
	Anthropomorphism	3.83±1.20	3.14±1.00	3.57±0.99	3.97±1.04	3.60±1.03	3.62±.08
	Geometric	3.85±1.28	2.96±1.12	3.40±.98	3.77±1.15	3.50±.93	3.49±.09
	Total	3.87±.11	3.07±.11	3.45±.10	3.88±.11	3.44±.09	-

Table 2

Multivariate Tests

	Pillai's Trace	**Wilks' Lambda**	**F**	**df**	**p**	**η^2**
Design forms (A)	0.094	0.906	4.347	(2, 84)	0.016	.063
Model body shapes (B)	0.394	0.606	13.316	(4, 82)	0.000	.221
Interaction: A × B	0.301	0.699	4.198	(8, 78)	0.000	.040

Table 3

ANOVA Results for Main Effects

	SS	**df**	**MS**	**F**	**p**
Design forms (A)	4.490	2	2.245	5.677	0.004
Model body shapes (B)	120.507	4	30.127	24.074	0.000
Interaction: A × B	8.621	8	1.078	3.514	0.001
Error (A)	67.217	170	0.395	-	-
Error (B)	425.484	340	1.251	-	-

$p < 0.05$, $p < 0.01$*, $p < 0.001$

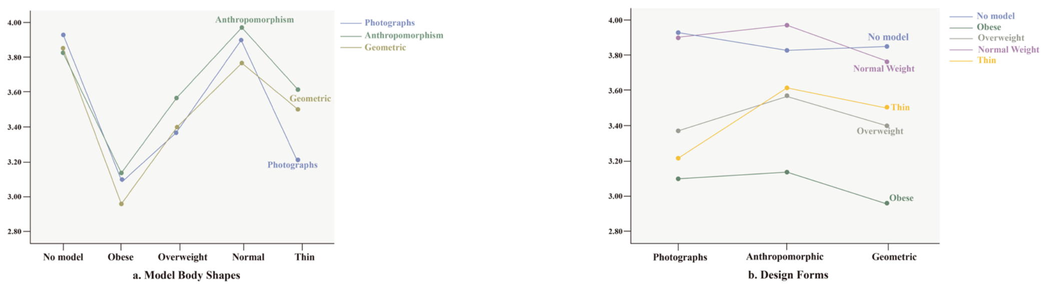

» **Figure 5:** *Image Form and Model Body Shape, (a) Model Body Shapes (b) Design Forms* design forms, while obese models were rated lowest. Figure 5b presents health perception ratings across design forms for each model body shape, demonstrating that anthropomorphic and photographic designs received higher ratings when they had normal or thin body shapes, whereas the geometric-obese condition received the lowest health perception ratings. These findings are consistent with the statistical results from the ANOVA, confirming that the combination of advertisement design forms and model body shapes significantly influences participants' health perception.

Effects of Image Form and Model Body Shape in Negative Emotional Responses

A two-way repeated measures ANOVA was also conducted to assess the impact of design forms and model body shapes on emotional responses. Table 4 presents the means and standard deviations for each condition. The results indicate that the "geometric-obese" (M = 3.56, SD = 1.64) and "photographic- obese" (M = 3.46, SD = 1.53) conditions elicited the highest emotional response ratings, whereas the "anthropomorphic-no model" (M = 2.171, SD = 1.168) and "geometric-no model" (M = 2.174, SD = 1.247) conditions had the lowest ratings. The main effect of design forms was not statistically significant (Pillai's Trace = 0.065, $F(2, 84) = 2.904$, $p = 0.060$, $\eta^2 = 0.041$), suggesting that design forms alone did not significantly affect emotional responses. However, the main effect of model body shapes was significant (Pillai's Trace = 0.460, $F(4, 82) = 17.470$, $p < 0.001$, $\eta^2 = 0.266$), indicating a substantial influence of model body shapes on participants' emotional reactions. Additionally, the interaction effect between design forms and model body shapes approached significance (Pillai's Trace = 0.173, $F(8, 78) = 2.040$, $p = 0.052$, $\eta^2 = 0.023$), suggesting a potential joint influence of these factors on emotional response (see Table 5).

Further pairwise comparisons among model body shapes revealed that the "obese" condition exhibited the greatest mean differences compared to other body shapes, particularly when contrasted with the "no model" condition (-1.254, $p < 0.001$) and the "normal" model condition (1.089, $p < 0.001$).

Table 4
Descriptive Statistics

		Model body shapes					
		No model (M±SD)	**Obese (M±SD)**	**Overweight (M±SD)**	**Normal (M±SD)**	**Thin (M±SD)**	**Total (M±SD)**
Design Forms	Photographs	2.31±1.15	3.46±1.53	2.84±1.31	2.36±1.16	3.12±1.58	2.82±.11
	Anthropomorphism	2.17±1.17	3.40±1.62	2.61±1.20	2.34±1.07	2.77±1.41	2.66±.11
	Geometric	2.17±1.25	3.56±1.64	2.93±1.33	2.45±1.27	2.86±1.41	2.80±.12
	Total	2.22±.10	3.47±.16	2.80±.12	2.38±.12	2.92±.15	-

Table 5
Multivariate Tests

	Pillai's Trace	Wilks' Lambda	F	df	p	η²
Design forms (A)	0.065	0.935	2.904	(2, 84)	0.060	.041
Model body shapes (B)	0.460	0.540	17.470	(4, 82)	0.000	.266
Interaction: A × B	0.173	0.827	2.040	(8, 78)	0.052	.023

Table 6
LSD Post Hoc Test

Comp.	MD	p-Value	Comp.	MD	p-Value
No model vs Obese	-1.254	0.000	Obese vs Normal	1.089	0.000
No model vs Overweight	-0.576	0.000	Obese vs Thin	0.556	0.000
No model vs Normal	-0.165	0.041	Overweight vs Normal	0.411	0.000
No model vs Thin	-0.698	0.000	Overweight vs Thin	-0.123	0.350
Obese vs Overweight	0.678	0.000	Normal vs Thin	-0.534	0.000

MD = mean difference

A significant difference was also observed between the "normal" and "thin" model conditions (-0.534, $p < 0.001$). These findings suggest that model body shapes significantly modulate emotional reactions, corroborating the significant main effect observed in Table 6.

Conclusion and Suggestions

This study explored the impact of fruit and vegetable image design forms and model body shapes on consumers' health perceptions and emotional responses. The results indicate that the two variables interacted with health perceptions. Anthropomorphic and photographic fruit and vegetable designs matched with models of normal body shapes significantly enhanced consumers' health perceptions, particularly in anthropomorphic design.

However, when the model's body shape deviated from health standards (e.g., being thin or obese), geometric design forms weakened health perceptions, confirming Hypothesis A. In other words, the graphic design form of fruits and vegetables and the model's body shape interacted to affect consumers' health perceptions. Normal body shapes can best promote consumers' health perceptions. Although a thin body shape is often pursued as an ideal body type in contemporary society, people's health perceptions of this body shape remain relatively low. This is consistent with Yu et al., (2011).

However, this study also found that when thin body shapes were configured with illustration (geometric and anthropomorphic) forms, health perceptions improved. Perhaps the illustration form can distract people from reality and induce viewers to associate different motivations, thereby triggering a more positive feeling (Chrysochou & Grunert, 2014). However, this did not occur in the obese body types. Thus, exercise and food images do influence health behaviors (Wu et al., 2022), and different body shapes and fruit and vegetable design forms lead to different acceptability.

The emotional response analysis showed that the shape of the model's body was the main factor affecting emotional responses, and Hypothesis B was not supported. The subjects' reactions to underweight or obese models included significant negative emotions such as anxiety and discomfort; normal body shapes triggered a more stable emotional response. Notably, although thin models are often seen as a means of attracting consumers' attention (Antioco, Smeesters & Le Boedec, 2012), this study found that they may trigger negative emotions, echoing the findings of Janssen and Paas (2014) and Halliwell and Dittmar (2004).

Moreover, compared with photos and geometric forms, when the four body types were configured with anthropomorphic forms, negative emotions were reduced. Previous studies suggest that anthropomorphic fruits and vegetables make people naturally find them cute and friendly, and especially showing the anthropomorphic advantages in advertising can improve the views and preferences of advertising products than those without anthropomorphic design. Anthropomorphism can provide consumers with a sense of social connection and mitigate the negative feelings associated with social exclusion. (Mourey, Olson & Yoon, 2017).

A model's body shape is the main factor in negative emotions, because being too thin or obese could be a health issue, which can make people feel anxious, sad and uneasy (Styk, Wojtowicz & Zmorzynski, 2023).

Perhaps models with an "ideal body shape" (being lean) are attractive and can have better sales efficiency (Antioco, Smeesters & Le Boedec, 2012; Tsawaab, 2023). In fact, they can lead to consumers' negative emotions in healthy eating advertisements. Therefore, how to apply model body shapes in health or fashion appeals is something worth further discussing in the future.

Overall, anthropomorphic fruits and vegetables associated with models of normal or overweight body shapes in healthy eating advertisement designs can effectively enhance health perceptions and reduce negative emotions. Moreover, consumers tend to think that extreme body shapes (thin or obese) symbolize unhealthy characteristics, making it challenging for even positive behaviors such as running to reverse this impression.

Regarding practical suggestions, excessively abstract images and models with extreme body shapes should be avoided in advertisement design. We recommend using anthropomorphic designs and models with normal body shapes to enhance advertising effectiveness. Moreover, designers can use color contrast, situational plots, or other techniques to further optimize consumers' emotional responses.

Regarding research limitations and future directions, this study primarily explored the impact of static advertising images on health perceptions and emotional responses, without examining dynamic media or other interactive design forms.

Future research should be extended to explore the regulatory role of different visual elements (e.g., color, text messages, and sports situations) and audience characteristics (e.g., gender and age) on advertising effectiveness, testing the applicability of the results across cultural and market contexts.

Funding

This work was supported by the National Chin-Yi University of Technology.

References

Antioco, M., Smeesters, D. & Le Boedec, A. (2012) Take your pick: Kate Moss or the girl next door? The effectiveness of cosmetics advertising. *Journal of Advertising Research*. 52 (1), 15–30. Available from: doi: https://doi.org/10.2501/JAR-52-1-015-030.

Bower, A. B. (2001) Highly attractive models in advertising and the women who loathe them: The implications of negative affect for spokesperson effectiveness. *Journal of Advertising*. 30 (3), 51–63. Available from: doi: https://doi.org/10.1080/00913367.2001.10673645.

Cachelin, F. M., Rebeck, R. M., Chung, G. H. & Pelayo, E. (2002) Does ethnicity influence body-size preference? A comparison of body image and body size. *Obesity Research*. 10 (3), 158–166. Available from: doi: https://doi.org/10.1038/oby.2002.25.

Chrysochou, P. & Grunert, K. G. (2014) Health-related ad information and health motivation effects on product evaluations. *Journal of Business Research*. 67 (6), 1209–1217. Available from: doi: https://doi.org/10.1016/j.jbusres.2013.05.001.

Chu, R., Hetherington, M. M. & Tang, T. (2024) Designers' needs in leveraging the evolving role of packaging for promoting healthy eating. *Sustainability*. 16 (15), 6365. Available from: doi: https://doi.org/10.3390/su16156365.

Cian, L., Krishna, A. & Elder, R. S. (2014) This logo moves me: Dynamic imagery from static images. *Journal of Marketing Research*. 51 (2), 184–197. Available from: doi: 10.1509/jmr.13.0023.

D'Alessandro, S. & Chitty, B. (2011) Real or relevant beauty? Body shape and endorser effects on brand attitude and body image. *Psychology & Marketing*. 28 (8), 843–878. Available from: doi: 10.1002/mar.20415.

Delbaere, M., McQuarrie, E. F. & Phillips, B. J. (2011) Personification in advertising. *Journal of Advertising*. 40 (1), 121–130. Available from: doi: https://doi.org/10.2753/JOA0091-3367400108

Dixon, H., Scully, M., Cotter, T., Maloney, S. & Wakefield, M. (2015) Healthy weight and lifestyle advertisements: an assessment of their persuasive potential. *Health Education Research*. 30 (4), 569-579.

Festinger, L. (1954). A theory of social comparison processes. *Human relations*. 7 (2), 117-140.

Garner, D. M., Garfinkel, P. E., Schwartz, D. & Thompson, M. (1980) Cultural expectations of thinness in women. *Psychological reports*. 47 (2), 483-491. Available from: doi: 10.2466/pr0.1980.47.2.483.

Halliwell, E. & Dittmar, H. (2004) Does size matter? The impact of model's body size on women's body-focused anxiety and advertising effectiveness. *Journal of Social and Clinical Psychology*. 23 (1), 104–122. Available from: doi: 10.1521/jscp.23.1.104.26989.

Horn, F. & Jongenelis, M. I. (2022) Outcomes of exposure to healthy weight and lifestyle advertising: An experimental study of adults from the United Kingdom. *Preventive Medicine Reports*. 25, 101679. Available from: doi: 10.1016/j.pmedr.2021.101679.

Ippolito, P. M. & Pappalardo, J. K. (2002) *Advertising Nutrition & Health - Evidence from Food Advertising 1977 - 1997*. Washington, D. C. Available from: https://www.ftc.gov/sites/default/files/documents/reports/advertising-nutrition-health-evidence-food-advertising-1977-1997/advertisingfinal.pdf [Accessed 2nd August, 2025].

Janssen, D. M. & Paas, L. J. (2014) Moderately thin advertising models are optimal, most of the time: Moderating the quadratic effect of model body size on ad attitude by fashion leadership. *Marketing Letters*. 25, 167-177. Available from: doi: https://doi.org/10.1007/s11002-013-9249-y.

Kozup, J. C., Creyer, E. H. & Burton, S. (2003) Making healthful food choices: the influence of health claims and nutrition information on consumers' evaluations of packaged food products and restaurant menu items. *Journal of Marketing*. 67 (2), 19-34. Available from: doi: https://doi.org/10.1509/jmkg.67.2.19.18608.

Lancki, N., Siddique, J., Schneider, J. A., Kanaya, A. M., Fujimoto, K., Dave, S. S., Puri-Tanejaa, A. & Kandula, N. R. (2018) Social network body size is associated with body size norms of South Asian adults. *Obesity Medicine*. 11, 25-30. Available from: doi: https://doi.org/10.1016/j.obmed.2018.06.001.

Mourey, J. A., Olson, J. G., & Yoon, C. (2017). Products as pals: Engaging with anthropomorphic products mitigates the effects of social exclusion. *Journal of Consumer Research*, 44(2), 414–431. Available from: doi: https://doi.org/10.1093/jcr/ucx038

Messaris, P. (ed.) & Humphreys, L. (ed.) (2006) *Digital media: Transformations in human communication*. New York, Peter Lang.

Oke, S. & Tan, M. (2022) Techniques for advertising healthy food in school settings to increase fruit and vegetable consumption. *INQUIRY: The Journal of Health Care Organization, Provision, and Financing*. 59. Available from: doi: https://doi.org/10.1177/00469580221100165.

Rosenblatt, D. H., Dixon, H., Wakefield, M. & Bode, S. (2019) Evaluating the influence of message framing and graphic imagery on perceptions of food product health warnings. *Food Quality and Preference*. 77, 32-42. Available from: doi: https://doi.org/10.1016/j.foodqual.2019.05.003.

Ruiter, R. (2019) Dynamism and congruency: A study on the effects of dynamism and congruency on consumer attitude and recall. University of Twente.

Saunders, J. F., Nutter, S. & Russell-Mayhew, S. (2022) Examining the conceptual and measurement overlap of body dissatisfaction and internalized weight stigma in predominantly female samples: a meta-analysis and measurement refinement study. *Frontiers in Global Women's Health*. 3, 877554. Available from: doi: 10.3389/fgwh.2022.877554.

Stephens, D. L., Hill, R. P. & Hanson, C. (1994). The beauty myth and female consumers: The controversial role of advertising. *Journal of Consumer Affairs*. 28 (1), 137-153. Available from: doi: https://doi.org/10.1111/j.1745-6606.1994.tb00819.x.

Styk, W., Wojtowicz, E. & Zmorzynski, S. (2023) I Don't Want to Be Thin! fear of weight change is not just a fear of obesity: research on the body mass anxiety scale. *International Journal of Environmental Research and Public Health.* 20 (4), 2888. Available from: doi: https://doi.org/10.3390/ijerph20042888.

Tsawaab, A. H. (2023) The impact of body positivity in fashion advertising on customer perceptions and purchase intentions. *International Journal of Multidisciplinary: Applied Business and Education Research*. 4 (8), 2769-2784. Available from: doi: https://doi.org/10.11594/ijmaber.04.08.10.

Wallhead, G., Furnham, A. & McClelland, A. (2025) The influence of idealised and non-idealised models on the effectiveness of advertisements and body appreciation in females. *Frontiers in Communication*. 10. Available from: doi: https://doi.org/10.3389/fcomm.2025.1529650.

Wu, Y., Harford, J., Petersen, J. & Prichard, I. (2022) "Eat clean, train mean, get lean": Body image and health behaviours of women who engage with fitspiration and clean eating imagery on Instagram. *Body image.* 42, 25-31. Available from: doi: https://doi.org/10.1016/j.bodyim.2022.05.003.

Yu, U. J., Damhorst, M. L. & Russell, D. W. (2011) The impact of body image on consumers' perceptions of idealized advertising images and brand attitudes. *Family and Consumer Sciences Research Journal.* 40 (1), 58-73. Available from: doi: https://doi.org/10.1111/j.1552-3934.2011.02088.x.